Universität Konstanz
Fachbereich Physik

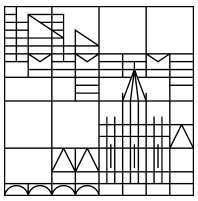

Quantum Control with Atoms and Photons in Optical Microresonators

Diplomarbeit

submitted by

Steffen Zeeb

2009

supervisors:
A-Prof. Dr. Scott Parkins
Prof. Dr. Howard Carmichael
Prof. Dr. Jürgen Audretsch
Prof. Dr. Guido Burkard

In Gedenken an meinen Vater

„Weine nicht weil etwas vorbei ist, sondern
lächle weil du es erleben durftest.“

Zusammenfassung

Die vorliegende Arbeit befasst sich mit der Untersuchung eines „cascaded cavity QED“ Systems, welches aus zwei über eine Glasfaser verbundenen, mikrotoroidalen Resonatoren besteht. In diesen breiten sich zwei entgegengesetzt laufende „whispering-gallery“ Moden aus, über deren evaneszente Feld jeweils ein einzelnes Atom an die Resonatoren gekoppelt ist.

Im ersten Teil der Arbeit wird die spontane Emission des Systems für den Fall eines anfänglich angeregten Atoms untersucht. Für das „bad-cavity“ Regime ist es möglich, die Resonatormoden adiabatisch zu beseitigen und dadurch analytische Ausdrücke für die Emissionsspektren herzuleiten. Diese Ergebnisse werden mit numerischen Resultaten, die aus dem vollständigen Modell gewonnen werden, verglichen. Dabei wird, so lange man sich im „bad-cavity“ Regime befindet, in welchem die Näherungen, die bei der Herleitung der analytischen Ergebnisse gemacht werden, ihre Gültigkeit besitzen, eine gute Übereinstimmung der analytischen und numerischen Ergebnisse gefunden. Des Weiteren wird für das „bad-cavity“ Regime die Mastergleichung, in welcher die Resonatormoden adiabatisch beseitigt sind, hergeleitet. Diese zeigt eine neuartige Struktur und kann die zuvor berechneten Emissionsspektren qualitativ erklären. Schließlich werden für das „strong-coupling“ Regime numerische Berechnungen durchgeführt, welche ein „vacuum Rabi splitting“ des Emissionsspektrums zeigen.

Im zweiten Teil wird das Verhalten des mit einer externen, kohärenten Lichtquelle (Laser) getriebenen Systems untersucht. Analytische Berechnungen werden für den Fall, dass keine Atome an die Mikroresonatoren gekoppelt sind, durchgeführt. Dabei zeigt sich, dass bei geeigneter Wahl der Parameter ein dem elektromagnetisch-induzierter-Transparenz-Effekt ähnliches Verhalten im Spektrum des Ausgangs-Photonenflusses auftreten kann. Des Weiteren wird das vollständige Modell numerisch, sowohl für das „bad-cavity“ als auch für das „strong-coupling“ Regime, untersucht. Durch Lösen der Mastergleichung im stationären Zustand wird der Photonenfluss berechnet. Ähnlich zum System der spontanen Emission tritt für das „strong-coupling“ Regime ein „vacuum Rabi splitting“ im Spektrum des Photonflusses auf. Außerdem zeigt sich, dass im „bad-cavity“ Regime die Linienbreite des Absorptions- bzw. Transmissionsspektrums für den Vorwärts- bzw. Rückwärtsfluss analog zum Spektrum des spontanen Emissionssystems skaliert. Zusätzlich wird eine Methode entwickelt, durch die das gekoppelte Mikroresonatorsystem mittels der Eigenschaften eines Einzelresonatorsystems anhand von Reflektions- und Transmissionskoeffizient

beschrieben wird. Die Übereinstimmung dieser Methode mit numerischen Resultaten des vollständigen Systems wird für den Fall eines nicht zu stark treibenden Feldes, d.h. solange die Kopplung der Mikroresonatoren linear ist, gezeigt.

Abstract

In this thesis we study a cascaded cavity QED system consisting of two microtoroidal resonators which are connected via an optical fibre. The toroids act as cavities with two counter-propagating whispering-gallery modes and a single atom is coupled to each of the toroids by the evanescent field of these cavity modes.

In the first part, we study the spontaneous emission of the system when one atom is initially excited. In the bad-cavity regime we are able to adiabatically eliminate the cavity modes and can derive analytical expressions for the emission spectra. These analytical results are compared to the emission spectra obtained from a numerical treatment of the full model. We find good agreement between the analytical and numerical results as long as we stay within the bad-cavity regime, for which the approximations made in the analytical investigation are valid. In addition, the master equation with the cavity modes adiabatically eliminated is derived. It shows a very novel behaviour and can qualitatively explain the emission spectra in the bad-cavity limit. For the strong-coupling regime a numerical investigation is carried out which shows a vacuum Rabi splitting of the emission spectra.

In the second part, we study the behaviour of the system when it is driven by an external, coherent light source. Analytical calculations are carried out for the case that no atoms are coupled to the toroids. For an appropriate choice of parameters the output flux can exhibit an electromagnetically-induced-transparency-like effect. In addition, we numerically investigate the "full" model for the strong-coupling and the bad-cavity regime. The output fluxes are computed by solving the master equation for the system in steady state in the weak excitation regime. Similar to the spontaneous emission, the photon flux shows a vacuum Rabi splitting for the strong-coupling regime. In the bad-cavity limit, we find that the linewidth of the absorption (transmission) spectrum of the forward (backward) flux scales analogously to the spectrum of the spontaneous emission system. Furthermore, a method to describe the cascaded system in terms of the properties of the single-toroid system, by means of reflection and transmission coefficients, is given. Its agreement with the numerical results for sufficiently weak driving fields (when the coupling of the toroids is essentially linear) is shown.

Acknowledgements

First of all, I would like to thank my supervisor A-Prof. Dr. Scott Parkins very much for giving me the opportunity to come to New Zealand and join the Quantum Optics group at the University of Auckland for doing my thesis. Scott always had time for me and patiently answered my questions whenever I popped into his office. I am also very grateful for his thorough proofreading of my thesis.

Many thanks also to my second supervisor Prof. Dr. Howard Carmichael for supporting me and helping me with my project. In particular, I would like to acknowledge Howard for all the useful comments and grammatical corrections he made throughout my thesis.

I am also very grateful to A-Prof. Dr. Leonhardt for his commitment prior to my arrival in New Zealand in guiding me through the jungle of bureaucracy at the University of Auckland (which seems to be worse than in any German institution). Without his help I would have given up organizing to come to New Zealand.

In addition, I am also very thankful to my supervisors Prof. Dr. Audretsch and Prof. Dr. Burkard at the Universität Konstanz who agreed on marking and supervising my thesis and therefore made it possible for me to come to New Zealand.

Very special thanks to Lloyd who took on the burden of proofreading my thesis and correcting the various mistakes I made.

Also, very special thanks to Klix for drawing most of the schematics in my thesis.

Last but not least there is more than just physics. Numerous people, too many to state, made my stay in Auckland very pleasant. I would like to thank them for a great and unforgettable year in New Zealand.

Auckland
July 2009

Steffen Zeeb

Contents

Chapter 1

Introduction

In 1901 Planck was able to solve the ultraviolet catastrophe problem by proposing that black-body radiation is emitted in discrete energy packets called quanta. Four years later, in 1905, Einstein explained the photoelectric effect by associating the formerly purely mathematical construct of an energy quantum with a real physical light particle, which was given the name "photon" years later, in 1926, by Lewis. This was the genesis of *quantization*. In 1913 Bohr applied the ideas of quantization to the atom and came up with the picture of an atom as a planetary-like system, where the electron is orbiting around the nucleus. On these grounds Heisenberg, Schrödinger and Dirac developed a rigorous mathematical treatment of what is now called *quantum mechanics* during the 1920s. The quantization of the radiation field, which combined the wave and particle-like aspects of light, was done by Dirac in 1927 and by Fermi in 1932. The development of quantum mechanics led to remarkable applications, such as lasers (1960), which had a big impact, not only on our society, but also on experiments in *quantum optics*.

Quantum optics is of special interest mainly for two reasons. First, it offers a way to prove the first principles of the fundamental theory of quantum mechanics, where we have come to create the conditions of the textbook examples in real experiments. A special domain of quantum optics is *cavity QED*. QED stands for *quantum electrodynamics*, which describes the interaction of some material (atoms) with the quantized electromagnetic field (photons), and is one of the most accurate physical theories constructed so far. Hence, cavity QED describes the interaction of atoms with light in a cavity, where cavity refers to an optical or microwave resonator. It was realized by Purcell, in 1946, that the emission spectrum of an atom can be altered when it is placed in a resonant cavity [Pur46]. For a weak atom-cavity coupling, e.g., where a photon emitted from the atom is lost out of the cavity before it can be reabsorbed by the atom, which is therefore an irreversible process, the spontaneous emission of light by the atom can either be inhibited or enhanced. This is referred to as the Purcell effect. The case of a strong atom-cavity coupling, where the photon is reabsorbed faster than it is lost out of the cavity, was first analysed by Jaynes and Cummings in 1963 [JC63] and the so-called vacuum Rabi splitting (a

splitting of the emission spectrum of the atom) was predicted. Not until 1992 was the technology advanced enough to observe the vacuum Rabi splitting for a single atom experimentally [TRK92].

The study of quantum optics is also appealing due to its implications for *quantum information* processing with atoms and photons [Mon02] and the pursuit of building a *quantum computer*. In 1982 Feynman proposed a computer running according to the laws of quantum physics rather than the laws of classical physics [Fey82]. Three years later, in 1985, Deutsch [Deu85] outlined the basic principles of such a quantum computer, which could, in principle, solve problems that are not efficiently solvable with a classical computer. A quantum computer consists of *quantum nodes*, where *quantum states* can be stored and locally manipulated; these states correspond to *qubits*, the quantum analogue of classical bits. These nodes are connected by *quantum channels* to distribute the information throughout the network. In order to do so, a reversible state transfer method is required. Cavity QED offers a promising approach, in which a quantum state can be mapped between light and matter in a reversible way. A first scheme for "Quantum State Transfer and Entanglement Distribution among Distant Nodes in a Quantum Network" was proposed by J. I. Cirac *et al.* in 1997 [CZKM97]. Ten years later, a reversible state transfer between light and an atom in a cavity – "the first verification of the fundamental primitive upon which the protocol" by J. I. Cirac *et al.* is based – was realized experimentally by A. D. Boozer *et al.* [BBM$^+$07].

A promising device for a future quantum network is an optical microtoroid which provides for a strong interaction between a single atom and a single photon. This was experimentally shown in 2006 by Takao Aoki *et al.* [ADW$^+$06a]. Hence, the microtoroid has the potential to be used as a quantum node, where quantum states can be stored and locally manipulated. A system of two coupled toroidal microcavities is the first step towards a more complex network and, in order to be able to understand these more complex networks, the coupled two toroid system has to be understood first. This thesis characterizes a system of two microtoroids coupled by a fibre. Knowledge of the behaviour of such systems may one day lead to applications in the field of quantum computing, or in related fields.

1.1 Outline

The thesis is divided into two sections. In Chapters 2-4 the background theory is presented. It is then applied in Chapters 5 and 6 to investigate cascaded quantum optical systems. No knowledge of quantum optics is assumed, but the reader is expected to be familiar with the concepts of quantum mechanics on an advanced level.

In Chapter 2, the basic concepts of quantum optics are introduced. The electromagnetic field is quantized and its interaction with an atom is discussed. The Jaynes-Cummings model, the fundamental model for the interaction of an atom with a cavity field, is introduced and some extensions to this model are made.

In Chapter 3, the theory of open quantum systems is presented. In particular, the master equation for treating dissipative systems and the quantum regression formula are derived.

Chapter 4 deals with more advanced topics in cavity QED. The input-output theory, which relates the input field to the output field of a cavity, is presented and cascaded systems, e.g, two coupled cavity QED systems, are discussed.

In Chapter 5, the spontaneous emission spectrum of a specific cascaded system consisting of two coupled microtoroids, with an atom coupled to each and one atom initially excited, is studied. The focus of the investigation lies on the so-called "bad-cavity" regime, where an analytical and numerical treatment is carried out. The system is also investigated numerically for the so-called "strong-coupling" regime.

In Chapter 6, the cascaded system studied in the previous chapter is extended by adding an external light source to drive the atoms. The system is investigated analytically for the case that no atoms are coupled to the toroids, where the output photon flux is computed. For the full model (consisting of two coupled microtoroids with a single atom coupled to each toroid), the output photon flux is studied numerically for the strong-coupling and the bad-cavity regime. Furthermore, an analytical treatment in terms of reflection and transmission coefficients is given.

Finally, Chapter 7 gives a summary of the results and discusses potential topics for future research.

Chapter 2

Atom-Photon Interaction

In this chapter we aim to derive some of the basic concepts of quantum optics which we can build on in later chapters. For many problems in quantum optics it is necessary to describe the light as a quantized field. This quantization of the electromagnetic field is done in the first section.

The following sections deal with a two-level atom and its interaction with a quantized field. In particular, the *Jaynes-Cummings model*, the fundamental model for the interaction of an atom with a cavity field, will be introduced and some extensions to this model will be made to describe more complex systems.

This review is by no means complete. A more comprehensive introduction to the basic concepts of quantum optics can be found in [Fox06] and, on a more advanced level, in [SZ97].

2.1 Quantization of the electromagnetic field

The free electric and magnetic field is obtained by solving Maxwell's equations in empty space, i.e., no sources of radiation and no charges are present. Free space is modelled as a cubic cavity of length $L \to \infty$, which imposes periodic boundary conditions, so that only certain electromagnetic waves with discrete wave vectors, of form $\vec{k} = \frac{2\pi}{L}(m_x, m_y, m_z)$, where (m_x, m_y, m_z) is a set of integers, can exist. Expanding the classical electric and magnetic fields in terms of travelling waves yields[1]

$$\vec{E}(\vec{r},t) = \sum_{\vec{k}} \sum_{\lambda=1}^{2} \vec{E}_{\vec{k},\lambda} e^{i(\vec{k}\cdot\vec{r}-\omega_k t)} + \text{c.c.}\,, \tag{2.1}$$

$$\vec{B}(\vec{r},t) = \sum_{\vec{k}} \sum_{\lambda=1}^{2} \vec{B}_{\vec{k},\lambda} e^{i(\vec{k}\cdot\vec{r}-\omega_k t)} + \text{c.c.}\,, \tag{2.2}$$

[1] A more detailed derivation and further discussions can be found in many textbooks on electrodynamics, for example in [Jac07].

with

$$\vec{E}_{\vec{k},\lambda} = i\omega_k \hat{e}_{\vec{k},\lambda} A_{\vec{k},\lambda} \,, \tag{2.3}$$

$$\vec{B}_{\vec{k},\lambda} = i(\vec{k} \times \hat{e}_{\vec{k},\lambda}) A_{\vec{k},\lambda} \,, \tag{2.4}$$

where ω_k is the frequency of the plane wave, $A_{\vec{k},\lambda}$ is an amplitude,[2] $\hat{e}_{\vec{k},\lambda}$ is a unit polarization vector (taken to be real for linearly polarized light) and the summation over λ accounts for the two perpendicular directions of linear polarization.

The energy of the field is given by

$$H_{\mathrm{F}} = \frac{1}{2} \int_V d^3r \left(\epsilon_0 \vec{E}(\vec{r},t) \cdot \vec{E}(\vec{r},t) + \frac{1}{\mu_0} \vec{B}(\vec{r},t) \cdot \vec{B}(\vec{r},t) \right) , \tag{2.5}$$

where ϵ_0 is the permittivity and μ_0 the permeability of free space.

We separate the mode amplitudes into real and imaginary parts by defining

$$A_{\vec{k},\lambda} := \frac{1}{\sqrt{4\epsilon_0 V}} \left(q_{\vec{k},\lambda} + \frac{i}{\omega_k} p_{\vec{k},\lambda} \right) , \tag{2.6}$$

where $q_{\vec{k},\lambda}$ and $p_{\vec{k},\lambda}$ comprise a pair of real variables and $V = L^3$ is the volume of the cubic cell that models free space.

Using equations (2.5), (2.1), (2.2) and (2.6), plus the orthogonality of different modes, we find for the energy

$$H_{\mathrm{F}} = \sum_{\vec{k}} \sum_{\lambda=1}^{2} \frac{1}{2} \left(p^2_{\vec{k},\lambda} + \omega_k^2 q^2_{\vec{k},\lambda} \right) . \tag{2.7}$$

This Hamiltonian corresponds to the Hamiltonian of an infinite set of harmonic oscillators with generalized coordinates $q_{\vec{k},\lambda}$ and canonical momenta $p_{\vec{k},\lambda}$ within Lagrangian/Hamiltonian mechanics. Each mode of the field is therefore formally equivalent to a mechanical harmonic oscillator.

The quantization is accomplished by using the *correspondence principle* and replacing the conjugate variables $p_{\vec{k},\lambda}$ and $q_{\vec{k},\lambda}$ by operators $\hat{p}_{\vec{k},\lambda}$ and $\hat{q}_{\vec{k},\lambda}$ which obey the fundamental commutation relations

$$\left[\hat{q}_{\vec{k},\lambda}, \hat{p}_{\vec{k}',\lambda'} \right] = i\hbar \delta_{\vec{k}\vec{k}'} \delta_{\lambda\lambda'} \,, \tag{2.8}$$

$$\left[\hat{q}_{\vec{k},\lambda}, \hat{q}_{\vec{k}',\lambda'} \right] = \left[\hat{p}_{\vec{k},\lambda}, \hat{p}_{\vec{k}',\lambda'} \right] = 0 \,. \tag{2.9}$$

Usually a canonical transformation to the *annihilation* and *creation operators* is made, by introducing

$$a_{\vec{k},\lambda} = \frac{1}{\sqrt{2\hbar\omega_k}} \left(\omega_k \hat{q}_{\vec{k},\lambda} + i\hat{p}_{\vec{k},\lambda} \right) , \tag{2.10}$$

$$a^\dagger_{\vec{k},\lambda} = \frac{1}{\sqrt{2\hbar\omega_k}} \left(\omega_k \hat{q}_{\vec{k},\lambda} - i\hat{p}_{\vec{k},\lambda} \right) , \tag{2.11}$$

[2] To be more precise, it is the amplitude of the vector potential.

which obey the commutation relations

$$\left[a_{\vec{k},\lambda}, a^{\dagger}_{\vec{k}',\lambda'}\right] = \delta_{\vec{k}\vec{k}'}\delta_{\lambda\lambda'}\,, \tag{2.12}$$

$$\left[a_{\vec{k},\lambda}, a_{\vec{k}',\lambda'}\right] = \left[a^{\dagger}_{\vec{k},\lambda}, a^{\dagger}_{\vec{k}',\lambda'}\right] = 0\,. \tag{2.13}$$

In terms of $a_{\vec{k},\lambda}$ and $a^{\dagger}_{\vec{k},\lambda}$, the field operators can be written as

$$\hat{\vec{E}}(\vec{r},t) = \sum_{\vec{k}}\sum_{\lambda=1}^{2} \vec{\mathcal{E}}_{\vec{k},\lambda} a_{\vec{k},\lambda} e^{i(\vec{k}\cdot\vec{r}-\omega_k t)} + \text{H.c.}\,, \tag{2.14}$$

$$\hat{\vec{B}}(\vec{r},t) = \sum_{\vec{k}}\sum_{\lambda=1}^{2} \vec{\mathcal{B}}_{\vec{k},\lambda} a_{\vec{k},\lambda} e^{i(\vec{k}\cdot\vec{r}-\omega_k t)} + \text{H.c.}\,, \tag{2.15}$$

with

$$\vec{\mathcal{E}}_{\vec{k},\lambda} = i\sqrt{\frac{\hbar\omega_k}{2\epsilon_0 V}}\hat{e}_{\vec{k},\lambda}\,, \tag{2.16}$$

$$\vec{\mathcal{B}}_{\vec{k},\lambda} = i\sqrt{\frac{\hbar}{2\epsilon_0 V\omega_k}}(\vec{k}\times\hat{e}_{\vec{k},\lambda})\,, \tag{2.17}$$

and the Hamiltonian of the quantized radiation field becomes

$$H_{\text{F}} = \sum_{\vec{k}}\sum_{\lambda=1}^{2} \hbar\omega_k \left(a^{\dagger}_{\vec{k},\lambda} a_{\vec{k},\lambda} + \frac{1}{2}\right)\,. \tag{2.18}$$

Note that in the Heisenberg picture the time evolution for the annihilation operator is given by

$$\frac{d}{dt}a_{\vec{k},\lambda} = \frac{i}{\hbar}\left[H, a_{\vec{k},\lambda}\right] = -i\omega_k a_{\vec{k},\lambda}\,, \tag{2.19}$$

with the solution

$$a_{\vec{k},\lambda}(t) = a_{\vec{k},\lambda}(0)e^{-i\omega_k t}\,. \tag{2.20}$$

Similarly, we find for the time evolution of the creation operator

$$a^{\dagger}_{\vec{k},\lambda}(t) = a^{\dagger}_{\vec{k},\lambda}(0)e^{i\omega_k t}\,. \tag{2.21}$$

Note that the above expansion give the field operators in the Heisenberg picture, equations (2.14) and (2.15), where the $a_{\vec{k},\lambda}$ correspond to what is called $a_{\vec{k},\lambda}(0)$ in equation (2.20).

2.2 The two-level atom

In quantum optics the atom is often assumed to be a two-energy-level system with E_g the energy of the lower state, called the ground state, and E_e the energy of the upper state, called the excited state. The atom can be excited from the ground to the upper state by absorbing a photon of energy

$$\hbar\omega_A = E_e - E_g\,, \tag{2.22}$$

where ω_A is the transition frequency; from here it can relax back to the ground state by emitting a photon of the same energy.

The Hamiltonian of the *two-level atom* can be written in the basis of the energy eigenstates, as

$$H_A = E_g|g\rangle\langle g| + E_e|e\rangle\langle e|\,, \tag{2.23}$$

where $|g\rangle$ denotes the ground state and $|e\rangle$ the excited state of the atom. The first term in the Hamiltonian can be removed by setting the zero of energy to be the energy of the ground state. Introducing the *atomic lowering* and *raising operators*

$$\sigma^- := |g\rangle\langle e| \qquad \text{and} \qquad \sigma^+ := |e\rangle\langle g|\,, \tag{2.24}$$

the Hamiltonian of the two-level atom becomes

$$H_A = \hbar\omega_A\sigma^+\sigma^-\,. \tag{2.25}$$

Note that in the Heisenberg picture the time evolution for the atomic lowering operator is given by

$$\frac{d}{dt}\sigma^- = \frac{i}{\hbar}\left[H, \sigma^-\right] = -i\omega_A\sigma^-\,, \tag{2.26}$$

with solution

$$\sigma^-(t) = \sigma^-(0)e^{-i\omega_A t}\,. \tag{2.27}$$

Similarily we find for the time evolution of the atomic raising operator

$$\sigma^+(t) = \sigma^+(0)e^{i\omega_A t}\,. \tag{2.28}$$

The two-energy-level atom is of course an approximation. A real atom has many different energy levels with all possible transitions between them. But for a radiation field which interacts with an atom near one of its transition frequencies and is far off resonance from all others, the two-level atom is a very good approximation, since the probabilities for other transitions to occur are vanishingly small.

2.3 Atom-light interaction

When an atom is placed in an electric field its electrons interact with this field and the electronic charge distribution of the atom is distorted. For optical frequencies, where the wavelength of the electric field is much larger than the size of the atom, the field is effectively constant across the atom. Thus, all terms higher than the lowest can be neglected in a multipole expansion of the field. The remaining atom-field interaction term is the electric-dipole interaction and hence this is referred to as the *dipole approximation*.

The Hamiltonian for the interaction of the radiation field with an atom is, in the dipole approximation, given by[3]

$$H_{\mathrm{I}} = -\hat{\vec{d}} \cdot \hat{\vec{E}}\,, \tag{2.29}$$

where $\hat{\vec{E}}$ is the electric field operator at the position of the atom and $\hat{\vec{d}}$ is the electric-dipole moment operator of the atom, given by

$$\hat{\vec{d}} = -e \sum_i \hat{\vec{r}}_i\,, \tag{2.30}$$

where $\hat{\vec{r}}_i$ is the position operator of the i^{th} electron.

If we make the approximation of a two-level atom the dipole moment operator can be expanded in terms of the ground and excited state of the atom,

$$\hat{\vec{d}} = \sum_{n,m=\{g,e\}} \vec{\mu}_{nm} |n\rangle\langle m|\,, \tag{2.31}$$

where we have introduced the atomic dipole matrix elements

$$\vec{\mu}_{nm} = -e \sum_i \langle n|\hat{\vec{r}}_i|m\rangle\,. \tag{2.32}$$

Noticing that the energy eigenstates cannot have a permanent dipole moment,[4] i.e.,

$$\langle n|\hat{\vec{r}}_i|n\rangle = 0\,, \tag{2.33}$$

the dipole operator simplifies to

$$\hat{\vec{d}} = \vec{\mu}_{ge}\sigma^- + \vec{\mu}_{eg}\sigma^+\,. \tag{2.34}$$

The electric field operator is given by equation (2.14). In the Schrödinger picture and with the dipole approximation made, it yields

$$\hat{\vec{E}} = \sum_{\vec{k}} \left(\vec{\mathcal{E}}_{\vec{k}} a_{\vec{k}} + \vec{\mathcal{E}}^*_{\vec{k}} a^\dagger_{\vec{k}}\right)\,, \tag{2.35}$$

[3] A derivation of this Hamiltonian can be found in [Lou73, Chap. 8].

[4] For further information see [Sak94, p. 260].

where we considered only one direction of polarization for simplicity.

With equation (2.35) for the field operator and equation (2.34) for the dipole operator, the interaction term can be written as

$$-\hat{\vec{d}} \cdot \hat{\vec{E}} = -\sum_{\vec{k}} \left(\vec{\mu}_{ge}\sigma^- + \vec{\mu}_{eg}\sigma^+\right) \cdot \left(\vec{\mathcal{E}}_{\vec{k}} a_{\vec{k}} + \vec{\mathcal{E}}^*_{\vec{k}} a^\dagger_{\vec{k}}\right) . \tag{2.36}$$

In the next step we apply the *rotating wave approximation*. The free evolution of the annihilation and creation operators in the Heisenberg picture is given by equations (2.20) and (2.21), and the free evolution of the atomic operators is given by equations (2.27) and (2.28). Combining these dependencies we find

$$\sigma^-(t)a^\dagger_{\vec{k}}(t) = \sigma^-(0)a^\dagger_{\vec{k}}(0)e^{-i(\omega_\mathrm{A}-\omega_k)t} , \tag{2.37}$$

$$\sigma^+(t)a_{\vec{k}}(t) = \sigma^+(0)a_{\vec{k}}(0)e^{i(\omega_\mathrm{A}-\omega_k)t} , \tag{2.38}$$

and

$$\sigma^-(t)a_{\vec{k}}(t) = \sigma^-(0)a_{\vec{k}}(0)e^{-i(\omega_\mathrm{A}+\omega_k)t} , \tag{2.39}$$

$$\sigma^+(t)a^\dagger_{\vec{k}}(t) = \sigma^+(0)a^\dagger_{\vec{k}}(0)e^{i(\omega_\mathrm{A}+\omega_k)t} . \tag{2.40}$$

We see that $\sigma^-(t)a^\dagger_{\vec{k}}(t)$, which corresponds to the emission of a photon and the de-excitation of the atom, and $\sigma^+(t)a_{\vec{k}}(t)$, describing the absorption of a photon and the excitation of the atom, vary slowly in time near resonance. On the contrary, $\sigma^-(t)a_{\vec{k}}(t)$ and $\sigma^+(t)a^\dagger_{\vec{k}}(t)$ evolve at optical frequencies. On a timescale of a few optical periods the fast varying terms tend to average to zero. Thus, they may be neglected when evaluating the interaction Hamiltonian. This is referred to as the rotating wave approximation.

Finally, defining the dipole coupling constants as

$$g_{\vec{k}} := -\frac{\vec{\mu}_{eg} \cdot \vec{\mathcal{E}}_{\vec{k}}}{\hbar} \qquad \text{and} \qquad g^*_{\vec{k}} := -\frac{\vec{\mu}_{ge} \cdot \vec{\mathcal{E}}^*_{\vec{k}}}{\hbar} , \tag{2.41}$$

the interaction Hamiltonian in the rotating wave approximation is

$$H_\mathrm{I} = \hbar \sum_{\vec{k}} (g^*_{\vec{k}}\sigma^- a^\dagger_{\vec{k}} + g_{\vec{k}}\sigma^+ a_{\vec{k}}) . \tag{2.42}$$

2.4 Atom in a cavity – Jaynes-Cummings model

Combining the results from the previous sections we are now able to describe the interaction of atoms with the quantized modes of a cavity. The simplest case, the interaction of a two-level atom with a single cavity mode near resonance, is described by the Jaynes-Cummings model.[5]

[5] The model is named after Jaynes and Cummings who were the first to analyse the interaction between a resonant cavity and a molecule in their famous paper from 1963 [JC63].

2.4.1 The Hamiltonian

The Jaynes-Cummings Hamiltonian for the system of a two-state atom interacting with a cavity mode is

$$H = H_{\mathrm{A}} + H_{\mathrm{C}} + H_{\mathrm{AC}}\,, \tag{2.43}$$

where H_{A} is the Hamiltonian for the two-level atom, given by equation (2.25), H_{C} the Hamiltonian for the quantized cavity field, given by equation (2.18), reduced to a single mode and dropping the zero-point term as it does not contribute to the dynamics, and H_{AC} is the interaction Hamiltonian in the rotating wave approximation given by equation (2.42). Thus the Hamiltonian reads explicitly as

$$H = \hbar\omega_{\mathrm{A}}\sigma^+\sigma^- + \hbar\omega_{\mathrm{C}}a^\dagger a + \hbar(g^*a^\dagger\sigma^- + g\sigma^+a)\,, \tag{2.44}$$

where ω_{A} is the atomic transition frequency, ω_{C} the frequency of the cavity mode and g the dipole coupling constant.

2.4.2 Dressed states

For simplicity in the following considerations, we assume the atom to be on exact resonance with the cavity mode, i.e., $\omega_{\mathrm{A}} = \omega_{\mathrm{C}} =: \omega$. The system ground state is denoted by $|g,0\rangle$ and has the energy $E = 0$.

Let us start by considering the "bare" states of the uncoupled system, i.e., the coupling constant g in the Hamiltonian (2.44) is zero. In this case the (eigen-)states $|g,n\rangle$ and $|e,n-1\rangle$ (with $n > 0$, where n is the number of photons in the cavity mode) are degenerate and their energy is $E_n = n\hbar\omega$.

Taking the atom-cavity coupling into account lifts the degeneracy and we find

$$H|g,n\rangle = n\hbar\omega|g,n\rangle + \hbar g\sqrt{n}|e,n-1\rangle\,, \tag{2.45}$$

$$H|e,n-1\rangle = n\hbar\omega|e,n-1\rangle + \hbar g^*\sqrt{n}|g,n\rangle\,, \tag{2.46}$$

for $n > 0$. The interaction term couples the two states $|g,n\rangle$ and $|e,n-1\rangle$ for each value of n, but does not couple any other states. Therefore we can consider each subspace $\mathcal{H}_n = \{|g,n\rangle, |e,n-1\rangle\}$ independently and write the total Hamiltonian as (see [MSI07, Chap. 14])

$$H = \sum_n H_n\,, \tag{2.47}$$

where H_n acts only in $\mathcal{H}_n$ and can be written as

$$H_n = \begin{pmatrix} n\hbar\omega & \hbar g\sqrt{n} \\ \hbar g^*\sqrt{n} & n\hbar\omega \end{pmatrix}. \tag{2.48}$$

Diagonalizing this Hamiltonian, we find the two eigenvalues

$$E_n^{\pm} = n\hbar\omega \pm \sqrt{n}\hbar|g|\,, \tag{2.49}$$

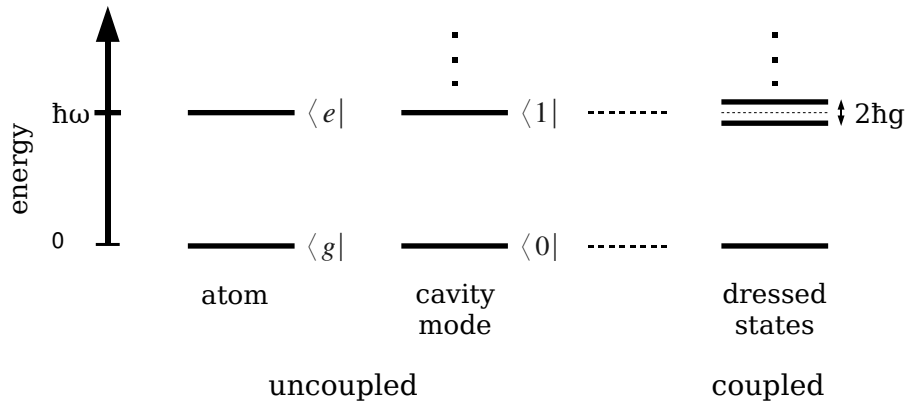

FIGURE 2.1: The Jaynes-Cummings ladder. Shown on the left are the energies of the uncoupled states of the atom and the cavity mode with their resonance frequencies taken equal. Shown on the right is the ladder of dressed states of a coupled atom-photon system.

which are the energies of the corresponding system eigenvectors,

$$|E_n^+\rangle = \frac{1}{\sqrt{2}}(|g,n\rangle + |e,n-1\rangle)\,, \tag{2.50}$$

$$|E_n^-\rangle = \frac{1}{\sqrt{2}}(|g,n\rangle - |e,n-1\rangle)\,. \tag{2.51}$$

These mixed atom-photon states are the so-called *dressed states*. The energy eigenvalues form a "ladder" of doublets, referred to as the *Jaynes-Cummings ladder*. This is illustrated in Figure 2.1.

Note that there is a splitting for even the first rung of the ladder, called the *vacuum Rabi splitting*, whose magnitude is determined by the coupling strength:

$$E_{\text{vacuum Rabi splitting}} = 2\hbar g\,. \tag{2.52}$$

2.5 Extensions to the Jaynes-Cummings model

The simple Jaynes-Cummings model can be extended in order to describe more sophisticated systems.

2.5.1 Microresonators – two-mode cavity

The simplest cavity QED system comprises a high-finesse optical Fabry-Perot cavity with an atom placed inside it. This is by no means the only cavity system possible. Many other (microfabricated) systems have been developed, especially because of the need for ultra high Q factors and scalability to large number of devices.[6] The Q

[6] For a review on optical microcavities see [Vah03].

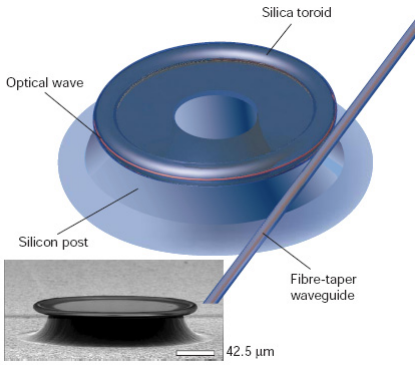

FIGURE 2.2: Rendering of an ultra-high Q microtoroid resonator. Picture taken from [Vah03].

factor of a cavity is a measure of its quality and is determined by the total energy stored in the cavity divided by the energy lost per cycle, or in other words, the Q factor is proportional to the confinement time in units of the optical period. Examples for ultra-high Q-factor small-mode-volume cavities are *spherical* or *toroidal microresonators*. These fused silicia microtoroids are fabricated on silicon wafers by standard lithographic techniques and can be accessed (i.e. light is coupled to and from the toroid) by fibre optic tapers. An example can be seen in Figure 2.2. Light in the microtorid executes orbits near the surface of the toroid, undergoing continuous internal reflections. There are two possible directions of propagation which account for the existence of two counter-propagating so-called *whispering-gallery modes* (WGMs).[7] These WGMs have very low loss rates and are strongly confined within the toroid, which leads to very large single-photon electric fields – described by the strong-coupling cavity QED regime. An atom which is brought close to the toroid can interact with it through the evanescent field of the WGMs. The strength of the atom-cavity coupling can be controlled by adjusting the distance between the toroid and the atom. In the same way, the coupling of the toroid to and from the fibre can be controlled.

Other very interesting types of cavity QED systems are found in solid state physics. Semiconductor *quantum dots* or *quantum wells* in micropillar, microdisk or photonic crystal cavities exhibit similar properties to their atom-microtoroid counterparts. A quantum dot is a semiconductor "island" (e.g., InAs) whose bond electron and hole pairs (so-called excitons) are confined in all three spatial dimensions. (In a quantum well the excitons are confined in one dimension.) As a result, quantum dots have a discrete energy spectrum rather than a continuous one and essentially behave like atoms.[8] The micropillar, microdisk and photonic crystal act as cavities. For example, a photonic crystal has a periodic variation in its refraction index on a length scale comparable to the wavelength of interest. In analogy to electrons in

[7] The WGMs are named after their acoustic equivalent.
[8] For an introduction to quantum dots see [Ree93].

an atomic crystal, there are so-called photonic bandgaps where no photon mode can exist. The prohibition of wave propagation in the forbidden gaps can be used to create a highly reflective mirror. A cavity is then formed by omitting one or two periods of the variation in the refractive index [Yab87]. When a quantum dot is placed within one of these cavities, a solid state optical cavity QED system is formed. The advantage of the quantum dot cavity QED system is that the quantum dot is firmly fixed to the cavity and therefore the experiments can be carried out on the same object, whereas in experiments with real atoms, an atom usually passes through the cavity, or the evanescent field of the resonator, and is lost after its transit.[9] On the other hand, semiconductor systems are much more complex. The parameters of the system and how they control the system's behaviour are much better understood in cavity QED systems using atoms.

Another system for studying the interaction of light and matter at the quantum level is the so-called *circuit QED system*, in which microwave photons are coupled to superconducting qubits, formed from *Josephson junctions* and superconducting islands, which act as artificial atoms. These systems can have a very strong atom-photon coupling.[10]

The system we will investigate in this thesis is assumed to consists of mico-toroids where the counter-propagating WGMs can interact with one another (e.g. by scattering at imperfections of the toroid), with the strength h, and each of the modes is coupled to the atom with the strength g. This system can be described by an extended Jaynes-Cummings model where we have to take the second (counter-propagating) cavity mode, b, into account, together with its interaction with the first mode, a. The extended Jaynes-Cummings Hamiltonian for a two-mode cavity with interaction of the modes is

$$\begin{aligned} H = {} & \hbar\omega_{\mathrm{C}}(a^\dagger a + b^\dagger b) + \hbar(ha^\dagger b + h^* b^\dagger a) \\ & + \hbar\omega_{\mathrm{A}}\sigma^+\sigma^- + \hbar(g^* a^\dagger \sigma^- + g\sigma_1^+ a) + \hbar(gb^\dagger\sigma^- + g^*\sigma^+ b)\,. \end{aligned} \tag{2.53}$$

2.5.2 Driven Jaynes-Cummings model

When a cavity is irradiated by an external coherent light source (e.g. a laser), the light can couple into the cavity and, in the case of the right frequency, provide the cavity modes with energy. If the probe frequency is near resonance with a cavity mode and the cavity has sufficiently high finesse this interaction is well approximated by a linear coupling, of strength ϵ. The number of photons in the input mode is usually very large so that quantum effects do not play a role. Hence, the input field can be treated classically, i.e., the field operator, $\hat{E}$, can be replaced by a classical complex field amplitude, E_0.

We assume the input light to be of the form

$$E_{\mathrm{in}}(t) = E_0 e^{-i\omega t}\,. \tag{2.54}$$

[9] Although, cavity QED experiments with an atom trapped inside a cavity have been conducted [YVK99, BMB+04].

[10] An introduction to circuit QED can for example be found in [SG08].

The Hamiltonian describing the interaction between a cavity mode, a, and the input light can then be written as

$$H_{\text{driv}} = \hbar\mathcal{E}^* e^{i\omega_{\text{p}}t} a + \hbar\mathcal{E} e^{-i\omega_{\text{p}}t} a^\dagger \tag{2.55}$$

where the coupling constant, ϵ, a transmission coefficient (typically a factor $\sqrt{2\kappa}$, with κ the cavity damping rate) which accounts for the coupling into the cavity, and a possible phase change on transmission, $e^{-i\phi}$, are all absorbed into the complex field amplitude $\mathcal{E}$.

Chapter 3

Quantum Theory of Open Systems

After having developed the essential theoretical background to the interaction between atoms and light, with and without a cavity present, we consider the leakage of light out of the cavity and its implications in this chapter. In the previous chapter, the cavity system was assumed to be sealed from its environment. However, in a real system, dissipation is always present. Also, one is usually interested in the light emitted from the cavity rather than the intracavity light. For an accurate description of a cavity system we therefore have to treat it as an *open quantum system*, a system which interacts with its environment and, in particular, loses photons to the environment. In this chapter, the general *master equation* – the central equation for treating open quantum systems – will be derived, and then be applied to a specific example: the single atom-toroid system.

3.1 Derivation of the master equation

The system, S, that we are interested in has some leakage to, or some interaction with, its environment, and cannot be considered as a closed system. Hence, to describe the system accurately we have to take its environment into account as well. The environment is typically much larger than the system and can be seen as a reservoir, R. The combination of the system S and the reservoir R is assumed to be a closed quantum system, $S \otimes R$, described by the density operator $\chi(t)$.[1] The total Hamiltonian, H, of the closed system can be decomposed as follows:

$$H = H_{\mathrm{S}} + H_{\mathrm{R}} + H_{\mathrm{SR}}\,, \tag{3.1}$$

where H_{S} and H_{R} are the Hamiltonians for the system and reservoir, respectively, and H_{SR} is the Hamiltonian, describing their interaction.

[1] We usually only have knowledge of the system S, and due to its dissipation even this knowledge is limited. Therefore we cannot describe the system by a state vector, but have to use the density operator instead.

3.1.1 Reduced density operator

The evolution of the closed system $S \otimes R$ is governed by the *von Neumann equation*

$$\dot{\chi}(t) = -\frac{i}{\hbar}\left[H, \chi\right] , \tag{3.2}$$

where H is the closed system Hamiltonian. In general this equation is very complex, in particular, because of the complex nature of the reservoir, and cannot be solved. Since we are only interested in the system, S, not in the reservoir, we can trace over the reservoir states and obtain the reduced density operator

$$\rho = \mathrm{Tr}_{\mathrm{R}}\left[\chi(t)\right] , \tag{3.3}$$

describing the system, including the effects of the reservoir upon it, e.g., the damping of the system (into the reservoir). The reduced density operator is sufficient to calculate the averages of all operators, $\hat{O}$, acting on the system subspace, $\mathcal{H}_{\mathrm{S}}$, alone:

$$\langle \hat{O} \rangle = \mathrm{Tr}_{\mathrm{S}\otimes\mathrm{R}}\left[\hat{O}\chi(t)\right] = \mathrm{Tr}_{\mathrm{S}}\left\{\hat{O}\mathrm{Tr}_{\mathrm{R}}\left[\chi(t)\right]\right\} = \mathrm{Tr}_{\mathrm{S}}\left[\hat{O}\rho(t)\right] . \tag{3.4}$$

Our objective in the following is to obtain an equation of motion for $\rho(t)$.

3.1.2 The von Neumann equation in integro-differential form

To separate the fast motion of the system and reservoir from the slow motion due to their interaction, we move to an interaction picture defined by

$$\tilde{\chi}(t) := e^{\frac{i}{\hbar}(H_{\mathrm{S}}+H_{\mathrm{R}})t}\chi(t)e^{-\frac{i}{\hbar}(H_{\mathrm{S}}+H_{\mathrm{R}})t} . \tag{3.5}$$

The von Neumann equation (3.2) in the interaction picture yields

$$\begin{aligned}\dot{\tilde{\chi}}(t) &= \frac{i}{\hbar}(H_{\mathrm{S}}+H_{\mathrm{R}})\tilde{\chi}(t) - \frac{i}{\hbar}\tilde{\chi}(t)(H_{\mathrm{S}}+H_{\mathrm{R}}) + e^{\frac{i}{\hbar}(H_{\mathrm{S}}+H_{\mathrm{R}})t}\dot{\chi}(t)e^{-\frac{i}{\hbar}(H_{\mathrm{S}}+H_{\mathrm{R}})t} \\ &= -\frac{i}{\hbar}\left[\tilde{H}_{\mathrm{SR}}(t), \tilde{\chi}(t)\right] ,\end{aligned} \tag{3.6}$$

where $\tilde{H}_{\mathrm{SR}}(t)$ is explicitly time dependent, namely

$$\tilde{H}_{\mathrm{SR}}(t) = e^{\frac{i}{\hbar}(H_{\mathrm{S}}+H_{\mathrm{R}})t}H_{\mathrm{SR}}e^{-\frac{i}{\hbar}(H_{\mathrm{S}}+H_{\mathrm{R}})t} . \tag{3.7}$$

Integrating equation (3.6) formally, yields

$$\tilde{\chi}(t) = \tilde{\chi}(0) - \frac{i}{\hbar}\int_0^t dt' \left[\tilde{H}_{\mathrm{SR}}(t'), \tilde{\chi}(t')\right] . \tag{3.8}$$

Substituting this solution into equation (3.6) gives the *integro-differential* form of the von Neumann equation,

$$\dot{\tilde{\chi}}(t) = -\frac{i}{\hbar}\left[\tilde{H}_{\mathrm{SR}}(t), \tilde{\chi}(0)\right] - \frac{1}{\hbar^2}\int_0^t dt' \left[\tilde{H}_{\mathrm{SR}}(t), \left[\tilde{H}_{\mathrm{SR}}(t'), \tilde{\chi}(t')\right]\right] . \tag{3.9}$$

We have simply recast equation (3.2) into a more convenient form, from which we can construct an equation of motion for the reduced density operator of system S by making appropriate approximations.

3.1.3 Born approximation

Tracing over the reservoir in equation (3.9) gives the master equation for the reduced density operator, $\tilde{\rho}(t)$,

$$\dot{\tilde{\rho}}(t) = -\frac{i}{\hbar}\mathrm{Tr}_\mathrm{R}\left\{\left[\tilde{H}_\mathrm{SR}(t), \tilde{\chi}(0)\right]\right\} - \frac{1}{\hbar^2}\int_0^t dt' \mathrm{Tr}_\mathrm{R}\left\{\left[\tilde{H}_\mathrm{SR}(t), \left[\tilde{H}_\mathrm{SR}(t'), \tilde{\chi}(t')\right]\right]\right\} . \tag{3.10}$$

In the next step, we assume that the system and the reservoir are uncorrelated at time $t = 0$, so that the density operator for the composite system, $\tilde{\chi}(0)$, factorizes as

$$\tilde{\chi}(0) = \chi(0) = R_0\rho(0) , \tag{3.11}$$

where R_0 is the initial density operator of the reservoir. We further assume that

$$\mathrm{Tr}_\mathrm{R}\left[\tilde{H}_\mathrm{SR}(t)R_0\right] = 0 , \tag{3.12}$$

which can always be arranged by including $\mathrm{Tr}_\mathrm{R}\left[\tilde{H}_\mathrm{SR}(t)R_0\right]$ in the system Hamiltonian.[2] With these assumptions we can simplify the master equation (3.10) and arrive at

$$\dot{\tilde{\rho}}(t) = -\frac{1}{\hbar^2}\int_0^t dt' \mathrm{Tr}_\mathrm{R}\left\{\left[\tilde{H}_\mathrm{SR}(t), \left[\tilde{H}_\mathrm{SR}(t'), \tilde{\chi}(t')\right]\right]\right\} . \tag{3.13}$$

For a weak interaction between the system and reservoir, i.e., when the system perturbs the reservoir only slightly, we can expand the density operator of the composite system in terms of the interaction H_SR,

$$\tilde{\chi}(t) = R_0\tilde{\rho} + \mathcal{O}(H_\mathrm{SR}) . \tag{3.14}$$

Then, to a good approximation we may neglect terms in the master equation of higher order than second order in H_SR, and the density operator, $\tilde{\chi}(t)$, effectively factorizes for all times. This approximation is referred to as the *Born approximation* because of its similarity to an approximation encountered in scattering theory. Thus, substituting equation (3.14) into (3.13) yields the master equation in the Born approximation,

$$\dot{\tilde{\rho}}(t) = -\frac{1}{\hbar^2}\int_0^t dt' \mathrm{Tr}_\mathrm{R}\left\{\left[\tilde{H}_\mathrm{SR}(t), \left[\tilde{H}_\mathrm{SR}(t'), R_0\tilde{\rho}(t')\right]\right]\right\} . \tag{3.15}$$

This is still a complicated equation, which, in particular, still contains memory effects, i.e., the future evolution of $\tilde{\rho}(t)$ depends on its past history through the integration over t'. We will simplify it further in the next section by neglecting the memory effects.

[2] For more details see [Car99, Chap. 1 and Chap. 2].

3.1.4 Markov approximation

Typically, the reservoir is a very large system with many degrees of freedom which is in thermal equilibrium. Thus, the reservoir is essentially unaffected by the system and the perturbations induced by the system on it quickly die away. That means that the correlation time of the reservoir is much shorter than the timescale for significant changes of the system. In this case, the evolution of the system is essentially independent of its past and we can neglect the history of the system. We impose this approximation by replacing $\tilde{\rho}(t')$ in equation (3.15) with $\tilde{\rho}(t)$. This is called the *Markov approximation*. The evolution of the reduced density operator, $\tilde{\rho}(t)$, is then governed by the master equation in the Born-Markov approximation,

$$\dot{\tilde{\rho}}(t) = -\frac{1}{\hbar^2}\int_0^t dt' \mathrm{Tr}_\mathrm{R}\left\{\left[\tilde{H}_\mathrm{SR}(t),\left[\tilde{H}_\mathrm{SR}(t'), R_0\tilde{\rho}(t)\right]\right]\right\} . \tag{3.16}$$

3.1.5 Master equation in Lindblad form

We will derive the so-called *Lindblad form* of the master equation, which is commonly used in quantum optics, by making the model more specific. Let us assume that each system operator, s_i, of system S is coupled to a statistically independent reservoir operator, r_i, of reservoir R. Thus, we explicitly write the interaction Hamiltonian as

$$H_\mathrm{SR} = \hbar\sum_i s_i r_i . \tag{3.17}$$

The interaction Hamiltonian in the interaction picture is then

$$\begin{aligned}\tilde{H}_\mathrm{SR} &= \hbar\sum_i e^{\frac{i}{\hbar}(H_\mathrm{S}+H_\mathrm{R})t} s_i r_i e^{-\frac{i}{\hbar}(H_\mathrm{S}+H_\mathrm{R})t} \\ &= \hbar\sum_i (e^{\frac{i}{\hbar}H_\mathrm{S}t} s_i e^{-\frac{i}{\hbar}H_\mathrm{S}t})(e^{\frac{i}{\hbar}H_\mathrm{R}t} r_i e^{-\frac{i}{\hbar}H_\mathrm{R}t}) \\ &= \hbar\sum_i \tilde{s}_i(t)\tilde{r}_i(t) .\end{aligned} \tag{3.18}$$

Substituting this result in the master equation (3.16) yields

$$\dot{\tilde{\rho}}(t) = -\sum_{i,j}\int_0^t dt' \mathrm{Tr}_\mathrm{R}\left\{[\tilde{s}_i(t)\tilde{r}_i(t), [\tilde{s}_j(t')\tilde{r}_j(t'), R_0\tilde{\rho}(t)]]\right\} . \tag{3.19}$$

Evaluating the commutators and using the cyclic property of the trace — $\mathrm{Tr}(\hat{A}\hat{B}\hat{C}) = \mathrm{Tr}(\hat{B}\hat{C}\hat{A}) = \mathrm{Tr}(\hat{C}\hat{A}\hat{B})$ — gives

$$\begin{aligned}\dot{\tilde{\rho}}(t) = -\sum_{i,j}\int_0^t dt' \{ &\left(\tilde{s}_i(t)\tilde{s}_j(t')\tilde{\rho}(t) - \tilde{s}_j(t')\tilde{\rho}(t)\tilde{s}_i(t)\right)\mathrm{Tr}_\mathrm{R}\left[\tilde{r}_i(t)\tilde{r}_j(t')R_0\right] \\ &+ \left(\tilde{\rho}(t)\tilde{s}_j(t')\tilde{s}_i(t) - \tilde{s}_i(t)\tilde{\rho}(t)\tilde{s}_j(t')\right)\mathrm{Tr}_\mathrm{R}\left[\tilde{r}_j(t')\tilde{r}_i(t)R_0\right]\} .\end{aligned} \tag{3.20}$$

For notational simplifications later on, we formally replace several of the $\tilde{H}_{\mathrm{SR}}$ terms by their adjoints. This is possible, since the sum in equation (3.20) extends over all possible operators and the interaction Hamiltonian is Hermitian, i.e., for each operator in $\tilde{H}_{\mathrm{SR}}$ its adjoint is present as well. Thus we can write

$$\begin{aligned}\dot{\tilde{\rho}}(t) = -\sum_{i,j}\int_0^t dt' \Big\{ &\left(\tilde{s}_i^\dagger(t)\tilde{s}_j(t')\tilde{\rho}(t) - \tilde{s}_j(t')\tilde{\rho}(t)\tilde{s}_i^\dagger(t)\right)\langle\tilde{r}_i^\dagger(t)\tilde{r}_j(t')\rangle_{\mathrm{R}} \\ &+ \left(\tilde{\rho}(t)\tilde{s}_j^\dagger(t')\tilde{s}_i(t) - \tilde{s}_i(t)\tilde{\rho}(t)\tilde{s}_j^\dagger(t')\right)\langle\tilde{r}_j^\dagger(t')\tilde{r}_i(t)\rangle_{\mathrm{R}}\Big\}, \end{aligned} \tag{3.21}$$

where we have used the relations

$$\langle\tilde{r}_i^\dagger(t)\tilde{r}_j(t')\rangle_{\mathrm{R}} = \mathrm{Tr}_{\mathrm{R}}\left[\tilde{r}_i^\dagger(t)\tilde{r}_j(t')R_0\right], \tag{3.22}$$

$$\langle\tilde{r}_j^\dagger(t')\tilde{r}_i(t)\rangle_{\mathrm{R}} = \mathrm{Tr}_{\mathrm{R}}\left[\tilde{r}_j^\dagger(t')\tilde{r}_i(t)R_0\right], \tag{3.23}$$

to replace the traces by expectation values.

In the next step we assume that the system Hamiltonian, H_{S}, is constructed in terms of s_i in such a way that these operators are transformed as follows,

$$\tilde{s}_i(t) = e^{\frac{i}{\hbar}H_{\mathrm{S}}t}s_i e^{-\frac{i}{\hbar}H_{\mathrm{S}}t} = s_i e^{-i\omega_i t}. \tag{3.24}$$

Substituting this expression for $\tilde{s}_i$ into equation (3.21) and making a change of variable,

$$\tau = t - t', \tag{3.25}$$

we find

$$\begin{aligned}\dot{\tilde{\rho}}(t) = -\sum_{i,j}\int_0^t d\tau \Big\{ &\left(s_i^\dagger s_j\tilde{\rho}(t) - s_j\tilde{\rho}(t)s_i^\dagger\right)\langle\tilde{r}_i^\dagger(t)\tilde{r}_j(t-\tau)\rangle_{\mathrm{R}}e^{i(\omega_i-\omega_j)t}e^{i\omega_j\tau} \\ &+ \left(\tilde{\rho}(t)s_j^\dagger s_i - s_i\tilde{\rho}(t)s_j^\dagger\right)\langle\tilde{r}_j^\dagger(t-\tau)\tilde{r}_i(t)\rangle_{\mathrm{R}}e^{-i(\omega_i-\omega_j)t}e^{-i\omega_j\tau}\Big\}. \end{aligned} \tag{3.26}$$

For statistically independent reservoir operators the correlation functions, $\langle\tilde{r}_i^\dagger(t)\tilde{r}_j(t-\tau)\rangle_{\mathrm{R}}$ and $\langle\tilde{r}_j^\dagger(t-\tau)\tilde{r}_i(t)\rangle_{\mathrm{R}}$, are zero unless i is equal to j, since they factorize for $i \neq j$ and the mean of the reservoir operators, $\langle\tilde{r}_i(t)\rangle$, is assumed to be zero. Therefore, all the cross terms in the master equation (3.26) vanish and we obtain

$$\begin{aligned}\dot{\tilde{\rho}}(t) = -\sum_{i}\Big[&\left(s_i^\dagger s_i\tilde{\rho}(t) - s_i\tilde{\rho}(t)s_i^\dagger\right)\int_0^t d\tau\langle\tilde{r}_i^\dagger(t)\tilde{r}_i(t-\tau)\rangle_{\mathrm{R}}e^{i\omega_i\tau} \\ &+ \left(\tilde{\rho}(t)s_i^\dagger s_i - s_i\tilde{\rho}(t)s_i^\dagger\right)\int_0^t d\tau\langle\tilde{r}_i^\dagger(t-\tau)\tilde{r}_i(t)\rangle_{\mathrm{R}}e^{-i\omega_i\tau}\Big]. \end{aligned} \tag{3.27}$$

Defining

$$\gamma_i = 2\,\mathrm{Re}\left\{\int_0^t d\tau \langle \tilde{r}_i^\dagger(t)\tilde{r}_i(t-\tau)\rangle_\mathrm{R} e^{i\omega_i\tau}\right\},$$
$$\Delta_i = 2\,\mathrm{Im}\left\{\int_0^t d\tau \langle \tilde{r}_i^\dagger(t)\tilde{r}_i(t-\tau)\rangle_\mathrm{R} e^{i\omega_i\tau}\right\}, \tag{3.28}$$

we arrive at

$$\dot{\tilde{\rho}}(t) = \sum_i \left\{-i\frac{\Delta_i}{2}\left[s_i^\dagger s_i, \tilde{\rho}(t)\right] + \frac{\gamma_i}{2}\left(2s_i\tilde{\rho}(t)s_i^\dagger - s_i^\dagger s_i\tilde{\rho}(t) - \tilde{\rho}(t)s_i^\dagger s_i\right)\right\}. \tag{3.29}$$

Transforming this equation back to the Schrödinger picture finally yields the master equation in Lindblad form,

$$\dot{\rho}(t) = -\frac{i}{\hbar}\left[H_\mathrm{S}', \rho(t)\right] + \sum_i \frac{\gamma_i}{2}\left(2s_i\rho(t)s_i^\dagger - s_i^\dagger s_i\rho(t) - \rho(t)s_i^\dagger s_i\right), \tag{3.30}$$

with the effective system Hamiltonian,

$$H_\mathrm{S}' = H_\mathrm{S} + \sum_i \frac{\hbar\Delta_i}{2} s_i^\dagger s_i\,. \tag{3.31}$$

Note, in the derivation of this master equation, it was assumed that the system operators, s_i, couple to statistically independent reservoirs, which is a reasonable assumption in most cases in quantum optics. The first term on the RHS of equation (3.30) describes the unitary evolution of the density operator, and includes an energy shift of the system. This energy shift, by the term $\sum_i \frac{\hbar\Delta_i}{2} s_i^\dagger s_i$, is usually small (in regards to quantum optical systems) and is generally absorbed into the definition of the system's resonance frequency (i.e., the frequency of an atom or a cavity mode). The second term on the RHS describes the damping of the system, with damping constant γ_i.

The master equation in Lindblad form is sometimes expressed in terms of *jump operators* (or *collapse operators*), $\hat{C}_i = \sqrt{\gamma_i}s_i$, as shown

$$\dot{\rho}(t) = -\frac{i}{\hbar}\left[H_\mathrm{S}, \rho(t)\right] + \sum_i \left(\hat{C}_i\rho(t)\hat{C}_i^\dagger - \frac{1}{2}\hat{C}_i^\dagger\hat{C}_i\rho(t) - \frac{1}{2}\rho(t)\hat{C}_i^\dagger\hat{C}_i\right). \tag{3.32}$$

Another widely used form of the master equation is

$$\dot{\rho}(t) = -\frac{i}{\hbar}\left[H_\mathrm{S}, \rho(t)\right] + \mathcal{L}\rho(t)\,, \tag{3.33}$$

where $\mathcal{L}$ is the *Liouvillian superoperator*, which acts on other operators rather than on state vectors. It is given by

$$\mathcal{L}\cdot = \sum_i \frac{\gamma_i}{2}\left(2s_i\cdot s_i^\dagger - s_i^\dagger s_i\cdot - \cdot s_i^\dagger s_i\right). \tag{3.34}$$

Sometimes, the commutator in the master equation (3.33) is incorporated into the definition of the Liouvillian, so that the master equation is written in a more succinct form, namely,

$$\dot{\rho}(t) = \mathcal{L}\rho(t)\,. \tag{3.35}$$

3.2 Quantum regression formula

Solving the master equation gives us an explicit expression for the time dependence of the reduced density operator $\rho(t)$. This density operator in turn allows us to compute the time dependence of the expectation value of any operator defined on the system Hilbert space, $\mathcal{H}_{\mathrm{S}}$, by using equation (3.4). In this section we will show how the mean of a product of two operators evaluated at different times – the so-called *two-time correlation functions* – of the form

$$\langle \hat{O}_1(t)\hat{O}_2(t')\rangle\,, \tag{3.36}$$

can be computed.

3.2.1 Formal results

In the Heisenberg picture, two-time correlation functions are straightforward to evaluate by

$$\langle \hat{O}_1(t)\hat{O}_2(t')\rangle = \mathrm{Tr}_{\mathrm{S}\otimes\mathrm{R}}\left[\chi^{(H)}(0)\hat{O}_1^{(H)}(t)\hat{O}_2^{(H)}(t')\right]\,, \tag{3.37}$$

where the superscript (H) denotes that the operator is in the Heisenberg picture; whereas, in the Schrödinger picture – where operators are generally time independent – such an expression cannot be evaluated. In the following we will suppress the superscript for the sake of a more readable text. Operators which are explicitly time dependent, like $\hat{O}(t)$, are in the Heisenberg picture and operators without an explicit time dependence, like $\hat{O}$, are in the Schrödinger picture – vice versa for the density operator χ and $\chi(t)$. In order to use the master equation in the Schrödinger picture, derived in the previous section, we have to transform equation (3.37) into the Schrödinger picture. This shall be done here.

We can move from the Schrödinger picture to the Heisenberg picture by a unitary transformation of form

$$\hat{O}(t) = e^{\frac{i}{\hbar}Ht}\hat{O}e^{-\frac{i}{\hbar}Ht}\,, \tag{3.38}$$

where H is the Hamiltonian of the system. Using this transformation and the cyclic property of the trace, we can write equation (3.37) as

$$\begin{aligned}\langle \hat{O}_1(t)\hat{O}_2(t')\rangle &= \mathrm{Tr}_{\mathrm{S}\otimes\mathrm{R}}\left[e^{\frac{i}{\hbar}Ht}\chi(t)\hat{O}_1e^{\frac{i}{\hbar}H(t'-t)}\hat{O}_2e^{-\frac{i}{\hbar}Ht'}\right]\\ &= \mathrm{Tr}_{\mathrm{S}\otimes\mathrm{R}}\left[\hat{O}_2e^{-\frac{i}{\hbar}H(t'-t)}\chi(t)\hat{O}_1e^{\frac{i}{\hbar}H(t'-t)}\right]\\ &= \mathrm{Tr}_{\mathrm{S}}\left\{\hat{O}_2\mathrm{Tr}_{\mathrm{R}}\left[e^{-\frac{i}{\hbar}H(t'-t)}\chi(t)\hat{O}_1e^{\frac{i}{\hbar}H(t'-t)}\right]\right\}\,,\end{aligned} \tag{3.39}$$

which is now a Schrödinger picture expression.

We define

$$\chi_{\hat{O}_1}(\tau) := e^{-\frac{i}{\hbar}H\tau}\chi(t)\hat{O}_1e^{\frac{i}{\hbar}H\tau}\,,\quad \text{with}\quad \tau = t'-t\,, \tag{3.40}$$

which satisfies the equation of motion

$$\frac{d}{d\tau}\chi_{\hat{O}_1}(\tau) = -\frac{i}{\hbar}\left[H, \chi_{\hat{O}_1}(\tau)\right] . \tag{3.41}$$

Furthermore, the reduced operator of $\chi_{\hat{O}_1}(\tau)$ is given by

$$\rho_{\hat{O}_1}(\tau) := \mathrm{Tr}_\mathrm{R}\left[\chi_{\hat{O}_1}(\tau)\right] , \tag{3.42}$$

which for $\tau = 0$ is

$$\rho_{\hat{O}_1}(0) = \mathrm{Tr}_\mathrm{R}\left[\chi_{\hat{O}_1}(0)\right] = \mathrm{Tr}_\mathrm{R}\left[\chi(t)\hat{O}_1\right] = \mathrm{Tr}_\mathrm{R}\left[\chi(t)\right]\hat{O}_1 = \rho(t)\hat{O}_1 . \tag{3.43}$$

If we then assume that the density operator of the composite system factorizes, with $\chi(t) = \rho(t)R_0$, as discussed in Section 3.1.3 (Born approximation), we find

$$\chi_{\hat{O}_1}(0) = \chi(t)\hat{O}_1 = R_0(\rho(t)\hat{O}_1) = R_0\rho_{\hat{O}_1}(0) . \tag{3.44}$$

Equations (3.41), (3.42) and (3.44) are equivalent to the von Neumann equation for $\chi(t)$, equation (3.2), the definition of the reduced density operator $\rho(t)$ in equation (3.3) and the Born approximation given by equation (3.14). Noting that equations (3.41) and (3.2) share the same Hamiltonian, we can derive an equation of motion for the operator $\rho_{\hat{O}_1}(\tau)$ in an analogous way to the derivation of the master equation in the previous section. This eventually yields

$$\frac{d}{d\tau}\rho_{\hat{O}_1}(\tau) = \mathcal{L}\rho_{\hat{O}_1}(\tau) , \tag{3.45}$$

where the notation of equation (3.35) is used. The formal solution is

$$\rho_{\hat{O}_1}(\tau) = e^{\mathcal{L}\tau}(\rho_{\hat{O}_1}(0)) = e^{\mathcal{L}\tau}(\rho(t)\hat{O}_1) . \tag{3.46}$$

Substituting this result into equation (3.39) gives the *quantum regression formula*

$$\langle\hat{O}_1(t)\hat{O}_2(t+\tau)\rangle = \mathrm{Tr}\left[\hat{O}_2 e^{\mathcal{L}\tau}(\rho(t)\hat{O}_1)\right] , \tag{3.47}$$

where $\tau > 0$. Following the same procedure it can be shown that

$$\langle\hat{O}_1(t+\tau)\hat{O}_2(t)\rangle = \mathrm{Tr}\left[\hat{O}_1 e^{\mathcal{L}\tau}(\hat{O}_2\rho(t))\right] , \tag{3.48}$$

with $\tau > 0$.

3.2.2 Results for a complete set of operators

The rather formal expressions (3.47) and (3.48) can be reduced to a form which is often more convenient for doing calculations.

For a complete set of system operators $\hat{A}_\mu$, $\mu = 1, 2, \ldots$, which obey the relation

$$\mathrm{Tr}_\mathrm{S}\left[\hat{A}_\mu(\mathcal{L}\hat{O})\right] = \sum_\lambda M_{\mu,\lambda}\mathrm{Tr}_\mathrm{S}\left[\hat{A}_\lambda\hat{O}\right] , \tag{3.49}$$

where $\hat{O}$ is an arbitrary operator and the $M_{\mu,\lambda}$ are constants, we find (for $\tau > 0$)

$$\begin{aligned}\frac{d}{d\tau}\langle\hat{O}(t)\hat{A}_\mu(t+\tau)\rangle &= \frac{d}{d\tau}\mathrm{Tr_S}\left[\hat{A}_\mu e^{\mathcal{L}\tau}(\rho(t)\hat{O})\right] \\ &= \mathrm{Tr_S}\left[\hat{A}_\mu\left\{\mathcal{L}e^{\mathcal{L}\tau}(\rho(t)\hat{O})\right\}\right] \\ &= \sum_\lambda M_{\mu,\lambda}\mathrm{Tr_S}\left[\hat{A}_\lambda e^{\mathcal{L}\tau}(\rho(t)\hat{O})\right] \\ &= \sum_\lambda M_{\mu,\lambda}\langle\hat{O}(t)\hat{A}_\lambda(t+\tau)\rangle\,, \end{aligned} \tag{3.50}$$

where equation (3.47) was used. The operator $\hat{O}$ can be any system operator, not necessarily one of the $\hat{A}_\mu$. In an analogous manner, we find

$$\frac{d}{d\tau}\langle\hat{A}_\mu(t+\tau)\hat{O}(t)\rangle = \sum_\lambda M_{\mu,\lambda}\langle\hat{A}_\lambda(t+\tau)\hat{O}(t)\rangle\,, \tag{3.51}$$

where $\tau > 0$.

Note, from equation (3.49), it follows, in particular, that

$$\frac{d}{dt}\langle\hat{A}_\mu\rangle = \mathrm{Tr_S}\left[\hat{A}_\mu\dot{\rho}\right] = \mathrm{Tr_S}\left[\hat{A}_\mu(\mathcal{L}\rho)\right] = \sum_\lambda M_{\mu,\lambda}\mathrm{Tr_S}\left[A_\lambda\rho\right] = \sum_\lambda M_{\mu,\lambda}\langle A_\lambda\rangle\,, \tag{3.52}$$

which is conveniently used to determine the constants $M_{\mu,\lambda}$.

3.3 Master equation for a single-microtoroid cavity QED system

In Chapter 5 and Chapter 6 we will investigate a system consisting of microtoroidal resonators to which atoms are coupled. These microresonators were described in Section 2.5.1, and can be modelled by an extended Jaynes-Cummings model. In this model, the atom-cavity system is assumed to be closed, with no leakage of light out of the cavity taken into account. This is unrealistic; moreover, the quantity which is usually measured is the light exiting the cavity. In this chapter, we developed the mathematical tools to describe the damping of a system using the master equation. We will apply this technique to derive the master equation for a single-microtoroid system with and without an external driving source.

3.3.1 Non-driven system

In order to use equation (3.32), we require the jump operators, $\hat{C}_i$, of our system, corresponding to the different loss channels. The atom-toroid system is described by the extended Jaynes-Cummings model of Section 2.5. Within the microtoroid are two counter-propagating WGMs, a and b, which interact with one another at

strength h, and are coupled to an atom, described by the atom-cavity coupling rate, g. The atom is considered to be a two-level atom, described by the raising and lowering operators $\sigma^{\pm}$ and the transition frequency ω_{A}. The Hamiltonian for the system is

$$\begin{aligned} H_{\mathrm{S}} &= \hbar\omega_{\mathrm{C}}(a^{\dagger}a + b^{\dagger}b) + \hbar(ha^{\dagger}b + h^{*}b^{\dagger}a) \\ &\quad + \hbar\omega_{\mathrm{A}}\sigma^{+}\sigma^{-} + \hbar(g^{*}a^{\dagger}\sigma^{-} + g\sigma^{+}a) + \hbar(gb^{\dagger}\sigma^{-} + g^{*}\sigma^{+}b)\,, \end{aligned} \tag{3.53}$$

where ω_{C} is the frequency of the two microtoroid modes.

In this system, light can be lost by essentially three methods. First, the light of modes a and b can be lost to the fibre the toroid is coupled to, at the rate κ_{ex} (see Section 2.5.1). Second, the light of modes a and b can be lost out of the toroid and not be coupled back into the fibre, e.g., by imperfections in the toroid. This intrinsic loss is described by the cavity decay rate κ_{i}. Third, the atom can spontaneously emit photons in a direction other than that of the cavity modes, a process described by the atomic decay rate γ.[3]

Each of these loss channels corresponds to an independent reservoir that different system operators interact with. Hence, we find for the jump operators,

$$\hat{C}_a^{(\mathrm{ex})} = \sqrt{2\kappa_{\mathrm{ex}}}a\,, \qquad \hat{C}_b^{(\mathrm{ex})} = \sqrt{2\kappa_{\mathrm{ex}}}b\,, \tag{3.54}$$

$$\hat{C}_a^{(\mathrm{i})} = \sqrt{2\kappa_{\mathrm{i}}}a\,, \qquad \hat{C}_b^{(\mathrm{i})} = \sqrt{2\kappa_{\mathrm{i}}}b\,, \tag{3.55}$$

$$\hat{C}_{\gamma} = \sqrt{\gamma}\sigma^{-} \tag{3.56}$$

The factor of two for the cavity decay rates, κ_{ex} and κ_{i}, come from the fact that they are defined to correspond to the parameter γ_i in equation (3.30), i.e., they correspond to half-widths not full-widths.

We define the total cavity decay rate as

$$\kappa := \kappa_{\mathrm{ex}} + \kappa_{\mathrm{i}}\,, \tag{3.57}$$

and find for the master equation for a single two-mode toroid without driving

$$\begin{aligned} \dot{\rho} = &-\frac{i}{\hbar}[H_{\mathrm{S}}, \rho] + \kappa(2a\rho a^{\dagger} - a^{\dagger}a\rho - \rho a^{\dagger}a) + \kappa(2b\rho b^{\dagger} - b^{\dagger}b\rho - \rho b^{\dagger}b) \\ &+ \frac{\gamma}{2}(2\sigma^{-}\rho\sigma^{+} - \sigma^{+}\sigma^{-}\rho - \rho\sigma^{+}\sigma^{-})\ . \end{aligned} \tag{3.58}$$

3.3.2 Driven system

Having described the microtoroidal system without driving, we consider now a coherent light source (laser) which drives the system. In the general case, we allow for driving of both cavity modes, a and b, by two separate external light sources of the

[3] The decay rate is in reality determined by several factors, such as the atom decaying to other levels which represents a breakdown of the two-level atom approximation we are using, and will thus not be considered.

same frequency $\omega_{\rm p}$. As already described in Section 2.5.2, the coherent input field can be treated classically and the Hamiltonian for the interaction between the cavity modes and the classical input field is typically written as

$$H_{\rm driv} = \hbar\left(\mathcal{E}_a^* e^{i\omega_{\rm p}t}a + \mathcal{E}_a e^{-i\omega_{\rm p}t}a^\dagger\right) + \hbar\left(\mathcal{E}_b^* e^{i\omega_{\rm p}t}b + \mathcal{E}_b e^{-i\omega_{\rm p}t}b^\dagger\right) , \tag{3.59}$$

where $\mathcal{E}_a$ and $\mathcal{E}_b$ are complex field amplitudes.

When deriving the master equation the assumption was used that reservoir modes have a zero mean amplitude. The reservoir mode which is in a coherent state, and drives the system, certainly has no zero mean amplitude, but since it is included in the system Hamiltonian rather than in the reservoir, the remaining reservoir modes have zero mean amplitude. Therefore the master equation for the driven cascaded system can be derived in the same way as the non-driven cascaded master equation was. The only difference is that the system Hamiltonian, $H_{\rm S}$, of the non-driven system described in equation (3.53) is replaced by the system Hamiltonian for the driven system, which reads

$$H_{\rm S}^{\rm driv} = H_{\rm S} + \hbar\left(\mathcal{E}^* e^{i\omega_{\rm p}t}a + \mathcal{E} e^{-i\omega_{\rm p}t}a^\dagger\right) + \hbar\left(\mathcal{E}_b^* e^{i\omega_{\rm p}t}b + \mathcal{E}_b e^{-i\omega_{\rm p}t}b^\dagger\right) . \tag{3.60}$$

The master equation for the driven single-toroid system is now given by

$$\begin{aligned}\dot{\rho} = &-\frac{i}{\hbar}[H_{\rm S}^{\rm driv},\rho] + \kappa(2a\rho a^\dagger - a^\dagger a\rho - \rho a^\dagger a) + \kappa(2b\rho b^\dagger - b^\dagger b\rho - \rho b^\dagger b) \\ &+ \frac{\gamma}{2}(2\sigma^-\rho\sigma^+ - \sigma^+\sigma^-\rho - \rho\sigma^+\sigma^-) \ .\end{aligned} \tag{3.61}$$

Chapter 4

Advanced Topics in Cavity QED

After having developed the essential theoretical method to describe damped quantum systems in the previous chapter, we can now turn to more advanced topics in cavity QED. The master equation treatment describes the internal field of a damped cavity. It is based on treating the external field which the cavity is coupled to as a heat bath. In the first section of this chapter we will explicitly treat the heat bath as an external cavity field, in order to obtain an expression relating the intracavity field to the cavity output field, the field which is normally accessible in experiments. A further extension of this is to allow the output field of the cavity to couple into another cavity. These so-called *cascaded systems* are described in the second section.

4.1 Input-output theory

A general *input-output theory* for quantum dissipative systems was developed by Collett and Gardiner [CG84]. A good treatment can be found in the book of Walls and Milburn [WM94], which we will closely follow.

In the following we will, for simplicity, consider a single cavity mode coupled to a one-dimensional external (reservoir) field. The extension to a two-mode cavity is obvious and is left for the reader. The total Hamiltonian is

$$H = H_{\mathrm{S}} + H_{\mathrm{R}} + H_{\mathrm{SR}}\,, \tag{4.1}$$

where H_{S} is the free Hamiltonian for the intracavity field mode, H_{R} is the free Hamiltonian for the external (reservoir) field modes, and the interaction Hamiltonian is written as

$$H_{\mathrm{SR}} = i\hbar \int_{-\infty}^{\infty} d\omega \kappa(\omega) \left[a^{\dagger} r(\omega) - r^{\dagger}(\omega) a \right] , \tag{4.2}$$

where $\kappa(\omega)$ is a coupling constant, and a and $r(\omega)$ are annihilation operators for the intracavity and the external field, respectively, which satisfy the commutation

relations

$$\left[a, a^\dagger\right] = 1\,, \tag{4.3}$$

$$\left[r(\omega), r^\dagger(\omega')\right] = \delta(\omega - \omega')\,. \tag{4.4}$$

Note that actual physical frequencies are positive, and therefore the limits of the integral in equation (4.2) are strictly $(0, \infty)$. However, for optical systems it is usually convenient to move to a rotating frame, a frame rotating with some characteristic high frequency Ω of the system (e.g., the cavity resonance frequency). In this case the integration limits become $(-\Omega, \infty)$. For a large optical frequency, Ω, the lower limit can, to a good approximation, be extended to $-\infty$ (hence the integration limits in equation (4.2)).

The Heisenberg equation of motion for $r(\omega)$ is

$$\dot{r}(\omega) = -i\omega r(\omega) + \kappa(\omega) a\,. \tag{4.5}$$

This can be formally integrated. To obtain the input field, we have to solve it in terms of initial conditions at time $t_0 < t$, and to obtain the output field, in terms of the final conditions at time $t_1 > t$. The formal solution for $t_0 < t$ is

$$r(\omega) = e^{-i\omega(t-t_0)} r(\omega, t_0) + \kappa(\omega) \int_{t_0}^{t} dt' e^{-i\omega(t-t')} a(t')\,, \tag{4.6}$$

and for $t < t_1$

$$r(\omega) = e^{-i\omega(t-t_1)} r(\omega, t_1) - \kappa(\omega) \int_{t}^{t_1} dt' e^{-i\omega(t-t')} a(t')\,. \tag{4.7}$$

The Heisenberg equation of motion for the system operator is

$$\dot{a}(t) = -\frac{i}{\hbar}\left[a(t), H_{\mathrm{S}}\right] - \int_{-\infty}^{\infty} d\omega \kappa(\omega) r(\omega)\,. \tag{4.8}$$

Substituting the formal solution (4.6) for the reservoir operator, $r(\omega)$, into the equation of motion for the system operator yields

$$\begin{aligned}\dot{a}(t) = -\frac{i}{\hbar}\left[a(t), H_{\mathrm{S}}\right] &- \int_{-\infty}^{\infty} d\omega \kappa(\omega) e^{-i\omega(t-t_0)} r(\omega, t_0) \\ &- \int_{-\infty}^{\infty} d\omega \kappa(\omega)^2 \int_{t_0}^{t} dt' e^{-i\omega(t-t')} a(t')\,.\end{aligned} \tag{4.9}$$

We now assume that $\kappa(\omega)$ is independent of frequency over a band of frequencies about the cavity mode frequency (which is the case in quantum optics), and thus can set

$$\kappa(\omega)^2 = \kappa/\pi\,. \tag{4.10}$$

Then using the relation

$$\int_{-\infty}^{\infty} d\omega e^{-i\omega(t-t')} = 2\pi\delta(t-t')\,, \tag{4.11}$$

and defining the input field operator by

$$a_{\rm in}(t) := \frac{-1}{\sqrt{2\pi}} \int_{-\infty}^{\infty} d\omega e^{-i\omega(t-t_0)} r(\omega, t_0)\,, \tag{4.12}$$

which satisfies the commutation relation,

$$\left[a_{\rm in}(t), a_{\rm in}^{\dagger}(t')\right] = \delta(t-t')\,, \tag{4.13}$$

we can derive a quantum Langevin equation for the damped intracavity field operator as

$$\dot{a}(t) = -\frac{i}{\hbar}\left[a(t), H_{\rm S}\right] - \kappa a(t) + \sqrt{2\kappa}a_{\rm in}(t)\,. \tag{4.14}$$

In this Langevin equation the (quantum) noise term appears explicitly as the input field.

By substituting the formal solution (4.7) for the reservoir operator into equation (4.8), the time reversed Langevin equation for the intracavity field operator is obtained. It reads

$$\dot{a}(t) = -\frac{i}{\hbar}\left[a(t), H_{\rm S}\right] + \kappa a(t) - \sqrt{2\kappa}a_{\rm out}(t)\,, \tag{4.15}$$

where the output field is defined by

$$a_{\rm out}(t) := \frac{1}{\sqrt{2\pi}} \int_{-\infty}^{\infty} d\omega e^{-i\omega(t-t_1)} r(\omega, t_1)\,, \tag{4.16}$$

which has the opposite sign to the input field.

From the two Langevin equations, (4.14) and (4.15), the intracavity field can be related to the external (reservoir) fields. Equating the two expressions for $\dot{a}(t)$ gives

$$a_{\rm out}(t) + a_{\rm in}(t) = \sqrt{2\kappa}a(t)\,. \tag{4.17}$$

This is a boundary condition relating each of the far-field amplitudes outside the cavity to the internal cavity field. Note that interference terms, e.g., $\langle a(t)a_{\rm in}(t')\rangle$ and $\langle a^{\dagger}(t)a_{\rm in}(t')\rangle$, may contribute to the observed output field moments.

4.2 Cascaded systems

A cascaded system consists of (at least) two subsystems which are connected by a one-way (non-Hamiltonian) coupling. In the following we will restrict ourselves to a system consisting of two subsystems as can be seen in Figure 4.1. The first cavity,

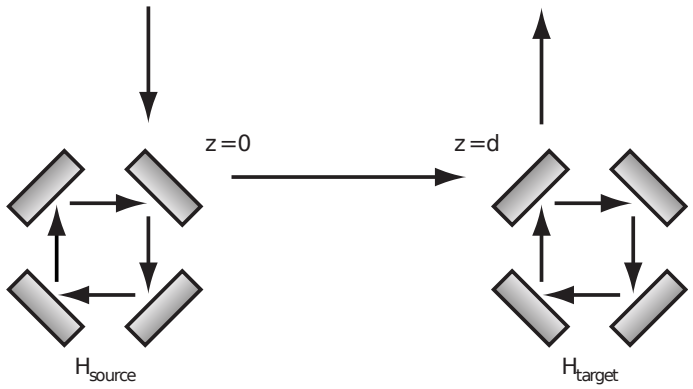

FIGURE 4.1: Schematic of a typical cascaded system. Light is coupled into the source cavity on the left, the output of which couples into the target cavity on the right. The output of the target system is finally measured.

at position $z = 0$, is called the source, which is driven by some input, and whose output couples to the second cavity at position $z = d$, called the target. This is a unidirectional coupling between source and target, where the output of the source is carried to the target by the reservoir. The main interest lies in the output of the target subsystem. In the simplest case the input to the source subsystem is just the thermal reservoir.

4.2.1 The cascaded systems master equation

Three different derivations of the cascaded systems master equation have been given [KS87, Gar93, Car93]. Here we closely follow the approach of Carmichael [Car93].

The Hamiltonian for the cascaded system can be divided up into the system Hamiltonian, H_{S}, the reservoir Hamiltonian, H_{R}, and the Hamiltonian of the interaction between the system and the reservoir, H_{SR}. Thus, it can be written as

$$H = H_{\mathrm{S}} + H_{\mathrm{R}} + H_{\mathrm{SR}} \,. \tag{4.18}$$

The system Hamiltonian consists of the source and target Hamiltonian (which describe the free cavity modes and any possible interactions inside the cavities) and is written as

$$H_{\mathrm{S}} = H_{\mathrm{source}} + H_{\mathrm{target}} \,. \tag{4.19}$$

The interaction Hamiltonian can be split up into

$$H_{\mathrm{SR}} = H_{SR}^{\mathrm{source}} + H_{SR}^{\mathrm{target}} \,, \tag{4.20}$$

where H_{SR}^{source} describes the interaction of the source with the reservoir and H_{SR}^{target} the interaction of the target with the reservoir. The interaction Hamiltonians are

given by

$$H_{SR}^{\text{source}} = \hbar\sqrt{2\kappa^{(1)}}\left(a_1\hat{\mathcal{E}}^\dagger(0) + a_1^\dagger\hat{\mathcal{E}}(0)\right), \tag{4.21}$$

$$H_{SR}^{\text{target}} = \hbar\sqrt{2\kappa^{(2)}}\left(a_2\hat{\mathcal{E}}^\dagger(d) + a_2^\dagger\hat{\mathcal{E}}(d)\right), \tag{4.22}$$

and the reservoir Hamiltonian is given by

$$H_{\text{R}} = \sum_j \hbar\omega_j r_j^\dagger r_j\,, \tag{4.23}$$

where a_1 and a_2 are the photon annihilation operators for the source and target modes, respectively, $\hat{\mathcal{E}}$ is the field operator of the reservoir, which contains the reservoir mode annihilation operators r_j. $\kappa^{(1)}$ and $\kappa^{(2)}$ are the cavity damping rates of the source and target, respectively.

The reservoirs that the two systems interact with can not be treated as independent, since the output from the source is carried by the reservoir to the target. In other words, although the source and target subsystem couple to different reservoir field operators, $\hat{\mathcal{E}}(0)$ and $\hat{\mathcal{E}}(d)$, there is a correlation between them so that the reservoirs are not independent. Therefore the standard method of deriving the master equation which was used for the harmonic oscillator (see Section 3.1) cannot be applied without some further work. However, the correlation between the reservoir fields at source and target enables us to relate $\hat{\mathcal{E}}(d)$ to $\hat{\mathcal{E}}(0)$, so that the source and output formally couple to the reservoir at the same spatial position. This can be done by introducing a unitary transformation U with

$$U(\tau) = \exp\left[-\frac{i}{\hbar}(H_{\text{source}} + H_{\text{R}} + H_{\text{SR}}^{\text{source}})\tau\right], \tag{4.24}$$

where τ is the time the light needs to travel from the source to the target. This unitary operator transforms the system in such a way that it performs a time retardation to the source subsystem and its interaction with the reservoir. In particular, it relates the reservoir field operator $\hat{\mathcal{E}}(d)$ to $\hat{\mathcal{E}}(0)$ by

$$\hat{\mathcal{E}}(d,\tau) = U^\dagger(\tau)\hat{\mathcal{E}}(d,0)U(\tau) = e^{i\phi_a}\left[\hat{\mathcal{E}}(0) - i\frac{1}{2}\sqrt{2\kappa^{(1)}}a_1\right]. \tag{4.25}$$

The field at the target at time $t = \tau$ is the time retarded input field at the source (with an additional phase factor $e^{i\phi_a}$ due to reflection at the mirror) which freely propagates between the source and target, plus a field which was radiated by the source at time $t = 0$.[1]

The Liouville equation for the density operator χ has also to be transformed by U so that it yields

$$\dot{\chi}_{\text{ret}} = -\frac{i}{\hbar}[H_{\text{ret}}, \chi_{\text{ret}}]\,, \tag{4.26}$$

[1] For a more detailed derivation of this relation between $\hat{\mathcal{E}}(d,\tau)$ and $\hat{\mathcal{E}}(0)$ see [Car08, p. 489].

with the time-retarded density operator

$$\chi_{\mathrm{ret}} = U^{\dagger}(\tau)\chi U(\tau)\,, \tag{4.27}$$

and the time-retarded Hamiltonian H_{ret} which differs only in the interaction term

$$(H_{\mathrm{SR}}^{\mathrm{target}})_{\mathrm{ret}} = \hbar\sqrt{2\kappa^{(2)}}\left(a_2\hat{\mathcal{E}}^{\dagger}(d,\tau) + a_2^{\dagger}\hat{\mathcal{E}}(d,\tau)\right)\,. \tag{4.28}$$

Substituting (4.25) into (4.28) yields, for the time-retarded Hamiltonian,

$$H_{\mathrm{ret}} = H_{\mathrm{sys}} + H_{\mathrm{R}} + H_{\mathrm{SR}}^{\mathrm{ret}}\,, \tag{4.29}$$

where the Hamiltonian H_{sys} describes the combined system of source and target

$$H_{\mathrm{sys}} = H_{\mathrm{source}} + H_{\mathrm{target}} + i\hbar\sqrt{\kappa^{(1)}\kappa^{(2)}}(e^{-i\phi_a}a_2a_1^{\dagger} - e^{i\phi_a}a_1a_2^{\dagger})\,, \tag{4.30}$$

and the Hamiltonian $H_{\mathrm{SR}}^{\mathrm{ret}}$ describes the interaction between the system and the reservoir

$$H_{\mathrm{SR}}^{\mathrm{ret}} = \hbar\left[\left(\sqrt{2\kappa^{(1)}}a_1 + e^{-i\phi_a}\sqrt{2\kappa^{(2)}}a_2\right)\hat{\mathcal{E}}^{\dagger}(0) + \mathrm{H.c.}\right]\,. \tag{4.31}$$

Both systems, i.e., the source described by the annihilation operator a_1 and the target described by the annihilation operator a_2, are now interacting with the same reservoir field $\hat{\mathcal{E}}^{\dagger}(0)$, the reservoir field at the same spatial position. This coupling between the reservoir and the atoms is a collective one with the jump operator

$$J = \sqrt{2\kappa^{(1)}}a_1 + e^{-i\phi_a}\sqrt{2\kappa^{(2)}}a_2\,. \tag{4.32}$$

This form of the coupling allows us to derive the master equation in the same way we did before (see Section 3.1). For this purpose, we start with equation (4.26) and introduce the reduced density operator

$$\rho_{\mathrm{ret}}(t) = \mathrm{tr}_{\mathrm{R}}\left[\chi_{\mathrm{ret}}(t)\right]\,, \tag{4.33}$$

where we have traced over the reservoir. From this point on the derivation is straightforward and we eventually obtain the master equation for the cascaded cavity system

$$\dot{\rho}_{\mathrm{ret}} = -\frac{i}{\hbar}[H_{\mathrm{sys}}, \rho_{\mathrm{ret}}] + \left(J\rho_{\mathrm{ret}}J^{\dagger} - \frac{1}{2}J^{\dagger}J\rho_{\mathrm{ret}} - \frac{1}{2}\rho_{\mathrm{ret}}J^{\dagger}J\right)\,, \tag{4.34}$$

where the source-retarded density operator, ρ_{ret}, describes the target subsystem at time t, and the source subsystem at time $t-\tau$.

Note that in general the system changes very slowly compared to the fast optical frequencies, therefore the retardation between the source and target can generally be neglected, apart from the effects of the free evolution of the light between the two cavities which takes place on a timescale of the optical period. This free evolution introduces a phase factor of $e^{i\omega\tau}$, where ω is the frequency of the field. Thus, in practice, we do not need to make a unitary transformation, but can simply replace

the input field, $\hat{\mathcal{E}}(d)$, in the interaction Hamiltonian of the target (equation (4.22)), by

$$\hat{\mathcal{E}}(d) = e^{i\omega\tau}e^{i\phi_a}\left[\hat{\mathcal{E}}(0) - i\frac{1}{2}\sqrt{2\kappa^{(1)}}a_1\right] . \tag{4.35}$$

If we redefine $\phi_a + \omega\tau \rightarrow \phi_a$, we formally obtain the same system Hamiltonian, given by equation (4.30), and the same master equation as before, but without the retardation of the source,

$$\dot{\rho} = -\frac{i}{\hbar}[H_{\text{sys}}, \rho] + \left(J\rho J^\dagger - \frac{1}{2}J^\dagger J\rho - \frac{1}{2}\rho J^\dagger J\right) . \tag{4.36}$$

The derivation of the master equation for cascaded systems introduced by Gardiner [Gar93] uses a different approach. The full derivation is omitted here, but a qualitative overview is outlined.[2]

This alternate approach starts with the quantum Langevin equations for the cavity modes, a_1 and a_2, of the source and target system, respectively. These equations are derived in Section 4.1. Similar to before, the time-retarded output field of the source is assumed to be the input, i.e., the noise term of the target system. The equations for a_1 and a_2 are combined to form a quantum Langevin equation of the whole system. This quantum Langevin equation is converted into a quantum Ito stochastic differential equation from which the master equation for the density operator ρ can be derived. The master equation yields

$$\begin{aligned}\dot{\rho} = -\frac{i}{\hbar}[H_{\text{S}}, \rho] &+ \kappa^{(1)}\left(2a_1\rho a_1^\dagger - a_1^\dagger a_1\rho - \rho a_1^\dagger a_1\right) \\ &+ \kappa^{(2)}\left(2a_2\rho a_2^\dagger - a_2^\dagger a_2\rho - \rho a_2^\dagger a_2\right) \\ &- 2\sqrt{\kappa^{(1)}\kappa^{(2)}}\left([a_2^\dagger, a_1\rho] + [\rho a_1^\dagger, a_2]\right) ,\end{aligned} \tag{4.37}$$

with $H_{\text{S}} = H_{\text{source}} + H_{\text{target}}$. At first glance this master equation looks different to equation (4.36) but it can be rearranged into the same form. Note that in this form the interaction between the two cavities is totally described in the damping term (the last line in equation (4.37)), whereas in the previous derivation the interaction is described by the system Hamiltonian plus, via the collective damping of the atoms, by the collective operator J.

4.2.2 Coherently driven cascaded systems

We consider now a coherent input into the source subsystem, corresponding to the irradiation of the source with a laser. As already described in Section 2.5.2, the coherent input field can be treated classically. The Hamiltonian for the interaction between the cavity mode a and the classical input field is typically written as

$$H_{\text{driv}} = \hbar\left(\mathcal{E}^* e^{i\omega_{\text{p}}t}a + \mathcal{E}e^{-i\omega_{\text{p}}t}a^\dagger\right) , \tag{4.38}$$

[2] For more details, consult [GZ04].

with frequency of the input field ω_p and a complex field amplitude $\mathcal{E}$. Note that in this notation, the factor $\sqrt{2\kappa}$, which appears, for example, in equations (4.21) and (4.22), is absorbed in the complex field amplitude $\mathcal{E}$.

After this recapitulation of how to describe a single coherently driven cavity, we now have to have a closer look at how a coherent input field drives a cascaded cavity system. Clearly the coherent light couples into the source cavity and drives the cavity mode a_1, which can be described by equation (4.38). The field coupling into the target system now consists of two parts: firstly, the output of the source plus the reservoir (which is described by the cascaded system formalism without driving), and secondly the coherent input field $\mathcal{E}(d)$ which does not couple into the source but is reflected to the target system. Thus the target is also directly driven by the coherent input field, with the addition of the phase factor $e^{i\phi_a}$ with respect to the input field, $\mathcal{E}(0)$, at the source, i.e., $\mathcal{E}(d) = e^{i\phi_a}\mathcal{E}(0)$. This phase factor is due to the reflection at the mirror of the source cavity and the free evolution between source and target.

The Hamiltonian for the driven system, $H_\mathrm{sys}^\mathrm{driv}$, can now be written as

$$\begin{aligned} H_\mathrm{sys}^\mathrm{driv} &= H_\mathrm{sys} + \hbar\left(\mathcal{E}^* e^{i\omega_\mathrm{p} t} a_1 + \mathcal{E} e^{-i\omega_\mathrm{p} t} a_1^\dagger\right) \\ &\quad + \hbar\sqrt{\frac{\kappa^{(2)}}{\kappa^{(1)}}}\left(\mathcal{E}^* e^{-i\phi_a} e^{i\omega_\mathrm{p} t} a_2 + \mathcal{E} e^{i\phi_a} e^{-i\omega_\mathrm{p} t} a_2^\dagger\right), \end{aligned} \tag{4.39}$$

where the factor $\sqrt{\frac{\kappa^{(2)}}{\kappa^{(1)}}}$ accounts for the notation in which $\kappa^{(1)}$ is absorbed in the complex field amplitude $\mathcal{E}$, and H_sys is the Hamiltonian of the non-driven system given by equation (4.30). The first driving term on the RHS of equation (4.39) describes the driving of the source and the second the driving of the target.

For deriving the master equation of the driven cascaded system we use the same argumentation as in Section 3.3.2, that the driving laser mode is included in the system Hamiltonian rather than in the reservoir, and that the remaining reservoir modes have a zero mean amplitude (as in our original derivation of the master equation). Therefore the master equation for the driven cascaded system can be derived in the same way as the non-driven cascaded master equation, only with the system Hamiltonian H_sys replaced by the driven system Hamiltonian $H_\mathrm{sys}^\mathrm{driv}$. The master equation for the driven cascaded system reads

$$\dot{\rho} = -\frac{i}{\hbar}[H_\mathrm{sys}^\mathrm{driv}, \rho] + \left(J\rho J^\dagger - \frac{1}{2}J^\dagger J\rho - \frac{1}{2}\rho J^\dagger J\right), \tag{4.40}$$

where J is the jump operator (4.32).

4.2.3 Cascaded systems consisting of two-mode cavities

The single two-mode cavity has already been described in Section 3.3, where we assumed that the system consisted of two counter-propagating cavity modes and a possible interaction between these modes. This is described by the Hamiltonian,

$$H = \hbar\omega(a^\dagger a + b^\dagger b) + \hbar(h a^\dagger b + h^* b^\dagger a), \tag{4.41}$$

where ω is the cavity frequency, a and b the counter-propagating cavity modes and h a complex coupling constant.

Let us initially ignore the interaction between the two modes (setting $h = 0$). In this case the counter-propagating modes in a single cavity are completely independent, and the coupling of the two cavities can be separately considered for the a modes, travelling clockwise, and for the b modes, travelling anti-clockwise. The coupling, in the case of the a modes, has already been derived in Section 4.2.1. In the same manner, the coupling for the b modes can be incorporated. The only difference is that for the b modes the former source becomes the target and vice versa – the modes b_1 and b_2 are travelling in the opposite direction. This eventually leads to the system Hamiltonian

$$H_{\text{sys}} = H_1 + H_2 + H_{12}\,, \tag{4.42}$$

with

$$H_1 = \hbar\omega_1(a_1^\dagger a_1 + b_1^\dagger b_1)\,, \tag{4.43}$$

$$H_2 = \hbar\omega_2(a_2^\dagger a_2 + b_2^\dagger b_2)\,, \tag{4.44}$$

$$\begin{aligned} H_{12} = {} & i\hbar\sqrt{\kappa^{(1)}\kappa^{(2)}}(e^{-i\phi_a}a_1^\dagger a_2 - e^{i\phi_a}a_2^\dagger a_1) \\ & + i\hbar\sqrt{\kappa^{(1)}\kappa^{(2)}}(e^{-i\phi_b}b_2^\dagger b_1 - e^{i\phi_b}b_1^\dagger b_2)\,, \end{aligned} \tag{4.45}$$

where H_1 describes the first cavity, H_2 the second cavity, and H_{12} the coupling between the two cavities. Included is a phase factor, $e^{-i\phi_b}$, due to reflection at the cavity mirror and the free evolution of the light from cavity 2 to cavity 1. Comparing H_{12} with the interaction term in equation (4.30), we see that there is an additional term describing a unidirectional coupling from cavity 2 to cavity 1 due to the b modes, which are travelling in the opposite direction to the a modes.

The master equation for the cascaded system consisting of two-mode cavities is then

$$\begin{aligned} \dot{\rho} = {} & -i\,[H_{\text{sys}}, \rho] + (J_a\rho J_a^\dagger - \frac{1}{2}J_a^\dagger J_a\rho - \frac{1}{2}\rho J_a^\dagger J_a) \\ & + (J_b\rho J_b^\dagger - \frac{1}{2}J_b^\dagger J_b\rho - \frac{1}{2}\rho J_b^\dagger J_b)\,, \end{aligned} \tag{4.46}$$

with jump operators

$$J_a = \sqrt{2\kappa^{(1)}}a_1 + e^{-i\phi_a}\sqrt{2\kappa^{(2)}}a_2\,, \tag{4.47}$$

$$J_b = \sqrt{2\kappa^{(2)}}b_2 + e^{-i\phi_b}\sqrt{2\kappa^{(1)}}b_1\,. \tag{4.48}$$

If we turn on the interaction between the two counter-propagating modes in each cavity (i.e., $h \neq 0$), the coupling between the two cavities no longer consists of two independent, unidirectional couplings for the a and b modes, respectively. Therefore, we cannot use the unitary transformation – equation (4.24) – in deriving the master equation. Nevertheless, as mentioned in the note below the master equation with

retardation of the source, equation (4.34), for a slow change of the system state (compared to the optical frequency), i.e., a small coupling h between the counter-propagating modes, the retardation is negligible, apart from a phase factor. Therefore we do not need to unitarily transform the system but can simply account for the effects of the time delay between the two cavities by writing the input fields for the interaction of the cavities with the reservoir in the manner of equation (4.35). From that point on, we can derive the master equation in the same way as before, eventually obtaining the same master equation as equation (4.46), i.e.,

$$\begin{aligned}\dot{\rho} = -i\left[H_{\mathrm{sys}}, \rho\right] &+ (J_a \rho J_a^\dagger - \frac{1}{2} J_a^\dagger J_a \rho - \frac{1}{2} \rho J_a^\dagger J_a) \\ &+ (J_b \rho J_b^\dagger - \frac{1}{2} J_b^\dagger J_b \rho - \frac{1}{2} \rho J_b^\dagger J_b)\,, \end{aligned} \tag{4.49}$$

where the system Hamiltonian is

$$H_{\mathrm{sys}} = H_1 + H_2 + H_{12}\,, \tag{4.50}$$

with

$$H_1 = \hbar\omega_1(a_1^\dagger a_1 + b_1^\dagger b_1) + \hbar(h_1 a_1^\dagger b_1 + h_1^* b_1^\dagger a_1)\,, \tag{4.51}$$

$$H_2 = \hbar\omega_2(a_2^\dagger a_2 + b_2^\dagger b_2) + \hbar(h_2 a_2^\dagger b_2 + h_2^* b_2^\dagger a_2)\,, \tag{4.52}$$

$$\begin{aligned} H_{12} = {} & i\hbar\sqrt{\kappa^{(1)}\kappa^{(2)}}(e^{-i\phi_a} a_1^\dagger a_2 - e^{i\phi_a} a_2^\dagger a_1) \\ & + i\hbar\sqrt{\kappa^{(1)}\kappa^{(2)}}(e^{-i\phi_b} b_2^\dagger b_1 - e^{i\phi_b} b_1^\dagger b_2)\,. \end{aligned} \tag{4.53}$$

This form now includes the interaction between the counter-propagating cavity modes.

Chapter 5

Spontaneous Emission in a Cascaded System

In the previous chapter the theory for describing cascaded systems was developed. We can now apply this theory to investigate the spontaneous emission of a cascaded system consisting of two toroids with a single atom coupled to each of them. We are, in particular, interested in the emission spectrum of the system when one atom is initially excited. The excited atom will eventually decay and light will be emitted. This is a non-stationary process.

In the first section we will outline the theoretical description. In the second, we will restrict ourself to the so-called "bad-cavity" regime where we are able to make certain simplifying assumptions and derive analytical expressions for the emission spectrum. These results will be compared to numerical calculations. In the third section we will briefly describe two special cases, namely a system where an atom is coupled to only one of the toroids and one consisting of only one toroid and a coupled atom. We will derive emission spectra in the bad-cavity regime for these simpler systems and compare them to the more complex case. In the fourth section, we will adiabatically eliminate the cavity modes in the bad-cavity limit and derive the associated master equation and its implications. Finally, in section five we will investigate the emission spectrum of our system in the so-called "strong-coupling" regime. This regime is of particular interest for future applications in quantum information where strong coupling between the atom and the photon is required.

5.1 The theoretical model

We want to investigate the system of two coupled microtoroids shown in Figure 5.1. The microresonators, described in Section 2.5.1, are connected via an optical fibre. The two counter-propagating WGMs, with annihilation operators a and b, couple to this fibre by the rate κ_{ex}. Also, light can be lost out of the toroid and not be coupled back into the fibre, e.g., due to imperfections in the toroid. This intrinsic loss is described by the rate κ_{i}. An atom, with spontaneous emission rate γ, is coupled

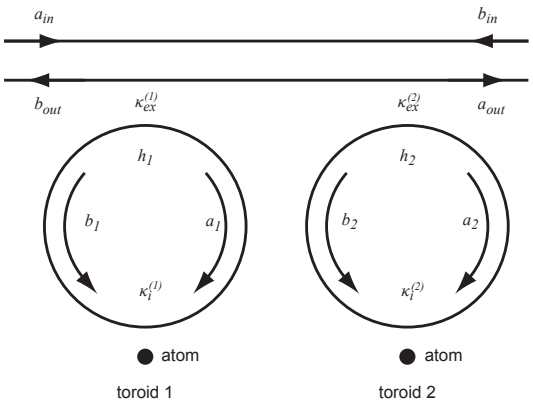

FIGURE 5.1: Schematic of a cascaded microtoroid system.

to each toroid via the evanescent field of the intracavity modes, with atom-cavity coupling constant g.

5.1.1 Hamiltonian and master equation

The master equation for a cascaded two-mode cavity system was derived in Section 4.2.3. We have to incorporate the intrinsic loss channels and the atoms (which couple to the toroids) in order to describe the system we are dealing with in this chapter. This can be done in an analogous way to the single-toroid case of Section 3.3.1. The atoms are considered to be two-level atoms, described by raising and lowering operators $\sigma^{\pm}$ and the transition frequency ω_{A}.

With the additional terms included, the Hamiltonian can be written in the form

$$H = H_1 + H_2 + H_{12}\,, \tag{5.1}$$

where H_1 describes the first cavity, H_2 the second cavity and H_{12} the coupling between the two cavities via the fibre. In their most general form these different parts read[1]

$$\begin{aligned} H_1 &= \omega_{\mathrm{C}_1}(a_1^\dagger a_1 + b_1^\dagger b_1) + (h_1 a_1^\dagger b_1 + h_1^* b_1^\dagger a_1) \\ &\quad + \omega_{\mathrm{A}_1}\sigma_1^+\sigma_1^- + (g_1^* a_1^\dagger \sigma_1^- + g_1\sigma_1^+ a_1) + (g_1 b_1^\dagger \sigma_1^- + g_1^*\sigma_1^+ b_1)\,, \qquad (5.2) \\ H_2 &= \omega_{\mathrm{C}_2}(a_2^\dagger a_2 + b_2^\dagger b_2) + (h_2 a_2^\dagger b_2 + h_2^* b_2^\dagger a_2) \\ &\quad + \omega_{\mathrm{A}_2}\sigma_2^+\sigma_2^- + (g_2^* a_2^\dagger \sigma_2^- + g_2\sigma_2^+ a_2) + (g_2 b_2^\dagger \sigma_2^- + g_2^*\sigma_2^+ b_2)\,, \qquad (5.3) \\ H_{12} &= i\sqrt{\kappa_{\mathrm{ex}}^{(1)}\kappa_{\mathrm{ex}}^{(2)}}(e^{-i\phi_a}a_1^\dagger a_2 - e^{i\phi_a}a_2^\dagger a_1) \\ &\quad + i\sqrt{\kappa_{\mathrm{ex}}^{(1)}\kappa_{\mathrm{ex}}^{(2)}}(e^{-i\phi_b}b_2^\dagger b_1 - e^{i\phi_b}b_1^\dagger b_2)\,, \qquad (5.4) \end{aligned}$$

[1] From here on we set $\hbar = 1$.

where ω_1 and ω_2 are the cavity mode frequencies, h_1 and h_2 the coupling strengths between the two counter-propagating modes in each toroid, g_1 and g_2 the atom-cavity coupling constants, and $e^{\pm i\phi_a}$ and $e^{\pm i\phi_b}$ phase factors taking into account the distance the light has to travel between the two cavities.

The master equation for the system now reads,

$$\begin{aligned}\dot{\rho} = -i\,[H,\rho] &+ (J_a\rho J_a^\dagger - \frac{1}{2}J_a^\dagger J_a\rho - \frac{1}{2}\rho J_a^\dagger J_a) + (J_b\rho J_b^\dagger - \frac{1}{2}J_b^\dagger J_b\rho - \frac{1}{2}\rho J_b^\dagger J_b)\\ &+ \kappa_{\mathrm{i}}^{(1)}(2a_1\rho a_1^\dagger - a_1^\dagger a_1\rho - \rho a_1^\dagger a_1) + \kappa_{\mathrm{i}}^{(1)}(2b_1\rho b_1^\dagger - b_1^\dagger b_1\rho - \rho b_1^\dagger b_1)\\ &+ \kappa_{\mathrm{i}}^{(2)}(2a_2\rho a_2^\dagger - a_2^\dagger a_2\rho - \rho a_2^\dagger a_2) + \kappa_{\mathrm{i}}^{(2)}(2b_2\rho b_2^\dagger - b_2^\dagger b_2\rho - \rho b_2^\dagger b_2)\\ &+ \frac{\gamma_1}{2}(2\sigma_1^-\rho\sigma_1^+ - \sigma_1^+\sigma_1^-\rho - \rho\sigma_1^+\sigma_1^-)\\ &+ \frac{\gamma_2}{2}(2\sigma_2^-\rho\sigma_2^+ - \sigma_2^+\sigma_2^-\rho - \rho\sigma_2^+\sigma_2^-)\,, \end{aligned} \tag{5.5}$$

with jump operators

$$J_a = \sqrt{2\kappa_{\mathrm{ex}}^{(1)}}a_1 + e^{-i\phi_a}\sqrt{2\kappa_{\mathrm{ex}}^{(2)}}a_2\,, \tag{5.6}$$

$$J_b = \sqrt{2\kappa_{\mathrm{ex}}^{(2)}}b_2 + e^{-i\phi_b}\sqrt{2\kappa_{\mathrm{ex}}^{(1)}}b_1\,. \tag{5.7}$$

This master equation has three different loss channels: A term describing the damping of the cavity modes into the fibre (κ_{ex}), an intrinsic loss channel for each cavity mode (κ_{i}) and a damping (free space spontaneous emission) term for each of the atoms (γ).

5.1.2 Separation of the Liouvillian

We want to calculate the emission spectrum for the initial state where only one atom is excited with the other in the ground state. Usually the emission spectrum is calculated by evaluating autocorrelation functions (of the form shown in equations (5.28)-(5.31)) with a dependency on two times. In the case of only one photon excitation, however, it is possible to factorize the two-time correlation functions and derive a simpler expression for the emission spectrum. We will follow closely the derivation of Carmichael [Car08, Chap. 13].

We start by separating the Liouvillian, $\mathcal{L}$, of the master equation, $\dot{\rho} = \mathcal{L}\rho$, into two parts, one acting on the one-energy-quantum subspace and the other generating transitions to the ground state. The master equation is then written as[2]

$$\dot{\rho} = (\mathcal{C} + \mathcal{D})\rho\,, \tag{5.8}$$

[2]There is a close connection between this derivation and Quantum Trajectory Theory. Exactly the same separation is done in Quantum Trajectory Theory, where the superoperator $\mathcal{C}$ governs the evolution of the system between the quantum jumps and the superoperator $\mathcal{D}$ executes the quantum jump. In the case of single-photon excitation, the system will be in the ground state after a quantum jump and no more evolution will take place. Unfortunately, a more detailed description of the Quantum Trajectory Theory is beyond the scope of this text, but the interested reader is referred to [Car08].

with $\mathcal{C}$ including the terms that act within the subspace of one-energy quantum and $\mathcal{D}$ the terms that generate transitions to the ground state, i.e.,

$$\begin{aligned}\mathcal{C} = -i\,[H,\cdot] - \frac{1}{2}[J_a^\dagger J_a,\cdot]_+ - \frac{1}{2}[J_a^\dagger J_a,\cdot]_+ \\ - \kappa_{\mathrm{i}}^{(1)}[a_1^\dagger a_1 + b_1^\dagger b_1,\cdot]_+ - \kappa_{\mathrm{i}}^{(2)}[a_2^\dagger a_2 + b_2^\dagger b_2,\cdot]_+ \\ - \frac{\gamma_1}{2}[\sigma_1^+\sigma_1^-,\cdot]_+ - \frac{\gamma_2}{2}[\sigma_2^+\sigma_2^-,\cdot]_+\,,\end{aligned} \tag{5.9}$$

and

$$\begin{aligned}\mathcal{D} = (J_a\cdot J_a^\dagger) + (J_b\cdot J_b^\dagger) + 2\kappa_i^{(1)}(a_1\cdot a_1^\dagger) + 2\kappa_i^{(1)}(b_1\cdot b_1^\dagger) \\ + 2\kappa_{\mathrm{i}}^{(2)}(a_2\cdot a_2^\dagger) + 2\kappa_{\mathrm{i}}^{(2)}(b_2\cdot b_2^\dagger) \\ + \gamma_1(\sigma_1^-\cdot\sigma_1^+) + \gamma_2(\sigma_2^-\cdot\sigma_2^+)\,.\end{aligned} \tag{5.10}$$

$[\cdot,\cdot]_+$ denotes the anti-commutator. The initial density operator, with only atom 1 excited, reads

$$\rho(0) = (|e\rangle\langle e|)_{A_1}(|g\rangle\langle g|)_{A_2}(|0\rangle\langle 0|)_{a_1}(|0\rangle\langle 0|)_{b_1}(|0\rangle\langle 0|)_{a_2}(|0\rangle\langle 0|)_{b_2}\,. \tag{5.11}$$

For times $t > 0$ a photon has either been emitted, with the probability P_{spon}, and the system is in the ground state,

$$|G\rangle = |g\rangle_{A_1}|g\rangle_{A_2}|0\rangle_{a_1}|0\rangle_{b_1}|0\rangle_{a_2}|0\rangle_{b_2}\,, \tag{5.12}$$

or no photon has been emitted and the system is still in the one-energy-quantum subspace described by the pure state

$$\begin{aligned}|\bar{\psi}(t)\rangle = \alpha(t)|eg0000\rangle + \xi(t)|ge0000\rangle + \beta(t)|gg1000\rangle \\ + \delta(t)|gg0100\rangle + \gamma(t)|gg0010\rangle + \eta(t)|gg0001\rangle\,,\end{aligned} \tag{5.13}$$

with $\alpha(t)$ and $\xi(t)$ the probability amplitudes for the excitation of atoms 1 and 2, respectively, $\beta(t)$ the probability amplitude for the excitation of cavity mode a_1 and so on. Thus, the density operator decomposes into two parts for $t > 0$

$$\rho(t) = \rho_0(t) + \rho_1(t)\,, \tag{5.14}$$

with

$$\rho_0(t) = P_{\mathrm{spon}}(t)|G\rangle\langle G|\,, \tag{5.15}$$

$$\rho_1(t) = |\bar{\psi}(t)\rangle\langle\bar{\psi}(t)|\,. \tag{5.16}$$

This decomposition of the density operator separates the master equation into two solvable pieces

$$\dot{\rho}_1(t) = \mathcal{C}\rho_1\,, \tag{5.17}$$

$$\dot{\rho}_0(t) = \mathcal{D}\rho_1\,. \tag{5.18}$$

From the second equation we get a differential equation for the probability $P_{\text{spon}}(t)$:

$$\begin{aligned}\frac{d}{dt}P_{\text{spon}}(t) &= \langle G|\dot{\rho}_0(t)|G\rangle \\ &= 2\kappa^{(1)}|\beta(t)|^2 + 2\kappa^{(1)}|\delta(t)|^2 + 2\kappa^{(2)}|\gamma(t)|^2 + 2\kappa^{(2)}|\eta(t)|^2 \\ &\quad + \gamma_1|\alpha(t)|^2 + \gamma_2|\xi(t)|^2\,, \end{aligned} \tag{5.19}$$

with $\kappa^{(1)} = \kappa_{\text{i}}^{(1)} + \kappa_{\text{ex}}^{(1)}$ and $\kappa^{(2)} = \kappa_{\text{i}}^{(2)} + \kappa_{\text{ex}}^{(2)}$. Then since the density operator $\rho_1(t)$ describes a pure state, the first equation yields a non-unitary Schrödinger equation for the quantum state $|\bar{\psi}(t)\rangle$,

$$\frac{d}{dt}|\bar{\psi}(t)\rangle = -iH_{\text{NH}}|\bar{\psi}(t)\rangle\,, \tag{5.20}$$

where the non-Hermitian Hamiltonian, H_{NH}, is

$$\begin{aligned}H_{\text{NH}} = H - i\frac{1}{2}(&J_a^\dagger J_a + J_b^\dagger J_b + 2\kappa_i^{(1)}a_1^\dagger a_1 + 2\kappa_i^{(1)}b_1^\dagger b_1 \\ &+ 2\kappa_{\text{i}}^{(2)}a_2^\dagger a_2 + 2\kappa_{\text{i}}^{(2)}b_2^\dagger b_2 + \gamma_1\sigma_1^+\sigma_1^- + \gamma_2\sigma_2^+\sigma_2^-)\,. \end{aligned} \tag{5.21}$$

This Schrödinger equation leads to a system of coupled differential equations for the probability amplitudes:

$$\dot{\alpha} = \left(-i\omega_{\text{A}_1} - \frac{\gamma_1}{2}\right)\alpha - ig_1\beta - ig_1^*\delta\,, \tag{5.22}$$

$$\dot{\xi} = \left(-i\omega_{\text{A}_2} - \frac{\gamma_2}{2}\right)\xi - ig_2\gamma - ig_2^*\eta\,, \tag{5.23}$$

$$\dot{\beta} = -ig_1^*\alpha + \left(-i\omega_{\text{C}_1} - \kappa^{(1)}\right)\beta - ih_1\delta\,, \tag{5.24}$$

$$\dot{\delta} = -ig_1\alpha - ih_1^*\beta + \left(-i\omega_{\text{C}_1} - \kappa^{(1)}\right)\delta - 2\sqrt{\kappa_{ex}^{(1)}\kappa_{\text{ex}}^{(2)}}e^{i\phi_b}\eta\,, \tag{5.25}$$

$$\dot{\gamma} = -ig_2^*\xi - 2\sqrt{\kappa_{\text{ex}}^{(1)}\kappa_{\text{ex}}^{(2)}}e^{i\phi_a}\beta + \left(-i\omega_{\text{C}_2} - \kappa^{(2)}\right)\gamma - ih_2\eta\,, \tag{5.26}$$

$$\dot{\eta} = -ig_2\xi - ih_2^*\gamma + \left(-i\omega_{\text{C}_2} - \kappa^{(2)}\right)\eta\,. \tag{5.27}$$

We will see in the next section that the emission spectrum can be expressed in terms of these probability amplitudes. Thus, we have to solve the differential equations (5.22)-(5.27), from which we compute the emission spectrum.

5.1.3 The emission spectrum

The property we are interested in, in particular, is the emission spectrum. The spontaneous emission is a non-stationary process. Its spectrum can be computed, in general, from double integrals over two-time correlation functions. In the present case, we can divide the emission into two parts. First, the emission of light "out of the sides" of the cavity (following the nomenclature of a standard cavity). This

emission consists of the spontaneous emission of the atoms to modes other than the cavity modes (spectrum denoted by $T_{\text{side},\sigma}$) – i.e., the emission of light by the atoms into free space – and the emission of light due to scattering of the WGMs (spectrum denoted by $T_{\text{side,modes}}$). Second, the emission from the toroids into the fibre (spectrum denoted by T_{axis}), which we will call the emission "along the axis" of the cavity.

The spectrum out of the sides of the cavity is determined by

$$T^{(j)}_{\text{side},\sigma}(\omega) = \frac{\gamma_j}{2\pi}\int_0^\infty dt \int_0^\infty dt'\, e^{-i\omega(t-t')}\langle \sigma_j^+(t)\sigma_j^-(t')\rangle\,, \tag{5.28}$$

$$T^{(j)}_{\text{side,modes}}(\omega) = \frac{\kappa_{\text{i}}^{(j)}}{\pi}\int_0^\infty dt \int_0^\infty dt'\, e^{-i\omega(t-t')}\left(\langle a_j^\dagger(t)a_j(t')\rangle + \langle b_j^\dagger(t)b_j(t')\rangle\right)\,, \tag{5.29}$$

where the index j stands for either cavity 1 or cavity 2, and the spectrum along the cavity axis is determined by

$$T_{\text{axis},a_{\text{out}}}(\omega) = \frac{1}{2\pi}\int_0^\infty dt \int_0^\infty dt'\, e^{-i\omega(t-t')}\langle a_{\text{out}}^\dagger(t)a_{\text{out}}(t')\rangle\,, \tag{5.30}$$

$$T_{\text{axis},b_{\text{out}}}(\omega) = \frac{1}{2\pi}\int_0^\infty dt \int_0^\infty dt'\, e^{-i\omega(t-t')}\langle b_{\text{out}}^\dagger(t)b_{\text{out}}(t')\rangle\,, \tag{5.31}$$

where the indices a_{out} and b_{out} denote the different directions of propagation in the fibre, due to the different directions of propagation of the a and b modes in the cavity. The normalization in these expressions has been chosen so that the probabilities of a photon being eventually emitted out of the sides of the cavities, $P_{\text{side}}(\infty)$, and along the cavity axis, $P_{\text{axis}}(\infty)$, sum to unity, i.e.,

$$P_{\text{side}}(\infty) + P_{\text{axis}}(\infty) = 1\,, \tag{5.32}$$

with the probabilities determined by

$$P_{\text{side}} = \int_{-\infty}^{\infty} d\omega T_{\text{side}}(\omega)\,, \tag{5.33}$$

$$P_{\text{axis}} = \int_{-\infty}^{\infty} d\omega T_{\text{axis}}(\omega)\,. \tag{5.34}$$

The output operators were derived in Section 4.1 via the input-output formalism. They read

$$a_{\text{out}}(t) = -a_{\text{in}}(t) + J_a(t)\,, \tag{5.35}$$

$$b_{\text{out}}(t) = -b_{\text{in}}(t) + J_b(t)\,, \tag{5.36}$$

where the inputs, a_{in} and b_{in}, correspond to vacuum noise.

We will now determine the autocorrelation functions, where we derive, to provide one explicit example, an expression for the correlation function $\langle \sigma_1^+(t)\sigma_1^-(t')\rangle$ in terms

of the probability amplitudes.[3] The other correlation functions are derived in the same way and only the results will be stated.

Using equation (3.47), from the quantum regression formula we find, for $t' \geq t$,

$$\langle \sigma_1^+(t)\sigma_1^-(t')\rangle = \mathrm{Tr}\left[\sigma_1^- e^{(\mathcal{C}+\mathcal{D})(t'-t)}(\rho(t)\sigma_1^+)\right] . \tag{5.37}$$

The term $\rho(t)\sigma_1^+$ in the trace can be replaced by

$$\rho(t)\sigma_1^+ = \alpha^*(t)|\bar{\psi}(t)\rangle\langle G| , \tag{5.38}$$

where we have used equations (5.13)-(5.16). The next step is to analyse how the exponential function in the trace acts on $|\bar{\psi}(t)\rangle\langle G|$. For this purpose we examine the effects of $\mathcal{C}$ and $\mathcal{D}$, which, by using (5.9) and (5.10), yield

$$\mathcal{C}\left(|\bar{\psi}(t)\rangle\langle G|\right) = \left(-iH_{\mathrm{NH}}|\bar{\psi}(t)\rangle\right)\langle G| , \tag{5.39}$$

$$\mathcal{D}\left(|\bar{\psi}(t)\rangle\langle G|\right) = 0 . \tag{5.40}$$

Thus we find (with $t' \geq t$)

$$\begin{aligned} e^{(\mathcal{C}+\mathcal{D})(t'-t)}|\bar{\psi}(t)\rangle\langle G| &= \left(e^{-iH_{\mathrm{NH}}(t'-t)}|\bar{\psi}(t)\rangle\right)\langle G| \\ &= |\bar{\psi}(t')\rangle\langle G| , \end{aligned} \tag{5.41}$$

where the state $|\bar{\psi}(t')\rangle$ denotes the state $|\bar{\psi}(t)\rangle$ propagated forward in time under the Schrödinger equation (5.20). With these results we are finally able to express the correlation function in term of probability amplitudes

$$\begin{aligned} \langle \sigma_1^+(t)\sigma_1^-(t')\rangle &= \alpha^*(t)\mathrm{tr}\left[|\bar{\psi}(t')\rangle\langle G|\right] \\ &= \alpha^*(t)\alpha(t') . \end{aligned} \tag{5.42}$$

Through this particular derivation, this result is only valid for $t' \geq t$, but with the relation

$$\langle \sigma_1^+(t)\sigma_1^-(t')\rangle = \langle \sigma_1^+(t')\sigma_1^-(t)\rangle^* , \tag{5.43}$$

it also holds for $t' < t$.

Substituting equation (5.43) into equation (5.28), we arrive at a simple expression for the spontaneous emission spectrum out of the side of the cavity of atom 1, namely

$$T^{(1)}_{\mathrm{side},\sigma}(\omega) = \frac{\gamma_1}{2\pi}\left|\int_0^\infty dt\, e^{i\omega t}\alpha(t)\right|^2 . \tag{5.44}$$

[3] This is only possible because of the decomposition of $\rho(t)$ shown in equation (5.14). In general we would need to derive a set of differential equations for the correlation functions via the quantum regression theorem (equations (3.50)-(3.52)) and solve this set of equations.

The other emission spectra can be derived in an analogous way. They are, for the emission out of the side of the cavity,

$$T^{(2)}_{\mathrm{side},\sigma}(\omega) = \frac{\gamma_2}{2\pi}\left|\int_0^\infty dt\, e^{i\omega t}\xi(t)\right|^2, \tag{5.45}$$

$$T^{(1)}_{\mathrm{side,mode}}(\omega) = \frac{\kappa_{\mathrm{i}}^{(1)}}{\pi}\left|\int_0^\infty dt\, e^{i\omega t}\beta(t)\right|^2 + \frac{\kappa_{\mathrm{i}}^{(1)}}{\pi}\left|\int_0^\infty dt\, e^{i\omega t}\delta(t)\right|^2, \tag{5.46}$$

$$T^{(2)}_{\mathrm{side,mode}}(\omega) = \frac{\kappa_{\mathrm{i}}^{(2)}}{\pi}\left|\int_0^\infty dt\, e^{i\omega t}\gamma(t)\right|^2 + \frac{\kappa_{\mathrm{i}}^{(2)}}{\pi}\left|\int_0^\infty dt\, e^{i\omega t}\eta(t)\right|^2, \tag{5.47}$$

and for the emission along the axis of the cavity,

$$\begin{aligned} T_{\mathrm{axis},a_{\mathrm{out}}}(\omega) = {} & \frac{\kappa_{\mathrm{ex}}^{(1)}}{\pi}\left|\int_0^\infty dt\, e^{i\omega t}\beta(t)\right|^2 + \frac{\kappa_{\mathrm{ex}}^{(2)}}{\pi}\left|\int_0^\infty dt\, e^{i\omega t}\gamma(t)\right|^2 \\ & + \frac{\sqrt{\kappa_{\mathrm{ex}}^{(1)}\kappa_{\mathrm{ex}}^{(2)}}}{\pi}e^{-i\phi_a}\int_0^\infty dt\, e^{-i\omega t}\beta^*(t)\int_0^\infty dt'\, e^{i\omega t'}\gamma(t') \\ & + \frac{\sqrt{\kappa_{\mathrm{ex}}^{(1)}\kappa_{\mathrm{ex}}^{(2)}}}{\pi}e^{i\phi_a}\int_0^\infty dt\, e^{-i\omega t}\gamma^*(t)\int_0^\infty dt'\, e^{i\omega t'}\beta(t'), \end{aligned} \tag{5.48}$$

$$\begin{aligned} T_{\mathrm{axis},b_{\mathrm{out}}}(\omega) = {} & \frac{\kappa_{\mathrm{ex}}^{(1)}}{\pi}\left|\int_0^\infty dt\, e^{i\omega t}\delta(t)\right|^2 + \frac{\kappa_{\mathrm{ex}}^{(2)}}{\pi}\left|\int_0^\infty dt\, e^{i\omega t}\eta(t)\right|^2 \\ & + \frac{\sqrt{\kappa_{\mathrm{ex}}^{(1)}\kappa_{\mathrm{ex}}^{(2)}}}{\pi}e^{i\phi_b}\int_0^\infty dt\, e^{-i\omega t}\delta^*(t)\int_0^\infty dt'\, e^{i\omega t'}\eta(t') \\ & + \frac{\sqrt{\kappa_{\mathrm{ex}}^{(1)}\kappa_{\mathrm{ex}}^{(2)}}}{\pi}e^{-i\phi_b}\int_0^\infty dt\, e^{-i\omega t}\eta^*(t)\int_0^\infty dt'\, e^{i\omega t'}\delta(t'). \end{aligned} \tag{5.49}$$

The special initial condition with the system in a one-energy-quantum state made it possible to decompose the density operator into two parts consisting of pure states. In turn, this made it possible to use a Schrödinger equation rather than a master equation, and express the system evolution in terms of probability amplitudes for the one-energy-quantum excitations. This eventually lead to the factorization of the two-time correlation functions and enabled the replacement of the two-time integrals by simpler one-time integrals over the probability amplitudes.

5.2 Bad-cavity limit – analytical & numerical investigations

We saw in the previous section that the emission spectra can be computed by integrals over the probability amplitudes for the one-energy-quantum excitation states shown by equations (5.44)-(5.49). Hence we have to solve the set of differential equations for the probability amplitudes given by equations (5.22)-(5.27) in order to be able to determine the emission spectra. For the general case, solving these equations

analytically becomes cumbersome and no further insight is achieved. If we want to derive manageable analytical results, certain simplifying assumptions have to be made.

5.2.1 The bad-cavity regime

The bad-cavity regime is characterized by a very high cavity damping rate, κ, which exceeds all other system rates, e.g., the spontaneous emission rate, γ, and the coupling rate between the atom and cavity, g, i.e.

$$\kappa \gg \gamma, g\,. \tag{5.50}$$

Due to the high cavity loss rate, the cavity modes decay on a much faster timescale than the timescale on which the atomic state is significantly changed. This enables us to adiabatically eliminate the cavity modes.

5.2.2 Adiabatic elimination of the cavity modes

In order to eliminate the cavity modes we transform the set of differential equations for the probability amplitudes, equations (5.22)-(5.27), to a frame that rotates at the atomic frequency ω_{A_1}. This ensures that κ is much larger than all other parameters. Then we can set the time derivatives of the probability amplitudes for the excited cavity modes, equations (5.24)-(5.27), to zero and solve these equations in steady state. The solutions for the cavity field modes can then be used to finally solve the differential equations for the probability amplitudes for the excited atoms.

The transformation to the rotating frame is done by the following substitutions:

$$\begin{aligned}
&\alpha' = \alpha e^{i\omega_{\mathrm{A}_1} t}, \quad \beta' = \beta e^{i\omega_{\mathrm{A}_1} t}, \quad \delta' = \delta e^{i\omega_{\mathrm{A}_1} t}\,, \\
&\xi' = \xi e^{i\omega_{\mathrm{A}_1} t}, \quad \gamma' = \gamma e^{i\omega_{\mathrm{A}_1} t}, \quad \eta' = \eta e^{i\omega_{\mathrm{A}_1} t}\,.
\end{aligned} \tag{5.51}$$

Hence, the system of differential equations in the rotating frame reads,

$$\dot{\alpha}' = -\frac{\gamma_1}{2}\alpha' - i g_1 \beta' - i g_1^* \delta'\,, \tag{5.52}$$

$$\dot{\xi}' = \left(-i(\omega_{\mathrm{A}_2} - \omega_{\mathrm{A}_1}) - \frac{\gamma_2}{2}\right)\xi' - i g_2 \gamma' - i g_2^* \eta'\,, \tag{5.53}$$

$$\dot{\beta}' = -i g_1^* \alpha' + \left(-i\Delta\omega_1 - \kappa^{(1)}\right)\beta' - i h_1 \delta'\,, \tag{5.54}$$

$$\dot{\delta}' = -i g_1 \alpha' - i h_1^* \beta' + \left(-i\Delta\omega_1 - \kappa^{(1)}\right)\delta' - 2\sqrt{\kappa_{\mathrm{ex}}^{(1)}\kappa_{\mathrm{ex}}^{(2)}}\, e^{i\phi_b}\eta'\,, \tag{5.55}$$

$$\dot{\gamma}' = -i g_2^* \xi' - 2\sqrt{\kappa_{\mathrm{ex}}^{(1)}\kappa_{\mathrm{ex}}^{(2)}}\, e^{i\phi_a}\beta' + \left(-i\Delta\omega_2 - \kappa^{(2)}\right)\gamma' - i h_2 \eta'\,, \tag{5.56}$$

$$\dot{\eta}' = -i g_2 \xi' - i h_2^* \gamma' + \left(-i\Delta\omega_2 - \kappa^{(2)}\right)\eta'\,, \tag{5.57}$$

with $\Delta\omega_1 = \omega_{\mathrm{C}_1} - \omega_{\mathrm{A}_1}$ and $\Delta\omega_2 = \omega_{\mathrm{C}_2} - \omega_{\mathrm{A}_1}$. We can now set the time derivative of equations (5.54)-(5.57) to zero, on the grounds mentioned above, from which we

obtain the following set of equations:

$$0 = -ig_1^*\alpha' + \left(-i\Delta\omega_1 - \kappa^{(1)}\right)\beta' - ih_1\delta' \,, \tag{5.58}$$

$$0 = -ig_1\alpha' - ih_1^*\beta' + \left(-i\Delta\omega_1 - \kappa^{(1)}\right)\delta' - 2\sqrt{\kappa_{\mathrm{ex}}^{(1)}\kappa_{\mathrm{ex}}^{(2)}}e^{i\phi_b}\eta' \,, \tag{5.59}$$

$$0 = -ig_2^*\xi' - 2\sqrt{\kappa_{\mathrm{ex}}^{(1)}\kappa_{\mathrm{ex}}^{(2)}}e^{i\phi_a}\beta' + \left(-i\Delta\omega_2 - \kappa^{(2)}\right)\gamma' - ih_2\eta' \,, \tag{5.60}$$

$$0 = -ig_2\xi' - ih_2^*\gamma' + \left(-i\Delta\omega_2 - \kappa^{(2)}\right)\eta' \,. \tag{5.61}$$

These equations have to be solved with respect to α' and ξ'.

Simplifying assumptions

The equations above are quite complicated in terms of the many different indices. Let us therefore take the two cavities to be identical so that we can simplify the equations and obtain analytical solutions. This is a reasonable assumption, because in experiments cavities with equal properties are commonly used. In particular we set

$$\omega_{\mathrm{C}_1} = \omega_{\mathrm{C}_2} =: \omega_{\mathrm{C}} \,, \quad \omega_{\mathrm{A}_1} = \omega_{\mathrm{A}_2} =: \omega_{\mathrm{A}} \,, \tag{5.62}$$

$$\kappa^{(1)} = \kappa^{(2)} =: \kappa \,, \quad \text{with} \quad \kappa_{\mathrm{i}} \approx 0 \,, \quad \text{and hence} \quad \kappa \approx \kappa_{\mathrm{ex}} \,, \tag{5.63}$$

$$g_1 = g_2 =: g \in \mathbb{R} \,. \tag{5.64}$$

Furthermore, we assume that the counter-propagating modes do not interact with each other and set the phase factors to zero (corresponding to choosing a specific distance between the toroids):

$$h_1 = h_2 = 0 \,, \quad \phi_a = \phi_b = 0 \,. \tag{5.65}$$

With these assumptions we obtain

$$0 = g\alpha' + (\Delta\omega - i\kappa)\,\beta' \,, \tag{5.66}$$

$$0 = g\alpha' + (\Delta\omega - i\kappa)\,\delta' - 2i\kappa\eta' \,, \tag{5.67}$$

$$0 = g\xi' - 2i\kappa\beta' + (\Delta\omega - i\kappa)\,\gamma' \,, \tag{5.68}$$

$$0 = g\xi' + (\Delta\omega - i\kappa)\,\eta' \,, \tag{5.69}$$

with solutions

$$\eta' = -\frac{g}{\Delta\omega - i\kappa}\xi' \,, \tag{5.70}$$

$$\gamma' = -\frac{g}{\Delta\omega - i\kappa}\xi' - \frac{2i\kappa g}{(\Delta\omega - i\kappa)^2}\alpha' \,, \tag{5.71}$$

$$\delta' = -\frac{2i\kappa g}{(\Delta\omega - i\kappa)^2}\xi' - \frac{g}{\Delta\omega - i\kappa}\alpha' \,, \tag{5.72}$$

$$\beta' = -\frac{g}{\Delta\omega - i\kappa}\alpha' \,, \tag{5.73}$$

Substituting these expressions into equations (5.52) and (5.53), the differential equations for the atomic probability amplitudes yield

$$\dot{\alpha}' = \left(-\frac{\gamma}{2} + 2i\frac{g^2}{\Delta\omega - i\kappa}\right)\alpha' - \frac{2\kappa g^2}{(\Delta\omega - i\kappa)^2}\xi' \,, \tag{5.74}$$

$$\dot{\xi}' = -\frac{2\kappa g^2}{(\Delta\omega - i\kappa)^2}\alpha' + \left(-\frac{\gamma}{2} + 2i\frac{g^2}{\Delta\omega - i\kappa}\right)\xi' \,. \tag{5.75}$$

We assume now that only the atom in cavity 1 is initially excited, and hence have to solve this set of differential equations for the initial values $\alpha(0) = 1$ and $\xi(0) = 0$. In the non-rotating frame, the resulting solutions for the probability amplitudes for the atoms are

$$\alpha(t) = \alpha'(t) \cdot e^{-i\omega_\mathrm{A} t} = \frac{1}{2}\left(e^{(\lambda_1 - i\omega_\mathrm{A})t} + e^{(\lambda_2 - i\omega_\mathrm{A})t}\right) \,, \tag{5.76}$$

$$\xi(t) = \xi'(t) \cdot e^{-i\omega_\mathrm{A} t} = \frac{1}{2}\left(e^{(\lambda_1 - i\omega_\mathrm{A})t} - e^{(\lambda_2 - i\omega_\mathrm{A})t}\right) \,, \tag{5.77}$$

with eigenvalues

$$\lambda_1 = -\frac{\gamma}{2} - 4g^2\frac{\kappa\Delta\omega^2}{(\Delta\omega^2 + \kappa^2)^2} + 2ig^2\frac{\Delta\omega(\Delta\omega^2 - \kappa^2)}{(\Delta\omega^2 + \kappa^2)^2} \,, \tag{5.78}$$

$$\lambda_2 = -\frac{\gamma}{2} - 4g^2\frac{\kappa^3}{(\Delta\omega^2 + \kappa^2)^2} + 2ig^2\frac{\Delta\omega(\Delta\omega^2 + 3\kappa^2)}{(\Delta\omega^2 + \kappa^2)^2} \,. \tag{5.79}$$

The probability amplitudes are exponentially decaying.

5.2.3 Analytical results

We eventually obtain for the integrals in equations (5.44) and (5.45)

$$\int_0^\infty dt\, e^{i\omega t}\alpha(t) = \frac{1}{2}\left(-\frac{1}{A + iB + i(\omega - \omega_\mathrm{A})} - \frac{1}{C + iD + i(\omega - \omega_\mathrm{A})}\right) \,, \tag{5.80}$$

$$\int_0^\infty dt\, e^{i\omega t}\xi(t) = \frac{1}{2}\left(-\frac{1}{A + iB + i(\omega - \omega_\mathrm{A})} + \frac{1}{C + iD + i(\omega - \omega_\mathrm{A})}\right) \,, \tag{5.81}$$

with

$$A = -\frac{\gamma}{2} - \frac{4g^2\kappa\Delta\omega^2}{(\Delta\omega^2 - \kappa^2)^2 + (2\kappa\Delta\omega)^2} \,, \tag{5.82}$$

$$B = \frac{2g^2\Delta\omega(\Delta\omega^2 - \kappa^2)}{(\Delta\omega^2 - \kappa^2)^2 + (2\kappa\Delta\omega)^2} \,, \tag{5.83}$$

$$C = -\frac{\gamma}{2} - \frac{4g^2\kappa^3}{(\Delta\omega^2 - \kappa^2)^2 + (2\kappa\Delta\omega)^2} \,, \tag{5.84}$$

$$D = \frac{2g^2\Delta\omega(\Delta\omega^2 - \kappa^2) + 8g^2\kappa^2\Delta\omega}{(\Delta\omega^2 - \kappa^2)^2 + (2\kappa\Delta\omega)^2} \,. \tag{5.85}$$

With these results we are finally able to compute the emission spectrum of the system given by equations (5.44)-(5.49). The emission spectrum for the atoms out of the side of the cavity, $T_{\text{side},\sigma}$, follows directly from equations (5.80) and (5.81). The other emission spectra, $T_{\text{side,mode}}$ and T_{axis}, are combinations of these two integrals, where we use the relations (5.70)-(5.73) to rewrite the spectra in terms of these integrals.

5.2.4 Numerical results

We will compare the analytical results which we obtained by adiabatically eliminating the cavity modes in the bad-cavity regime with numerical results obtained from the general model, and investigate how accurate the approximation is.

In the general model, the set of differential equations for the probability amplitudes, equations (5.52)-(5.57), is solved numerically. This is done with MATLAB where an explicit Runge-Kutta method is used to numerically integrate the set of ordinary differential equations for a given initial value. We assume the atom of the first cavity to be initially excited, i.e., $\alpha(0) = 1$ with all other initial probability amplitudes equal to zero. The obtained time series for the probability amplitudes ($\alpha(t_{\text{n}})$–$\eta(t_{\text{n}})$) must then be numerically integrated by way of equations (5.44)-(5.49) to obtain the emission spectra.

The emission spectra out of the side of the cavity, T_{side}, and along the axis of the cavity, T_{axis}, computed with adiabatic elimination and from the full model, are shown for different cavity damping rates in Figures 5.2-5.4. These spectra were calculated for zero detuning between the toroids and atoms ($\Delta\omega = 0$) and adopting the assumptions made when adiabatically eliminating the cavity modes, i.e., identical toroids and no direct coupling between the counter-propagating cavity modes. The analytical results (5.80) and (5.81) reduce, for zero detuning, to

$$\int_0^\infty dt\, e^{i\omega t}\alpha(t) = \frac{1}{2}\left(-\frac{1}{-\frac{\gamma}{2} + i(\omega - \omega_{\text{A}})} - \frac{1}{-\frac{\gamma}{2} - \frac{4g^2}{\kappa} + i(\omega - \omega_{\text{A}})}\right), \tag{5.86}$$

$$\int_0^\infty dt\, e^{i\omega t}\xi(t) = \frac{1}{2}\left(-\frac{1}{-\frac{\gamma}{2} + i(\omega - \omega_{\text{A}})} + \frac{1}{-\frac{\gamma}{2} - \frac{4g^2}{\kappa} + i(\omega - \omega_{\text{A}})}\right). \tag{5.87}$$

In Figure 5.2 the emission spectrum along the axis is plotted for zero atomic damping ($\gamma = 0$). In this case there is no emission out of the side of the cavity, since both of the potential loss channels (the atomic damping and the internal cavity damping) are set to zero. It can be seen that for a large cavity damping rate κ_{ex}, i.e., when we are clearly in the bad-cavity regime, the plot from the full model matches quite well the one with adiabatic elimination, whereas for smaller cavity losses the results of the two calculations start to deviate. With the adiabatic elimination, the emission along the axis ($T_{\text{axis},a_{\text{out}}}$ and $T_{\text{axis},b_{\text{out}}}$) is the same for both directions, but for the full model there is more light emitted in the direction of the b modes than of the a modes. Also, the adiabatic model can not explain the features (sharp peak or dip respectively on top of the broad curves of T_{axis}) which are caused by either spontaneous emission of the atoms (γ) (Figure 5.3) or internal cavity losses (κ_{i})

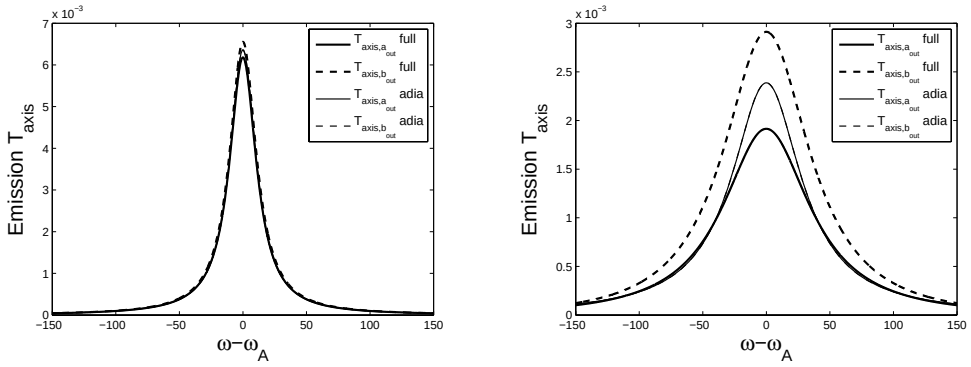

FIGURE 5.2: Emission spectra $T_{\mathrm{axis},a_{\mathrm{out}}}$ and $T_{\mathrm{axis},b_{\mathrm{out}}}$ as a function of frequency for two different cavity damping rates, $\kappa_{\mathrm{ex}} = 800$ (left) and $\kappa_{\mathrm{ex}} = 300$ (right). The emission spectra are obtained from the full model (thick lines) and with adiabatic elimination (thin lines). With adiabatic elimination, the emission spectra $T_{\mathrm{axis},a_{\mathrm{out}}}$ and $T_{\mathrm{axis},b_{\mathrm{out}}}$ completely coincide. The atomic decay rate and the internal cavity decay are set to zero ($\gamma = 0$, $\kappa_{\mathrm{i}} = 0$) and therefore there is no emission out of the side of the cavity ($T_{\mathrm{side}} = 0$). The other parameters are $g = 50$, $h = 0$ and $\Delta\omega = 0$. For the damping rate $\kappa_{\mathrm{ex}} = 800$ the emission spectra obtained from the two methods match quite well.

(Figure 5.4). When one of these loss channels is turned on, light can be emitted out of the side of the cavities and a sharp peak arises in the emission spectrum T_{side}, whose linewidth scales with γ or κ_{i}, respectively. The features in the emission along the axis tend to broaden the larger the damping, γ or κ_{i}, gets, i.e., the broader the emission out of the side of the cavity gets. In the case of a finite atomic damping rate γ (Figure 5.3) the dip in $T_{\mathrm{axis},b_{\mathrm{out}}}$ can be explained by the fact that some of the light can now be emitted by the atom and is therefore simply missing in the spectrum emitted along the axis. More will be said about these features in Section 5.4.4.

Note that the plots are approximately Lorentzian functions with, in the case of T_{axis}, a full width at half maximum of approximately $8\frac{g^2}{\kappa}$. In comparison the linewidth in the bad-cavity regime for cavity-enhanced spontaneous emission of a single atom in a single-mode cavity is approximately $2\frac{g^2}{\kappa}$ (if the atomic damping γ is neglected).[4] A deviation by a factor two can be explained by having two counter-propagating modes in the cavity, which yield a linewidth of $4\frac{g^2}{\kappa}$. The remaining factor of two is a first hint for the so-called *superradiance* [Dic54] where the linewidth for two atoms is, by a factor of two, larger. More will be said about this in Section 5.4.4.

5.3 Bad-cavity limit – special cases of the general system

In this section we will have a brief look at two obvious and simpler cases of our general system of two coupled toroids with an atom coupled to each. First, one

[4] For more information see for example [Car08].

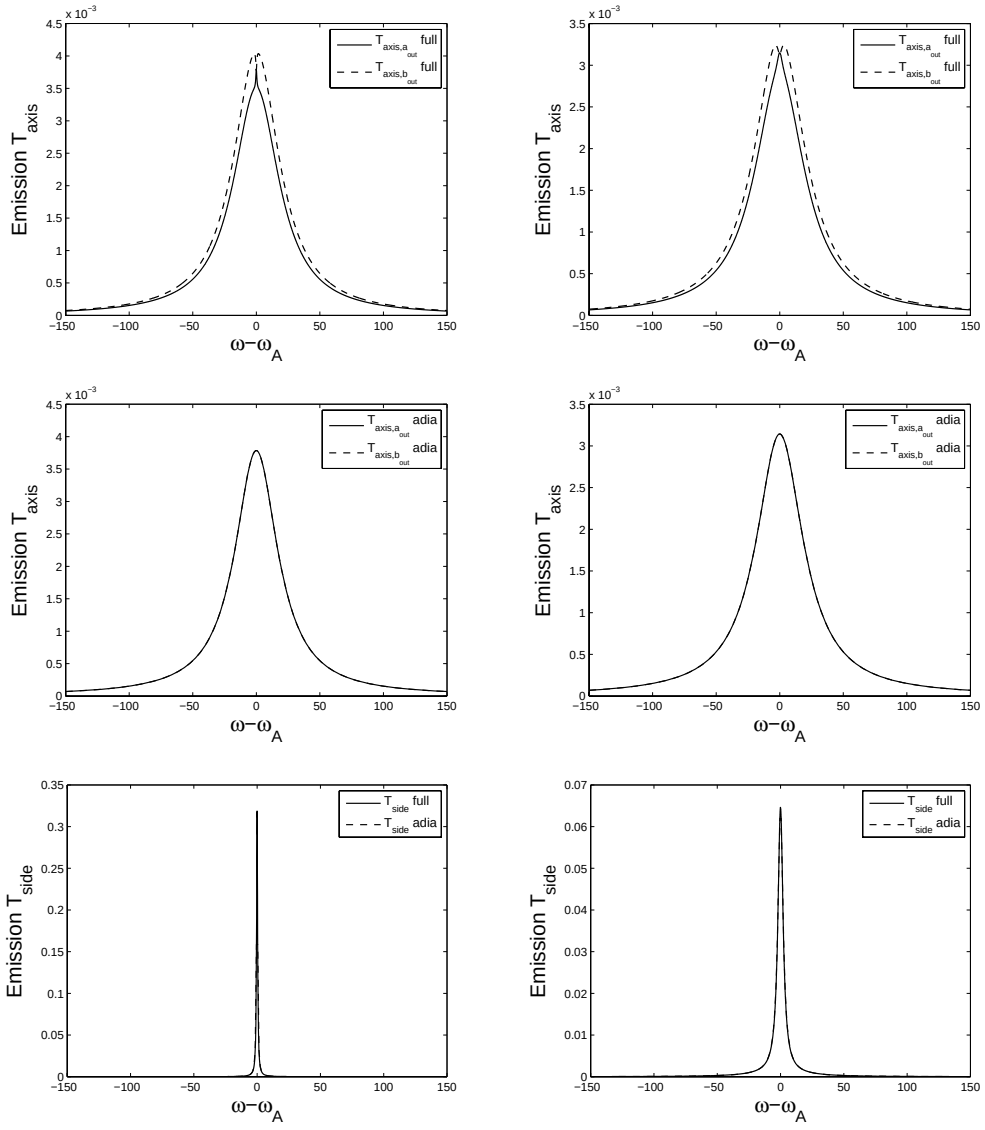

(a) $\gamma = 1$ (b) $\gamma = 5$

FIGURE 5.3: Emission spectra $T_{\mathrm{axis},a_{\mathrm{out}}}$, $T_{\mathrm{axis},b_{\mathrm{out}}}$ and $T_{\mathrm{side,total}}$ as a function of frequency for two different atomic decay rates, $\gamma = 1$ (left column) and $\gamma = 5$ (right column), obtained from the full model and with adiabatic elimination. With adiabatic elimination, the emission spectra $T_{\mathrm{axis},a_{\mathrm{out}}}$ and $T_{\mathrm{axis},b_{\mathrm{out}}}$ completely coincide. The other parameters are $\kappa_{\mathrm{ex}} = 500$, $g = 50$, $\kappa_{\mathrm{i}} = 0$, $h = 0$ and $\Delta\omega = 0$.

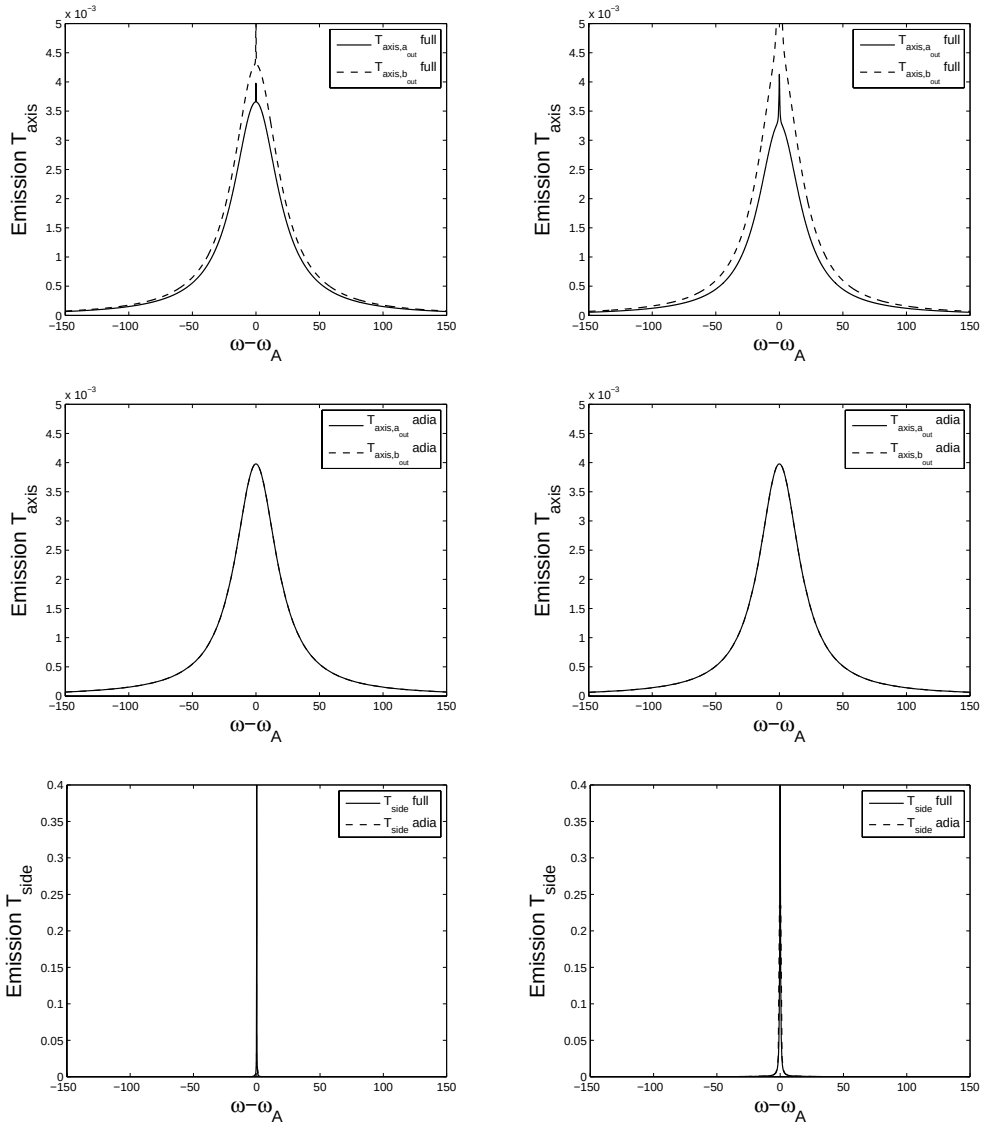

(a) $\kappa_\mathrm{i} = 1$ (b) $\kappa_\mathrm{i} = 20$

FIGURE 5.4: Emission spectra $T_{\mathrm{axis},a_\mathrm{out}}$, $T_{\mathrm{axis},b_\mathrm{out}}$ and $T_{\mathrm{side,total}}$ as a function of frequency for two different internal cavity decay rates, $\kappa_\mathrm{i} = 1$ (left column) and $\kappa_\mathrm{i} = 20$ (right column), obtained from the full model and with adiabatic elimination. With adiabatic elimination, the emission spectra $T_{\mathrm{axis},a_\mathrm{out}}$ and $T_{\mathrm{axis},b_\mathrm{out}}$ completely coincide. The other parameters are $\kappa_\mathrm{ex} = 500$, $g = 50$, $\gamma = 0$, $h = 0$ and $\Delta\omega = 0$.

atom can be taken away, thus we end up with two toroids with an atom coupled to only one of them. Second, an even simpler system is one in which we have one toroid with one atom. These systems can be described in a similar way to the more complex one already investigated. We will only give a short overview and state the results for the integrals that the emission spectra are calculated from in the bad-cavity regime. Then numerical results for these systems will be compared to the "full" system (consisting of two toroids with an atom coupled to each of them).

Hereafter, we will refer to the 2-toroids-2-atoms system as 2T2A system, to the 2-toroids-1-atom system as 2T1A system, to the 2-toroids-no-atom system as 2T0A system and to the 1-toroid-1-atom system as 1T1A system.

5.3.1 2-toroids-1-atom system

We consider the system where an atom is coupled to toroid 1 only. This can be described by the master equation (5.5) with the parameters g_2 and γ_2 set to zero. The separation of the Liouvillian can be done in the same manner as before. The pure state of the one energy quantum subspace is now

$$\begin{aligned}|\bar{\psi}(t)\rangle = \alpha(t)|e0000\rangle + \beta(t)|g1000\rangle + \delta(t)|g0100\rangle \\ + \gamma(t)|g0010\rangle + \eta(t)|g0001\rangle\,,\end{aligned} \tag{5.88}$$

where there is no probability amplitude ξ since no atom is coupled to the second toroid. We eventually arrive at the following set of differential equations for the probability amplitudes in the rotating frame:

$$\dot{\alpha}' = -\frac{\gamma_1}{2}\alpha' - ig_1\beta' - ig_1^*\delta'\,, \tag{5.89}$$

$$\dot{\beta}' = -ig_1^*\alpha' + \left(-i\Delta\omega_1 - \kappa^{(1)}\right)\beta' - ih_1\delta'\,, \tag{5.90}$$

$$\dot{\delta}' = -ig_1\alpha' - ih_1^*\beta' + \left(-i\Delta\omega_1 - \kappa^{(1)}\right)\delta' - 2\sqrt{\kappa_{\mathrm{ex}}^{(1)}\kappa_{\mathrm{ex}}^{(2)}}e^{i\phi_b}\eta'\,, \tag{5.91}$$

$$\dot{\gamma}' = -2\sqrt{\kappa_{\mathrm{ex}}^{(1)}\kappa_{\mathrm{ex}}^{(2)}}e^{i\phi_a}\beta' + \left(-i\Delta\omega_2 - \kappa^{(2)}\right)\gamma' - ih_2\eta'\,, \tag{5.92}$$

$$\dot{\eta}' = -ih_2^*\gamma' + \left(-i\Delta\omega_2 - \kappa^{(2)}\right)\eta'\,. \tag{5.93}$$

Adiabatically eliminating the cavity modes in the bad-cavity regime and assuming the same simplifying assumptions, we find

$$\beta' = \delta' = -\frac{g}{\Delta\omega - i\kappa}\alpha'\,, \tag{5.94}$$

$$\gamma' = -\frac{2i\kappa g}{(\Delta\omega - i\kappa)^2}\alpha'\,, \tag{5.95}$$

$$\eta' = 0\,. \tag{5.96}$$

Thus, all emission spectra, given by equations (5.44)-(5.49), can be computed from

$$\int_0^\infty dt\, e^{i\omega t}\alpha(t) = -\frac{1}{A + iB + i(\omega - \omega_{\mathrm{A}})}\,, \tag{5.97}$$

with

$$A = -\frac{\gamma}{2} - \frac{2\kappa g^2}{\Delta\omega^2 + \kappa^2}\,, \tag{5.98}$$

$$B = \frac{2g^2\Delta\omega}{\Delta\omega^2 + \kappa^2}\,. \tag{5.99}$$

5.3.2 1-toroid-1-atom system

We briefly state the results for the single-toroid system, described by the master equation

$$\begin{aligned}\dot\rho = &-i\,[H_1, \rho] + \kappa^{(1)}(2a_1\rho a_1^\dagger - a_1^\dagger a_1\rho - \rho a_1^\dagger a_1) + \kappa^{(1)}(2b_1\rho b_1^\dagger - b_1^\dagger b_1\rho - \rho b_1^\dagger b_1)\\ &+ \frac{\gamma_1}{2}(2\sigma_1^-\rho\sigma_1^+ - \sigma_1^+\sigma_1^-\rho - \rho\sigma_1^+\sigma_1^-)\,,\end{aligned} \tag{5.100}$$

with $\kappa^{(1)} = \kappa_{\mathrm{i}}^{(1)} + \kappa_{\mathrm{ex}}^{(1)}$ and the Hamiltonian H_1 from equation (5.2). This system is characterized in much detail for the driven case in [ADW$^+$06a, ADW$^+$06b, DPA$^+$08a, DPA$^+$08b].

Computing the emission spectra can be done in the same way as before. This time the pure state of the one-energy-quantum subspace is

$$|\bar\psi(t)\rangle = \alpha(t)|e00\rangle + \beta(t)|g10\rangle + \delta(t)|g01\rangle\,, \tag{5.101}$$

and we arrive at the following set of differential equations for the probability amplitudes:

$$\dot\alpha' = -\frac{\gamma_1}{2}\alpha' - ig_1\beta' - ig_1^*\delta'\,, \tag{5.102}$$

$$\dot\beta' = -ig_1^*\alpha' + \left(-i\Delta\omega_1 - \kappa^{(1)}\right)\beta' - ih_1\delta'\,, \tag{5.103}$$

$$\dot\delta' = -ig_1\alpha' - ih_1^*\beta' + \left(-i\Delta\omega_1 - \kappa^{(1)}\right)\delta'\,. \tag{5.104}$$

Using the same simplifying assumptions as before – except we do not have to set the coupling between the cavity modes to zero in order to get manageable analytical results – we adiabatically eliminate the cavity modes and obtain

$$\beta' = \delta' = -\frac{g}{\Delta\omega - i\kappa + h}\alpha'\,. \tag{5.105}$$

Thus, all the emission spectra given by equations (5.44)-(5.49) can be computed from

$$\int_0^\infty dt\, e^{i\omega t}\alpha(t) = -\frac{1}{A + iB + i(\omega - \omega_{\mathrm{A}})}\,, \tag{5.106}$$

with

$$A = -\frac{\gamma}{2} - \frac{2\kappa g^2}{(\Delta\omega + h)^2 + \kappa^2}\,, \tag{5.107}$$

$$B = \frac{2g^2(\Delta\omega + h)}{(\Delta\omega + h)^2 + \kappa^2}\,. \tag{5.108}$$

Note that the results for the probability amplitudes and the result for the integral (which were derived in the case of a possible coupling between the cavity modes) are the same as equations (5.94) and (5.97) for the 2T1A system (which were derived in the case of no coupling between the cavity modes) when the coupling is set to zero. Hence, it can be seen from equations (5.44)-(5.49) that, in the case of $h = 0$, the emission of the atom out of the side of the cavity, $T^{(1)}_{\text{side},\sigma}$, and the emission along the axis in the direction of the b mode, $T_{\text{axis},b_{\text{out}}}$, are the same for the 1T1A and the 2T1A system. This does make sense, since the light emitted in the direction of the b mode does not "see" the second cavity and is therefore not affected by it. The same is valid for the light directly emitted by the atom out of the side of the cavity.

5.3.3 Comparison between the three systems

In Figure 5.5 the emission spectra for the three systems (2T2A, 2T1A and 1T1A) are plotted. It can be seen that the emission spectra for the 2T1A and the 1T1A system match quite well, as we would expect (at least for $T_{\text{axis},b_{\text{out}}}$ and $T^{(1)}_{\text{side},\sigma}$) from the analytical results. For these two systems more light is emitted along the axis and less light out of the side of the cavity compared to the 2T2A system. This can be explained by the fact that in the 2T2A system, we have two atoms which can emit light out of the side of the toroids via spontaneous emission γ, whereas in the 2T1A and the 1T1A system, it is only one atom. However, the linewidth for the 2T2A system is approximately twice as large as the linewidth of the other systems. They are given by $8\frac{g^2}{\kappa}$ and $4\frac{g^2}{\kappa}$, respectively. The difference of a factor of two is explained by the occurrence of superradiance for the 2T2A system, where the two atoms can directly communicate (see Section 5.4.4). The linewidth for the 2T1A and the 1T1A system is due to cavity enhanced spontaneous emission of the atom (where the full width at half maximum is $2\frac{g^2}{\kappa}$ in the simplest case [Car08]) to either one of the cavity modes, a or b (giving the additional factor of two because of two decay channels). In the bad-cavity regime, the 2T1A and the 1T1A system are very similar in terms of the emission spectra. This is because in the 2T1A system the light which is emitted into the fibre from toroid 1 can hardly couple into the second toroid [PDAK09]. Hence, the 2T1A system is an effective 1T1A system in this case.

5.4 Bad-cavity limit – the adiabatic master equation

In this section another – more fundamental – way of adiabatically eliminating the cavity modes in the bad-cavity regime will be presented. In this limit the cavity damping rate, κ, exceeds the atomic spontaneous emission rate, γ, and the coupling rate between the atom and cavity, g. This means that the characteristic timescale of the cavity, i.e., the rate of decay of the cavity modes out of the cavity, is much faster than the timescale of the atom. The aim is to separate the slower varying behaviour from the fast decay of the cavity modes and to derive a master equation where the cavity modes have been adiabatically eliminated, i.e., a master equation

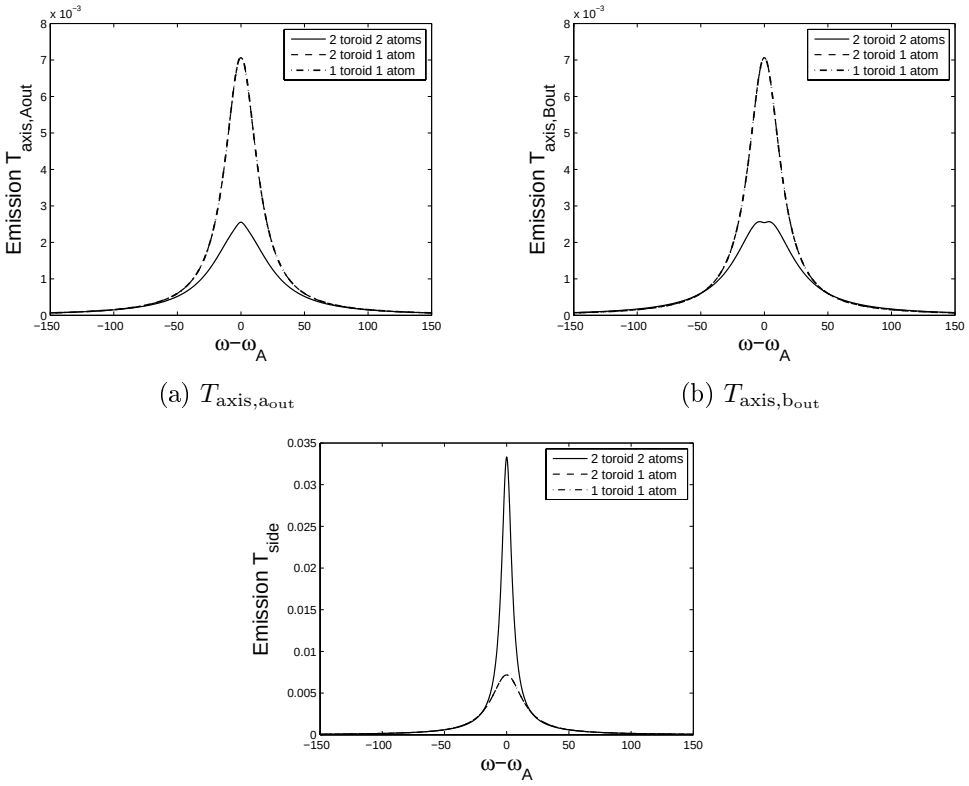

(a) $T_{\mathrm{axis,a_{out}}}$

(b) $T_{\mathrm{axis,b_{out}}}$

(c) $T_{\mathrm{side,total}}$

FIGURE 5.5: Emission spectra $T_{\mathrm{axis},a_{\mathrm{out}}}$ (a), $T_{\mathrm{axis},b_{\mathrm{out}}}$ (b) and $T_{\mathrm{side,total}}$ (c) as a function of frequency plotted for the three different systems (2T2A, 2T1A and 1T1A) where the atom (atom 1) is initially excited. The spectra for the 2T1A and the 1T1A system coincide. The parameters are $\kappa_{\mathrm{ex}} = 500$, $g = 50$, $\gamma = 10$, $\kappa_{\mathrm{i}} = 0$, $\Delta\omega = 0$ and $h = 0$.

which is written only in terms of the atomic operators. This master equation will be helpful in gaining more insight in the behaviour of the system.

5.4.1 Hamiltonian and master equation

This time the master equation describing our system is written in a slightly different way. We use the form (4.37) which was derived by Gardiner [GZ04]. A short sketch of the derivation can be found at the end of Section 4.2.1. In order to be able to carry out analytical calculations and to obtain some compact expressions we set the coupling between the cavity modes, h, to zero. In the bad-cavity regime we can assume $\kappa_\mathrm{i} = 0$ and hence $\kappa = \kappa_\mathrm{ex}$. For simplicity we also set the phase factors, ϕ_a and ϕ_b, to zero. The master equation then reads

$$\dot{\rho} = -i\,[H, \rho] + \mathcal{L}_\mathrm{C}\rho + \mathcal{L}_\mathrm{A}\rho\,, \tag{5.109}$$

with Hamiltonian

$$H = H_\mathrm{A} + H_\mathrm{C} + H_\mathrm{AC}\,, \tag{5.110}$$

where

$$H_\mathrm{A} = \omega_\mathrm{A}(\sigma_1^+\sigma_1^- + \sigma_2^+\sigma_2^-)\,, \tag{5.111}$$

$$H_\mathrm{C} = \omega_\mathrm{C}(a_1^\dagger a_1 + b_1^\dagger b_1 + a_2^\dagger a_2 + b_2^\dagger b_2)\,, \tag{5.112}$$

$$\begin{aligned} H_\mathrm{AC} = {} & (g_1^* a_1^\dagger \sigma_1^- + g_1 \sigma_1^+ a_1) + (g_1 b_1^\dagger \sigma_1^- + g_1^* \sigma_1^+ b_1) \\ & + (g_2^* a_2^\dagger \sigma_2^- + g_2 \sigma_2^+ a_2) + (g_2 b_2^\dagger \sigma_2^- + g_2^* \sigma_2^+ b_2)\,. \end{aligned} \tag{5.113}$$

Liouvillians describing the damping read

$$\mathcal{L}_\mathrm{C}\rho = \mathcal{L}_\mathrm{C}(a_1, a_2)\rho + \mathcal{L}_\mathrm{C}(b_1, b_2)\rho\,, \tag{5.114}$$

with

$$\begin{aligned} \mathcal{L}_\mathrm{C}(a_1, a_2)\rho = {} & \kappa_1(2a_1\rho a_1^\dagger - a_1^\dagger a_1\rho - \rho a_1^\dagger a_1) + \kappa_2(2a_2\rho a_2^\dagger - a_2^\dagger a_2\rho - \rho a_2^\dagger a_2) \\ & - 2\sqrt{\kappa_1\kappa_2}\left([a_2^\dagger, a_1\rho] + [\rho a_1^\dagger, a_2]\right)\,, \end{aligned} \tag{5.115}$$

$$\begin{aligned} \mathcal{L}_\mathrm{C}(b_1, b_2)\rho = {} & \kappa_1(2b_1\rho b_1^\dagger - b_1^\dagger b_1\rho - \rho b_1^\dagger b_1) + \kappa_2(2b_2\rho b_2^\dagger - b_2^\dagger b_2\rho - \rho b_2^\dagger b_2) \\ & - 2\sqrt{\kappa_1\kappa_2}\left([b_1^\dagger, b_2\rho] + [\rho b_2^\dagger, b_1]\right)\,, \end{aligned} \tag{5.116}$$

and

$$\mathcal{L}_\mathrm{A}\rho = \frac{\gamma_1}{2}(2\sigma_1^-\rho\sigma_1^+ - \sigma_1^+\sigma_1^-\rho - \rho\sigma_1^+\sigma_1^-) + \frac{\gamma_2}{2}(2\sigma_2^-\rho\sigma_2^+ - \sigma_2^+\sigma_2^-\rho - \rho\sigma_2^+\sigma_2^-)\,. \tag{5.117}$$

The master equation (5.109) is the same equation as (5.5), for the parameters assumed above, only with the parts of the equation arranged in a different way. It will turn out that some of the following calculations are easier when the master equation is written in this form.

5.4.2 Adiabatic elimination - theory

In the bad-cavity limit the cavity modes change on a much faster timescale than any rate of change associated with the atom. The idea then is to treat the cavity as a reservoir, because the light escapes from it quickly compared to the interaction time with the atom. Therefore we can trace out the cavity modes to derive a master equation for the atomic density operator $\rho_{\rm A}$.

The cavity is assumed to be in steady state with the density operator factorized in the form

$$\rho = \rho_{\rm C}^{\rm ss} \otimes \rho_{\rm A}\,. \tag{5.118}$$

We move to an interaction picture defined by

$$\tilde{\rho} = e^{i(H_{\rm A}+H_{\rm C})t}\rho e^{-i(H_{\rm A}+H_{\rm C})t}\,. \tag{5.119}$$

Tracing over the cavity modes yields the density operator in the interaction picture for the atom,

$$\tilde{\rho}_{\rm A} = {\rm Tr}_{\rm C}\{\tilde{\rho}\}\,. \tag{5.120}$$

Then following the standard derivation in the Born-Markov approximation (similar to what was done in Section 3.1, where $H_{\rm A}$ is now the system Hamiltonian and $H_{\rm C}$ the Hamiltonian for the reservoir) we arrive at

$$\dot{\tilde{\rho}}_{\rm A} = -\int_0^t dt' {\rm Tr}_{\rm C}\{[\tilde{H}_{\rm AC}(t), e^{\mathcal{L}_{\rm C}(t-t')}[\tilde{H}_{\rm AC}(t'), \tilde{\rho}_{\rm A}(t')\otimes\tilde{\rho}_{\rm C}(t')]]\} + \tilde{\mathcal{L}}_{\rm A}\tilde{\rho}_{\rm A}\,, \tag{5.121}$$

with

$$\begin{aligned}\tilde{H}_{\rm AC}(t) &= e^{i(H_{\rm A}+H_{\rm C})t}H_{\rm AC}e^{-i(H_{\rm A}+H_{\rm C})t} &(5.122)\\ &= g_1^* a_1^\dagger \sigma_1^-(t)e^{i\omega_{\rm C}t} + g_1 a_1\sigma_1^+(t)e^{-i\omega_{\rm C}t}\\ &\quad + g_1 b_1^\dagger\sigma_1^-(t)e^{i\omega_{\rm C}t} + g_1^* b_1\sigma_1^+(t)e^{-i\omega_{\rm C}t}\\ &\quad + g_2^* a_2^\dagger\sigma_2^-(t)e^{i\omega_{\rm C}t} + g_2 a_2\sigma_2^+(t)e^{-i\omega_{\rm C}t}\\ &\quad + g_2 b_2^\dagger\sigma_2^-(t)e^{i\omega_{\rm C}t} + g_2^* b_2\sigma_2^+(t)e^{-i\omega_{\rm C}t}\,, &(5.123)\end{aligned}$$

and the slowly varying atomic raising and lowering operators

$$\sigma^\pm(t) = e^{iH_{\rm A}t}\sigma^\pm e^{-iH_{\rm A}t}\,, \tag{5.124}$$

and where $\tilde{\mathcal{L}}_{\rm A}\tilde{\rho}_{\rm A}$ denotes the atomic damping term in the interaction picture

$$\begin{aligned}\tilde{\mathcal{L}}_{\rm A}\tilde{\rho}_{\rm A} &= \frac{\gamma_1}{2}\left(2\sigma_1^-(t)\tilde{\rho}_{\rm A}(t)\sigma_1^+(t) - \sigma_1^+(t)\sigma_1^-(t)\tilde{\rho}_{\rm A}(t) - \tilde{\rho}_{\rm A}(t)\sigma_1^+(t)\sigma_1^-(t)\right)\\ &\quad + \frac{\gamma_2}{2}\left(2\sigma_2^-(t)\tilde{\rho}_{\rm A}(t)\sigma_2^+(t) - \sigma_2^+(t)\sigma_2^-(t)\tilde{\rho}_{\rm A}(t) - \tilde{\rho}_{\rm A}(t)\sigma_2^+(t)\sigma_2^-(t)\right)\,.\end{aligned} \tag{5.125}$$

Substituting (5.123) into (5.121) yields

$$\begin{aligned}
\dot{\tilde{\rho}}_{\mathrm{A}} = -\Big(& |g_1|^2 \int_0^t dt' \mathrm{Tr}_{\mathrm{C}} \left[a_1 e^{\mathcal{L}_{\mathrm{C}}(t-t')} a_1^\dagger \tilde{\rho}_{\mathrm{C}}^{\mathrm{ss}}(t') \right] e^{-i\omega_{\mathrm{C}}(t-t')} \\
& \cdot \left(\sigma_1^+(t)\sigma_1^-(t')\tilde{\rho}_{\mathrm{A}}(t') - \sigma_1^-(t')\tilde{\rho}_{\mathrm{A}}(t')\sigma_1^+(t) \right) \\
& + |g_1|^2 \int_0^t dt' \mathrm{Tr}_{\mathrm{C}} \left[a_1^\dagger e^{\mathcal{L}_{\mathrm{C}}(t-t')} \tilde{\rho}_{\mathrm{C}}^{\mathrm{ss}}(t') a_1 \right] e^{i\omega_{\mathrm{C}}(t-t')} \\
& \cdot \left(\tilde{\rho}_{\mathrm{A}}(t')\sigma_1^+(t')\sigma_1^-(t) - \sigma_1^-(t)\tilde{\rho}_{\mathrm{A}}(t')\sigma_1^+(t') \right) \\
& + |g_2|^2 \int_0^t dt' \mathrm{Tr}_{\mathrm{C}} \left[a_2 e^{\mathcal{L}_{\mathrm{C}}(t-t')} a_2^\dagger \tilde{\rho}_{\mathrm{C}}^{\mathrm{ss}}(t') \right] e^{-i\omega_{\mathrm{C}}(t-t')} \\
& \cdot \left(\sigma_2^+(t)\sigma_2^-(t')\tilde{\rho}_{\mathrm{A}}(t') - \sigma_2^-(t')\tilde{\rho}_{\mathrm{A}}(t')\sigma_2^+(t) \right) \\
& + |g_2|^2 \int_0^t dt' \mathrm{Tr}_{\mathrm{C}} \left[a_2^\dagger e^{\mathcal{L}_{\mathrm{C}}(t-t')} \tilde{\rho}_{\mathrm{C}}^{\mathrm{ss}}(t') a_2 \right] e^{i\omega_{\mathrm{C}}(t-t')} \\
& \cdot \left(\tilde{\rho}_{\mathrm{A}}(t')\sigma_2^+(t')\sigma_2^-(t) - \sigma_2^-(t)\tilde{\rho}_{\mathrm{A}}(t')\sigma_2^+(t') \right) \\
& + g_1^* g_2 \int_0^t dt' \mathrm{Tr}_{\mathrm{C}} \left[a_2 e^{\mathcal{L}_{\mathrm{C}}(t-t')} a_1^\dagger \tilde{\rho}_{\mathrm{C}}^{\mathrm{ss}}(t') \right] e^{-i\omega_{\mathrm{C}}(t-t')} \\
& \cdot \left(\sigma_2^+(t)\sigma_1^-(t')\tilde{\rho}_{\mathrm{A}}(t') - \sigma_1^-(t')\tilde{\rho}_{\mathrm{A}}(t')\sigma_2^+(t) \right) \\
& + g_1 g_2^* \int_0^t dt' \mathrm{Tr}_{\mathrm{C}} \left[a_2^\dagger e^{\mathcal{L}_{\mathrm{C}}(t-t')} \tilde{\rho}_{\mathrm{C}}^{\mathrm{ss}}(t') a_1 \right] e^{i\omega_{\mathrm{C}}(t-t')} \\
& \cdot \left(\tilde{\rho}_{\mathrm{A}}(t')\sigma_1^+(t')\sigma_2^-(t) - \sigma_2^-(t)\tilde{\rho}_{\mathrm{A}}(t')\sigma_1^+(t') \right) \\
& + \dots \\
& + b \text{ terms} \Big) + \tilde{\mathcal{L}}_{\mathrm{A}} \tilde{\rho}_{\mathrm{A}} \,. \qquad (5.126)
\end{aligned}$$

In total we get $4 \cdot 8 \cdot 8 = 254$ terms representing all possible combinations of the operators $a_1^\dagger \sigma_1^-$, $a_1 \sigma_1^+$, ... in equation (5.123). These expressions can be further analysed with the quantum regression theorem of Section 3.2. It turns out that the terms written explicitly above (and the corresponding terms for the b modes) are the only ones which do not vanish.

We can relate the traces to two-time correlation functions using equations

$$\langle \hat{O}_1(t)\hat{O}_2(t+\tau)\rangle = \mathrm{Tr}\left[\hat{O}_2 e^{\mathcal{L}\tau}(\rho(t)\hat{O}_1)\right] , \qquad (5.127)$$

$$\langle \hat{O}_1(t+\tau)\hat{O}_2(t)\rangle = \mathrm{Tr}\left[\hat{O}_1 e^{\mathcal{L}\tau}(\hat{O}_2\rho(t))\right] . \qquad (5.128)$$

Furthermore a system of differential equations for these second-order correlation functions can be derived from equations (3.50)-(3.52). The initial values for solving this system can be found by assuming the cavity is in the vacuum state; thus, the only non-zero initial values for the steady state are

$$\langle a_1 a_1^\dagger\rangle_{\mathrm{ss}} = \langle a_2 a_2^\dagger\rangle_{\mathrm{ss}} = \langle b_1 b_1^\dagger\rangle_{\mathrm{ss}} = \langle b_2 b_2^\dagger\rangle_{\mathrm{ss}} = 1 \,. \qquad (5.129)$$

In the bad-cavity limit where the cavity damping is very fast this is a reasonable assumption. After some simple but laborious calculations we find for the non-zero two-time correlation functions in steady state:[5]

$$\langle a_1(t')a_1^\dagger(t)\rangle_{\rm ss} = {\rm Tr_C}\left[a_1 e^{\mathcal{L}_{\rm C}(t-t')}a_1^\dagger\tilde{\rho}_{\rm C}^{\rm ss}(t')\right] = e^{(-\kappa+i\omega_{\rm A})(t-t')}\,, \tag{5.130}$$

$$\langle a_2(t')a_2^\dagger(t)\rangle_{\rm ss} = {\rm Tr_C}\left[a_2 e^{\mathcal{L}_{\rm C}(t-t')}a_2^\dagger\tilde{\rho}_{\rm C}^{\rm ss}(t')\right] = e^{(-\kappa+i\omega_{\rm A})(t-t')}\,, \tag{5.131}$$

$$\langle a_1(t')a_2^\dagger(t)\rangle_{\rm ss} = {\rm Tr_C}\left[a_2 e^{\mathcal{L}_{\rm C}(t-t')}a_1^\dagger\tilde{\rho}_{\rm C}^{\rm ss}(t')\right] = -2\kappa(t-t')e^{(-\kappa+i\omega_{\rm A})(t-t')}\,, \tag{5.132}$$

– with $\langle a_1(t)a_1^\dagger(t')\rangle_{\rm ss}$, $\langle a_2(t)a_2^\dagger(t')\rangle_{\rm ss}$ and $\langle a_2(t)a_1^\dagger(t')\rangle_{\rm ss}$ their complex conjugates – and similar equations for the b modes. For simplicity we assumed the damping rates of the two cavities to be the same, i.e., $\kappa_1 = \kappa_2 = \kappa$.

Applying these results, from equation (5.126), we obtain

$$\begin{aligned}
\dot{\tilde{\rho}}_{\rm A} = -\Big(&|g_1|^2\int_0^t dt' e^{(-\kappa-i\Delta\omega)(t-t')}\cdot(\sigma_1^+(t)\sigma_1^-(t')\tilde{\rho}_{\rm A}(t') \\
&\qquad - \sigma_1^-(t')\tilde{\rho}_{\rm A}(t')\sigma_1^+(t)) \\
&+|g_1|^2\int_0^t dt' e^{(-\kappa+i\Delta\omega)(t-t')}\cdot(\tilde{\rho}_{\rm A}(t')\sigma_1^+(t')\sigma_1^-(t) \\
&\qquad - \sigma_1^-(t)\tilde{\rho}_{\rm A}(t')\sigma_1^+(t')) \\
&+|g_2|^2\int_0^t dt' e^{(-\kappa-i\Delta\omega)(t-t')}\cdot(\sigma_2^+(t)\sigma_2^-(t')\tilde{\rho}_{\rm A}(t') \\
&\qquad - \sigma_2^-(t')\tilde{\rho}_{\rm A}(t')\sigma_2^+(t)) \\
&+|g_2|^2\int_0^t dt' e^{(-\kappa+i\Delta\omega)(t-t')}\cdot(\tilde{\rho}_{\rm A}(t')\sigma_2^+(t')\sigma_2^-(t) \\
&\qquad - \sigma_2^-(t)\tilde{\rho}_{\rm A}(t')\sigma_2^+(t')) \\
&-g_1^*g_2\int_0^t dt' 2\kappa(t-t')e^{(-\kappa-i\Delta\omega)(t-t')}\cdot(\sigma_2^+(t)\sigma_1^-(t')\tilde{\rho}_{\rm A}(t') \\
&\qquad - \sigma_1^-(t')\tilde{\rho}_{\rm A}(t')\sigma_2^+(t)) \\
&-g_1g_2^*\int_0^t dt' 2\kappa(t-t')e^{(-\kappa+i\Delta\omega)(t-t')}\cdot(\tilde{\rho}_{\rm A}(t')\sigma_1^+(t')\sigma_2^-(t) \\
&\qquad - \sigma_2^-(t)\tilde{\rho}_{\rm A}(t')\sigma_1^+(t')) \\
&+ \text{b terms}\Big) + \tilde{\mathcal{L}}_{\rm A}\tilde{\rho}_{\rm A}\,.
\end{aligned} \tag{5.133}$$

In the Markov approximation we assume that the future evolution of the density operator is independent of its past and hence replace $\tilde{\rho}_{\rm A}(t')$ by $\tilde{\rho}_{\rm A}(t)$. The atomic operator $\sigma^\pm(t')$ is slowly varying compared to the cavity damping rate, κ, so it can be assumed constant under the integration (and be replaced by $\sigma^\pm(t)$). For a large

[5] The entire calculations can be found in Appendix A.

κ, i.e., in the limit $\kappa t >> 1$, the remaining integrals can easily be evaluated as

$$\lim_{\kappa t\to\infty}\int_0^t dt' e^{(-\kappa-i\Delta\omega)(t-t')} = \frac{\kappa - i\Delta\omega}{\kappa^2+\Delta\omega^2}\,, \tag{5.134}$$

$$\lim_{\kappa t\to\infty}\int_0^t dt' e^{(-\kappa+i\Delta\omega)(t-t')} = \frac{\kappa + i\Delta\omega}{\kappa^2+\Delta\omega^2}\,, \tag{5.135}$$

$$\lim_{\kappa t\to\infty}\int_0^t dt' 2\kappa(t-t') e^{(-\kappa-i\Delta\omega)(t-t')} = \frac{2\kappa}{(\kappa+i\Delta\omega)^2}\,, \tag{5.136}$$

$$\lim_{\kappa t\to\infty}\int_0^t dt' 2\kappa(t-t') e^{(-\kappa+i\Delta\omega)(t-t')} = \frac{2\kappa}{(\kappa-i\Delta\omega)^2}\,, \tag{5.137}$$

$$\tag{5.138}$$

and a compact form of the master equation is obtained.

5.4.3 The master equation

Moving back out of the interaction picture we finally arrive at the master equation with the cavity modes adiabatically eliminated,

$$\begin{aligned}\dot\rho = -i\,[H,\rho] &+ \frac{\Gamma_1}{2}(2\sigma_1^-\rho\sigma_1^+ - \sigma_1^+\sigma_1^-\rho - \rho\sigma_1^+\sigma_1^-)\\ &+ \frac{\Gamma_2}{2}(2\sigma_2^-\rho\sigma_2^+ - \sigma_2^+\sigma_2^-\rho - \rho\sigma_2^+\sigma_2^-)\\ &+ \frac{\Pi_1}{2}(2\sigma_1^-\rho\sigma_2^+ - \sigma_2^+\sigma_1^-\rho - \rho\sigma_2^+\sigma_1^-)\\ &+ \frac{\Pi_2}{2}(2\sigma_2^-\rho\sigma_1^+ - \sigma_1^+\sigma_2^-\rho - \rho\sigma_1^+\sigma_2^-)\,,\end{aligned} \tag{5.139}$$

with

$$\begin{aligned}H = \omega_{\rm A}\left(\sigma_1^+\sigma_1^- + \sigma_2^+\sigma_2^-\right) + \left(-2\frac{\Delta\omega}{\kappa^2+\Delta\omega^2}\right)\left(|g_1|^2\sigma_1^+\sigma_1^- + |g_2|^2\sigma_2^+\sigma_2^-\right)\\ + 4\frac{\kappa^2\Delta\omega}{(\kappa^2-\Delta\omega^2)^2+4\kappa^2\Delta\omega^2}\left(g_1^*g_2\sigma_2^+\sigma_1^- + g_1g_2^*\sigma_1^+\sigma_2^-\right)\,,\end{aligned} \tag{5.140}$$

$$\Gamma_1 = \gamma_1 + 4|g_1|^2\frac{\kappa}{\kappa^2+\Delta\omega^2}\,, \tag{5.141}$$

$$\Gamma_2 = \gamma_2 + 4|g_2|^2\frac{\kappa}{\kappa^2+\Delta\omega^2}\,, \tag{5.142}$$

$$\Pi_1 = -4g_1^*g_2\frac{\kappa(\kappa^2-\Delta\omega^2)}{(\kappa^2-\Delta\omega^2)^2+4\kappa^2\Delta\omega^2}\,, \tag{5.143}$$

$$\Pi_2 = -4g_1g_2^*\frac{\kappa(\kappa^2-\Delta\omega^2)}{(\kappa^2-\Delta\omega^2)^2+4\kappa^2\Delta\omega^2}\,. \tag{5.144}$$

This master equation is unique in the sense that depending on the detuning it either describes a collective atomic decay, the so-called superradiance, an individual decay of each atom, or a combination of both. In the following two sections we explicitly present the master equations for these two limiting cases and investigate them further.

5.4.4 Collective atomic decay

If we assume the atom-cavity coupling and the atomic damping rates of both atoms to be equal — i.e., $g_1 = g_2 =: g$ and $\gamma_1 = \gamma_2 =: \gamma$ — we obtain $\Gamma_1 = \Gamma_2 := \Gamma$ and $\Pi_1 = \Pi_2 =: \Pi$. Thus, we can write the master equations for the two limiting cases in a very compact form by introducing the collective atomic lowering and raising operators

$$J^{\pm} = \sigma_1^{\pm} - \sigma_2^{\pm} \,. \tag{5.145}$$

In the case of zero detuning, $\Delta\omega = 0$, the Hamiltonian vanishes, apart from the atomic energy terms. The parameter Γ becomes the negative of Π with the atomic damping rate, γ, added. The master equation reads

$$\begin{aligned}\dot{\rho} = -i\,[H,\rho] &+ \frac{X}{2}(2J^-\rho J^+ - J^+J^-\rho - \rho J^+J^-) \\ &+ \frac{\gamma}{2}(2\sigma_1^-\rho\sigma_1^+ - \sigma_1^+\sigma_1^-\rho - \rho\sigma_1^+\sigma_1^-) \\ &+ \frac{\gamma}{2}(2\sigma_2^-\rho\sigma_2^+ - \sigma_2^+\sigma_2^-\rho - \rho\sigma_2^+\sigma_2^-)\,,\end{aligned} \tag{5.146}$$

with

$$H = \omega_{\mathrm{A}}\left(\sigma_1^+\sigma_1^- + \sigma_2^+\sigma_2^-\right) , \tag{5.147}$$

$$X = 4\frac{g^2}{\kappa} \,. \tag{5.148}$$

If the natural damping of the atoms is very small ($\gamma \approx 0$) the atoms mainly decay collectively, as described by the collective atomic operator J. This effect is called superradiance, since the decay rate is larger than the spontaneous decay rate of the individual atoms.[6] It occurs when the atoms can directly "communicate" with each other because they couple to the same reservoir, e.g., because they are confined within a cubic wavelength or couple through a single mode – the so-called single-mode model [BSH71]. More information on superradiance can be found, for example, in [Leh70a, Leh70b, Aga70]. Neglecting the spontaneous emission ($\gamma \approx 0$), the decay rate is given by X, which corresponds to the full width at half maximum (of the emission spectrum). This factor, together with the fact that there are two modes in the cavity that the atom can decay to, explains the linewidth of $8\frac{g^2}{\kappa}$ in the bad-cavity limit mentioned in Section 5.2.4.

Note that we can write the one excited atom state of our system as a superposition of Bell states,

$$|\psi^+\rangle = \frac{1}{\sqrt{2}}(|eg\rangle + |ge\rangle)\,, \tag{5.149}$$

$$|\psi^-\rangle = \frac{1}{\sqrt{2}}(|eg\rangle - |ge\rangle)\,, \tag{5.150}$$

[6] Dicke, who was the first to investigate a collective spontaneous atomic decay in a gas [Dic54], spoke of "super-radiant" states due to the "abnormally large spontaneous radiation rates".

where the first entry in the ket vector denotes atom 1 and the second entry atom 2. Hence, the initial state with one atom excited is

$$|eg\rangle = \frac{1}{\sqrt{2}}(|\psi^+\rangle + |\psi^-\rangle)\,. \tag{5.151}$$

We then find for the action of the collective atomic operators $J^{\pm}$, given by equation (5.145), on the Bell states:

$$J^+|\psi^+\rangle = 0\,, \qquad J^-|\psi^+\rangle = 0\,, \tag{5.152}$$

$$J^+|\psi^-\rangle = \frac{2}{\sqrt{2}}|ee\rangle\,, \qquad J^-|\psi^-\rangle = \frac{2}{\sqrt{2}}|gg\rangle\,. \tag{5.153}$$

It follows that the Bell state $|\psi^+\rangle$ is a dark state, i.e., if we can neglect the spontaneous decay, γ, the state does not decay. Instead, the state and the associated density operator evolves unitarily in time under the Liouville equation

$$\dot{\rho} = -i\,[H, \rho]\ . \tag{5.154}$$

In this case the radiation travels back and forth between the atoms, always exciting them and being emitted again. It is trapped between the atoms until it eventually leaves the cavity due to the decay of the atom out the sides of the cavity, at rate γ.

Numerical results

We illustrate the behaviour described by the master equation with adiabatic elimination, discussed in the previous section, by means of numerical results obtained from the full model by solving equations (5.22)-(5.27). These investigations will enable us to explain the features which occurred in the numerical solutions of the full model shown in Figures 5.3 and 5.4.

In Figure 5.6 the evolution of the probabilities α for atom 1 being in the excited state and ξ for atom 2 being in the excited state are shown for an initial state of atom 1 being excited ($\alpha(0) = 1$ and all other initial probability amplitudes zero). It can be seen that without any possible losses out of the side of the cavity ($\gamma = 0$, $\kappa_{\rm i} = 0$) the probability for atom 1 being excited rapidly decays from the initial value of $|\alpha|^2 = 1$ to a constant, non-zero value of $|\alpha|^2 = 0.25$, whereas the probability for atom 2 being excited increases from the initial value of $|\xi|^2 = 0$ to $|\xi|^2 = 0.25$. Hence, with the probability $P = 0.5$ the system is trapped in a state where the photon is transferred back and forth between the two atoms due to the dark state, and with the probability $P_{\rm ground} = 0.5$ the system decays to the ground state due to the decay of the state $|\psi^-\rangle$. If we allow for spontaneous emission out of the side of the cavity ($\gamma \neq 0$) the probability for either atom 1 or atom 2 being excited eventually decays to zero on a timescale of γ^{-1}, i.e., the dark state eventually decays via the additional loss channel.

In Figure 5.7 the emission spectra are plotted for initial states $|\psi(0)\rangle = |\psi^+\rangle$ and $|\psi(0)\rangle = |\psi^-\rangle$ with a possible atomic damping of $\gamma = 5$. The graphs were once again

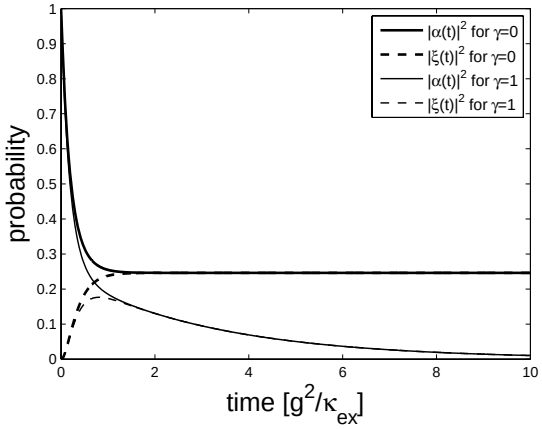

FIGURE 5.6: Evolution of the probabilities for atom 1 to be excited (α) and for atom 2 to be excited (ξ), plotted with ($\gamma = 1$) and without ($\gamma = 0$) a possibly spontaneous emission of the atoms. Atom 1 is initially excited, the cavity damping rate is $\kappa_{\rm ex} = 800$ and the other parameters are $g = 50$, $\kappa_{\rm i} = 0$, $h = 0$ and $\Delta\omega = 0$.

obtained from the full model. If the system is initially in the dark state, there is almost no emission along the axis. Instead, almost all the radiation is emitted via spontaneous emission of the atom out the side of the cavity. The emission probability (obtained from equations (5.33) and (5.34)) for emission along the axis is $P_{\rm axis} = 0.02$ and for emission out of the side of the cavity $P_{\rm side} = 0.98$. The small emission along the axis arises because we are not perfectly in the bad-cavity regime. The broad linewidth in this case relates to the cavity linewidth, κ, with the sharp dip in the middle due to the strong emission out of the side of the cavity by the atom in this frequency range. In contrast, the linewidth of the emission out of the side of the cavity, which relates to the atomic decay, γ, is very small. For the initial state $|\psi(0)\rangle = |\psi^-\rangle$, most of the light is emitted along the axis ($P_{\rm axis} = 0.87$) and only a small part is emitted out of the sides of the cavity ($P_{\rm side} = 0.12$) due to the small atomic decay rate, γ. The linewidth of the emission spectra in this case is determined by the decay rate $4\frac{g^2}{\kappa}$ from the master equation (5.146).

The same is true if light is emitted out the side of the cavity by the internal loss, κ_i, instead of the atomic damping, γ. In Figure 5.8 the emission spectra are plotted for an internal loss of $\kappa_i = 20$. In the case of the dark state, $|\psi^+\rangle$, most of the light is emitted out of the side of the cavity ($P_{\rm axis} = 0.09$ and $P_{\rm side} = 0.91$), whereas, in the case of the state $|\psi^-\rangle$ most of the light is emitted along the axis ($P_{\rm axis} = 0.89$ and $P_{\rm side} = 0.10$). Note that for the dark state, the internal loss causes a very narrow and high peak for both emissions, $T_{\rm axis}$ and $T_{\rm side}$. For emission $T_{\rm axis}$ the high peak occurs on top of the broad cavity linewidth. This is in contrast to the previous case with $\gamma \neq 0$ and $\kappa_i = 0$ (Figure 5.7).

The combination of the graphs for the initial states $|\psi^+\rangle$ and $|\psi^-\rangle$ can now qualitatively describe the features seen on the graphs for an initial state of atom 1

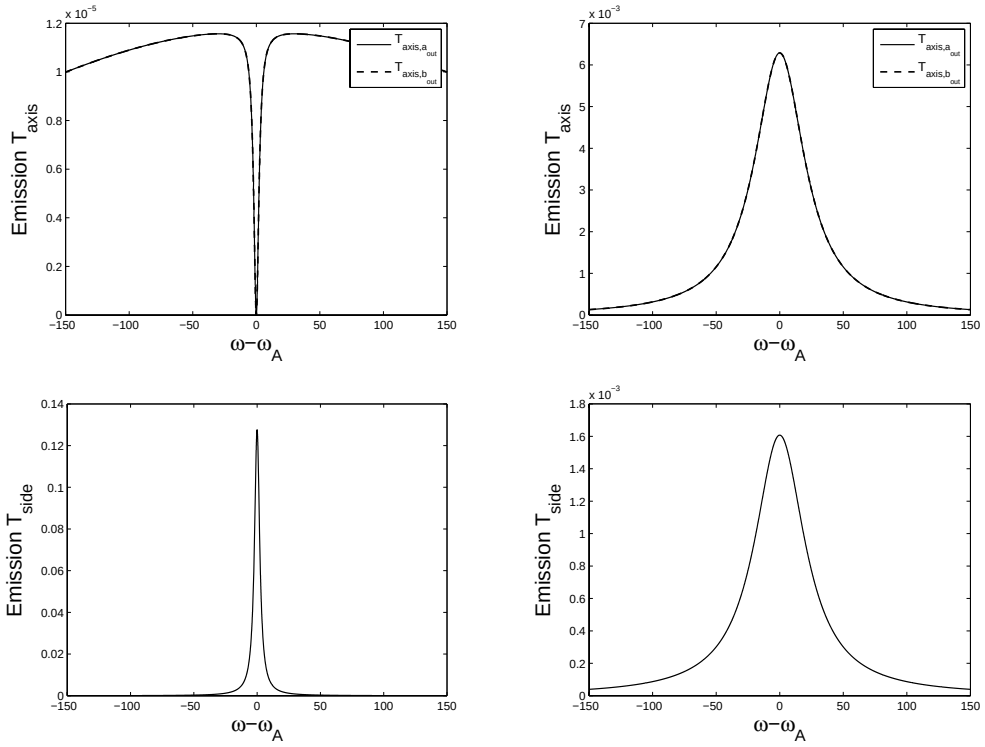

(a) initial state $|\psi^+\rangle$ (b) initial state $|\psi^-\rangle$

FIGURE 5.7: Emission spectra $T_{\text{axis},a_{\text{out}}}$, $T_{\text{axis},b_{\text{out}}}$ (top row) and $T_{\text{side,total}}$ (bottom row) as a function of frequency, plotted for the initial state $|\psi^+\rangle$ (left column) and $|\psi^-\rangle$ (right column) in the case of spontaneous emission, $\gamma = 5$. $T_{\text{axis},a_{\text{out}}}$ and $T_{\text{axis},b_{\text{out}}}$ coincide. The other parameters are $\kappa_{\text{ex}} = 500$, $g = 50$, $\kappa_{\text{i}} = 0$, $h = 0$ and $\Delta\omega = 0$.

being excited (Figures 5.3 and 5.4). Especially the sharp peak on top of the broad emission for T_{axis}, in the case of a finite internal loss, κ_{i}, (see Figure 5.4). This can be explained by the high peak for T_{axis} when the system is initially in the dark state (see Figure 5.8).

5.4.5 Individual atomic decay

In the individual atomic decay scenario we make the same simplifying assumptions as in the previous section. Then, in the case that the detuning is equal to the damping rate of the cavity, $\Delta\omega = \kappa$, the parameter Π vanishes and Γ reduces to the cavity-enhanced spontaneous emission rate [Car08]. The Hamiltonian can be written in terms of the atomic energy part (for the two atoms) plus an additional energy term

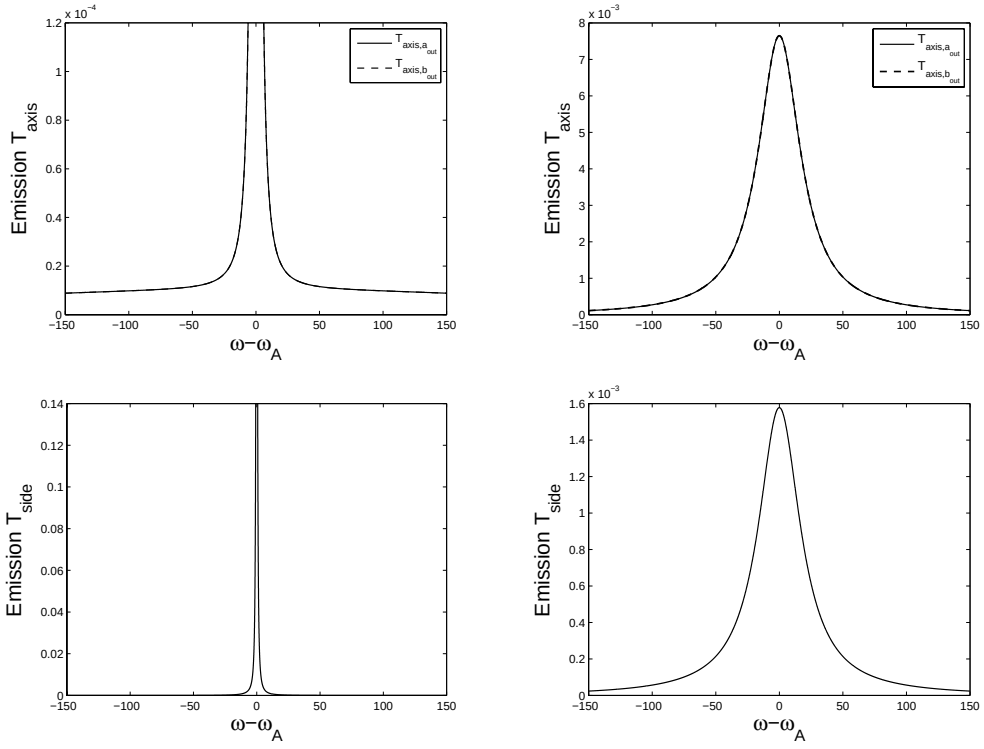

(a) initial state $|\psi^+\rangle$ (b) initial state $|\psi^-\rangle$

FIGURE 5.8: Emission spectra $T_{\text{axis},a_{\text{out}}}$, $T_{\text{axis},b_{\text{out}}}$ (top row) and $T_{\text{side,total}}$ (bottom row) as a function of frequency, plotted for the initial state $|\psi^+\rangle$ (left column) and $|\psi^-\rangle$ (right column) in the case of internal cavity decay, $\kappa_{\text{i}} = 20$. $T_{\text{axis},a_{\text{out}}}$ and $T_{\text{axis},b_{\text{out}}}$ coincide. The other parameters are $\kappa_{\text{ex}} = 500$, $g = 50$, $\gamma = 0$, $h = 0$ and $\Delta\omega = 0$.

for a collective atom ($-\frac{g^2}{\kappa}J^+J^-$). The master equation reads

$$\dot{\rho} = -i\,[H,\rho] + \frac{Y}{2}(2\sigma_1^-\rho\sigma_1^+ - \sigma_1^+\sigma_1^-\rho - \rho\sigma_1^+\sigma_1^-) + \frac{Y}{2}(2\sigma_2^-\rho\sigma_2^+ - \sigma_2^+\sigma_2^-\rho - \rho\sigma_2^+\sigma_2^-)\,, \tag{5.155}$$

with

$$H = \omega_{\mathrm{A}}\left(\sigma_1^+\sigma_1^- + \sigma_2^+\sigma_2^-\right) - \frac{g^2}{\kappa}J^+J^-\,, \tag{5.156}$$

$$Y = \gamma + 2\frac{g^2}{\kappa}\,. \tag{5.157}$$

Here, in contrast to the collective decay (5.146), the atoms decay independently, at a rate determined mainly by $\frac{g^2}{\kappa}$.

Note that the energy of the Bell state $|\psi^-\rangle$ is shifted by

$$-\frac{g^2}{\kappa}J^+J^-|\psi^-\rangle = -2\frac{g^2}{\kappa}|\psi^-\rangle\,, \tag{5.158}$$

whereas the energy of the Bell state $|\psi^+\rangle$ is not shifted,

$$-\frac{g^2}{\kappa}J^+J^-|\psi^+\rangle = 0\,. \tag{5.159}$$

Numerical results

The energy shift of the Bell state $|\psi^-\rangle$ is the key to explaining the behaviour of the emission spectra for the case of an initial state with only atom 1 excited and detuning $\Delta\omega = \kappa$ (Figure 5.9). The emission spectra for the two Bell states are plotted in Figure 5.10 for an atomic decay rate of $\gamma = 5$.[7] The peak for the state $|\psi^-\rangle$ is indeed shifted by approximately $-2\frac{g^2}{\kappa}$ as anticipated from the master equation with adiabatic elimination. Also, the full widths at half maximum of the emission spectra for $|\psi^+\rangle$ and $|\psi^-\rangle$ are approximately $2\frac{g^2}{\kappa}$, as predicted, by this master equation. The emission spectra for the case of atom 1 initially excited can now be qualitatively explained as a combination of the spectra for $|\psi^+\rangle$ and $|\psi^-\rangle$ plus some interference terms. We find that the linewidth is approximately the sum of the two linewidths of the Bell states and that the linewidth decreases with increasing κ_{ex}, since the peak of the Bell state $|\psi^-\rangle$ is less shifted. Also, the dip in the emission spectrum $T_{\mathrm{axis},b_{\mathrm{out}}}$ moves towards zero detuning with increasing κ_{ex} (c.f. Figure 5.11).

[7] The case $\gamma = 0$, $\kappa_{\mathrm{i}} \neq 0$ (which was plotted for the collective atomic decay) is omitted, since the overall shape of the graphs are qualitatively similar to the case $\gamma = 0$, $\kappa_{\mathrm{i}} \neq 0$, plotted in Figure 5.10.

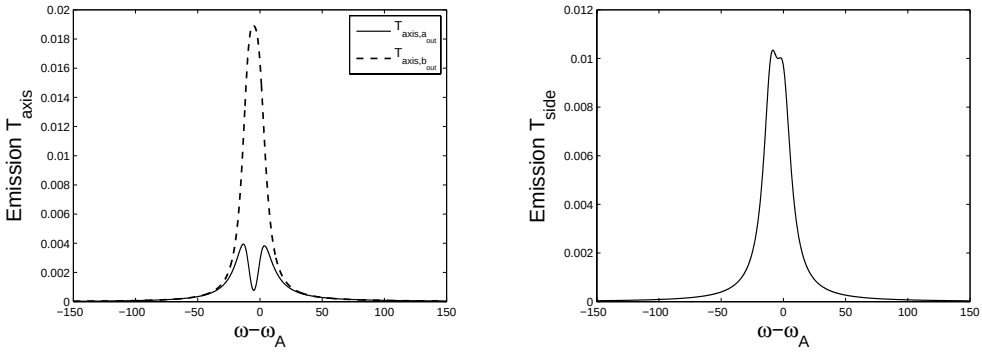

FIGURE 5.9: Emission spectra $T_{\mathrm{axis},a_{\mathrm{out}}}$, $T_{\mathrm{axis},b_{\mathrm{out}}}$ (left) and $T_{\mathrm{side,total}}$ (right) as a function of frequency, plotted for an initial state of atom 1 excited with detuning $\Delta\omega = \kappa$. The other parameters are $\kappa_{\mathrm{ex}} = 500$, $g = 50$, $\gamma = 5$, $\kappa_{\mathrm{i}} = 0$ and $h = 0$.

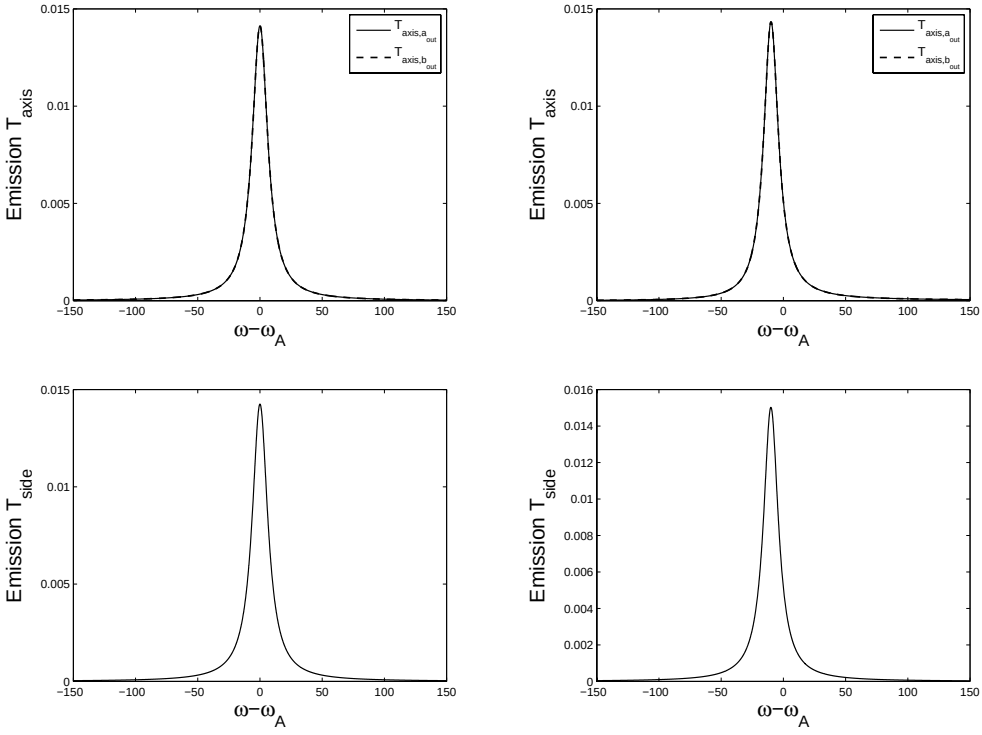

(a) initial state $|\psi^+\rangle$ (b) initial state $|\psi^-\rangle$

FIGURE 5.10: Emission spectra $T_{\mathrm{axis},a_{\mathrm{out}}}$, $T_{\mathrm{axis},b_{\mathrm{out}}}$ (top row) and $T_{\mathrm{side,total}}$ (bottom row) as a function of frequency, plotted for the initial state $|\psi^+\rangle$ (left column) and $|\psi^-\rangle$ (right column) in the case of detuning $\Delta\omega = \kappa$. $T_{\mathrm{axis},a_{\mathrm{out}}}$ and $T_{\mathrm{axis},b_{\mathrm{out}}}$ coincide. The other parameters are $\kappa_{\mathrm{ex}} = 500$, $g = 50$, $\gamma = 5$, $\kappa_{\mathrm{i}} = 0$ and $h = 0$.

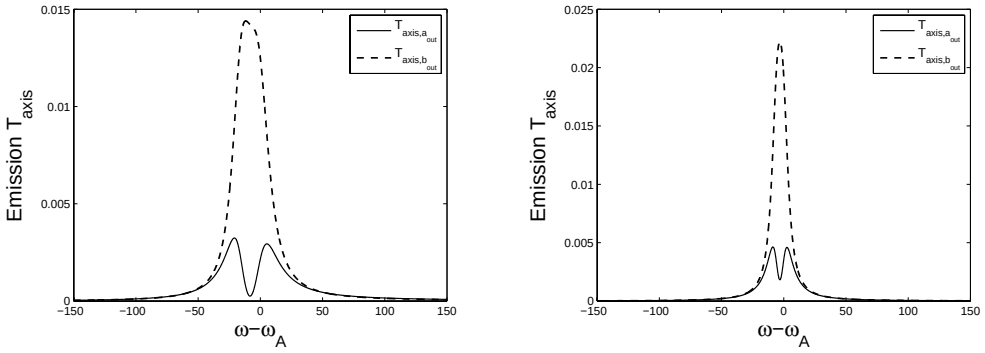

(a) $\kappa_{\mathrm{ex}} = 300$ (b) $\kappa_{\mathrm{ex}} = 800$

FIGURE 5.11: Emission spectra $T_{\mathrm{axis},a_{\mathrm{out}}}$ and $T_{\mathrm{axis},b_{\mathrm{out}}}$ as a function of frequency for the initial state of atom 1 excited. Plotted for a cavity decay rate of $\kappa_{\mathrm{ex}} = 300$ (left) and $\kappa_{\mathrm{ex}} = 800$ (right) in the case of detuning $\Delta\omega = \kappa$. The other parameters are $g = 50$, $\gamma = 5$, $\kappa_{\mathrm{i}} = 0$ and $h = 0$.

5.5 Strong-coupling limit

In this section we will investigate the emission spectra in the strong-coupling limit. This limit is of particular interest for future applications in quantum information where a strong coupling between the atom and the photon is required. The strong-coupling regime is determined by a large atom-cavity coupling, g, compared to the damping rates of the cavity, κ, and the atom, γ,

$$g >> \kappa, \gamma\,. \tag{5.160}$$

In this limit we cannot make the same simplifying assumptions we did for the bad-cavity regime (in particular we cannot adiabatically eliminate the cavity modes). Hence, an analytical treatment of the full system is much more complicated and we will only consider the numerical treatment. We start with the simplest system, the 1T1A system. The insights we gain from this simple case will then be applied to the more complex systems.

5.5.1 1-toroid-1-atom system

The emission spectrum of a two-level atom coupled to a resonant cavity mode has been investigated theoretically, for example, in [SMNE83] and [CBR$^+$89]. For the strong-coupling limit the emission spectrum is found to be a doublet, split by the vacuum Rabi splitting (here $2\sqrt{2}g$). The fullwidth of each peak of the doublet is $\kappa + \frac{\gamma}{2}$. These results are reproduced by solving the 1T1A model from Section 5.3.2 numerically in the strong-coupling limit (see Figure 5.12). However, now we allow for two counter-propagating WGMs that the atom can decay to and a coupling between the modes with strength h. When the coupling is turned on, an imbalance between the two peaks occurs and they are shifted by h. This can be explained by the different

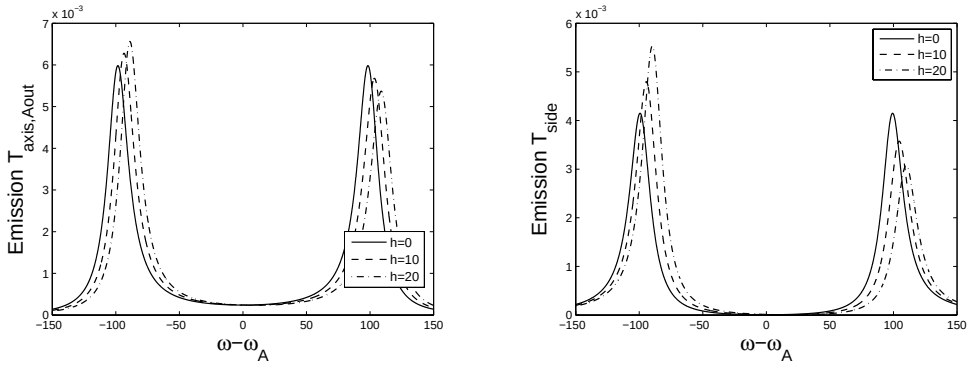

FIGURE 5.12: Emission spectra $T_{\mathrm{axis},a_{\mathrm{out}}}$ (left) and T_{side} (right) as a function of frequency for the 1T1A system. Note that the emission spectrum $T_{\mathrm{axis},b_{\mathrm{out}}}$ is the same as $T_{\mathrm{axis},a_{\mathrm{out}}}$ and is omitted. The emission spectra are plotted for $h = 0$ (solid line), $h = 10$ (dashed line) and $h = 20$ (dash-dot line). The other parameters are $\kappa_{\mathrm{ex}} = 15$, $g = 70$, $\gamma = 10$, $\kappa_{\mathrm{i}} = 0$ and $\Delta\omega = 0$.

coupling of the atom to the two normal modes of the system. We can express the system Hamiltonian and the damping terms in the master equation in terms of the normal modes of the cavity [DPA+08b], defined by

$$A = \frac{a+b}{\sqrt{2}} \qquad \text{and} \qquad B = \frac{a-b}{\sqrt{2}}\,. \tag{5.161}$$

Explicitly, we have

$$\begin{aligned}\dot{\rho} = &-i\,[H,\rho] + \kappa(2A\rho A^\dagger - A^\dagger A\rho - \rho A^\dagger A) + \kappa(2B\rho B^\dagger - B^\dagger B\rho - \rho B^\dagger B)\\ &+ \frac{\gamma}{2}(2\sigma^-\rho\sigma^+ - \sigma^+\sigma^-\rho - \rho\sigma^+\sigma^-)\,,\end{aligned} \tag{5.162}$$

with

$$\begin{aligned}H = &(\omega_{\mathrm{C}} + h)A^\dagger A + (\omega_{\mathrm{C}} - h)B^\dagger B + \omega_A\sigma^+\sigma^-\\ &+ \sqrt{2}\mathrm{Re}\{g\}(A^\dagger\sigma^- + \sigma^+A) - i\sqrt{2}\mathrm{Im}\{g\}(B^\dagger\sigma^- - \sigma^+B)\,.\end{aligned} \tag{5.163}$$

Thus, for a real valued g (as was chosen in Figure 5.12), the atom is only coupled to the normal mode A, with the cavity frequency $\omega_{\mathrm{C}} + h$, which accounts for the shift of the peaks.

5.5.2 More complex systems

We will consider the 2T1A system and the "full" 2T2A system. The following results were again obtained by solving equations (5.89)-(5.93) and (5.52)-(5.57), respectively, numerically, where we assume the cavity parameters to be the same and set the phase factors, ϕ_a and ϕ_b, to zero.

When adding another cavity (Figure 5.13) or another cavity with an atom in the ground state also coupled (Figure 5.14) the overall shape of the graphs still remains the same. In particular, there is still the doublet, split by a factor of $2\sqrt{2}g$ and with the same dependence on h (e.g., imbalance between the peaks and shift of the peaks by h). But there are also obvious differences. The emission spectra $T_{\text{axis},a_{\text{out}}}$ and $T_{\text{axis},b_{\text{out}}}$ are not the same any more since adding another cavity (in the case that only one of the atoms is initially excited) breaks the symmetry. Also, in the case of a coupling between the cavity modes ($h \neq 0$), a dispersive-like feature occurs in between the two peaks at the position of $\omega - \omega_{\text{A}} = -h$, which is connected to an increased emission of the atom out of the side of the cavity at this frequency. For the 2T2A system, in the case of no coupling between the modes, the atoms emit light very strongly at their natural frequency (sharp peak for the emission spectrum T_{side} at $\omega = \omega_{\text{A}}$) and hence a dip occurs in the emission spectrum T_{axis} at this frequency. This does not occur in the 2T1A system. In the 2T2A system the peaks of the doublet also have a more complicated shape. We cannot explain all the features which occur here, but the dispersive-like feature is clearly connected to the value of h and is shifted in the opposite direction to the peaks. Hence, its occurrence is probably due to the coupling of the atom to what we called the normal mode B of the cavity in the 1T1A system, which has frequency $\omega - h$.[8] Further investigation is required in order to understand the origin of these features.

[8] To be correct, in the case of coupled cavities we need to find the normal modes of the total Hamiltonian and cannot just use the "local" normal modes of the separate cavities (which would be A and B). This involves finding the eigenvalues of the total Hamiltonian which seems not possible to do analytically.

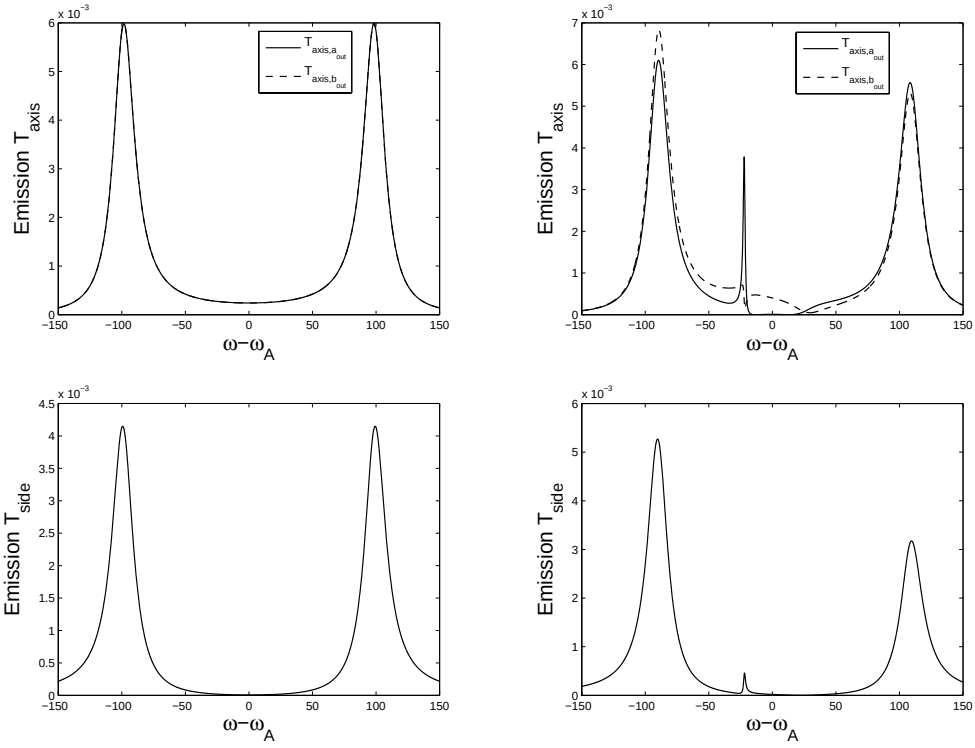

(a) $h = 0$ (b) $h = 20$

FIGURE 5.13: Emission spectra $T_{\mathrm{axis},a_{\mathrm{out}}}$, $T_{\mathrm{axis},b_{\mathrm{out}}}$ (top row) and $T_{\mathrm{side,total}}$ (bottom row) as a function of frequency for the 2T1A system, plotted for a coupling constant $h = 0$ (left column) and $h = 20$ (right column). The other parameters are $\kappa_{\mathrm{ex}} = 15$, $g = 70$, $\gamma = 10$, $\kappa_{\mathrm{i}} = 0$ and $\Delta\omega = 0$.

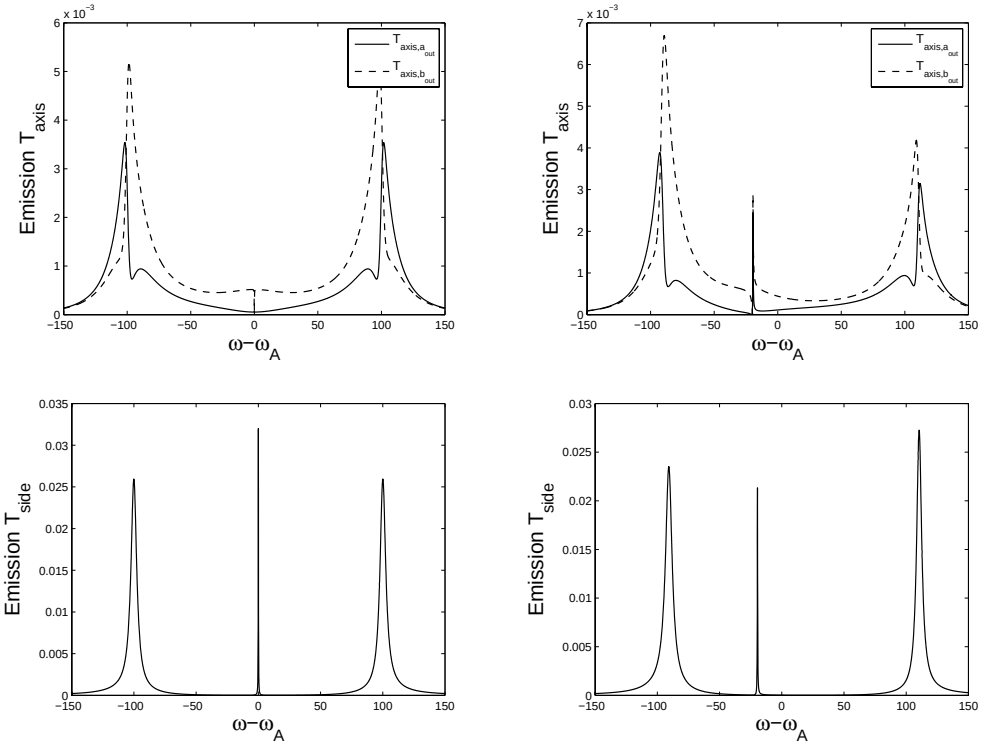

(a) $h = 0$ (b) $h = 20$

FIGURE 5.14: Emission spectra $T_{\mathrm{axis},a_{\mathrm{out}}}$, $T_{\mathrm{axis},b_{\mathrm{out}}}$ (top row) and $T_{\mathrm{side,total}}$ (bottom row) as a function of frequency for the 2T2A system, plotted for a coupling constant $h = 0$ (left column) and $h = 20$ (right column). The other parameters are $\kappa_{\mathrm{ex}} = 15$, $g = 70$, $\gamma = 10$, $\kappa_{\mathrm{i}} = 0$ and $\Delta\omega = 0$. Atom 1 is initially excited.

Chapter 6

Driven Cascaded System

In this chapter we will study an extension of the spontaneous emission system presented in the previous chapter. Instead of an atom being initially excited and observing the emission spectrum, we drive the cascaded system with a coherent light source (laser) and examine the output flux of the driven system.

The theoretical model will be presented in the first section. In the second section we will present analytical results which are obtained for a simpler system, namely the 2T0A system. The general system is too complicated to analyse analytically, hence we will restrict ourselves to a numerical investigation. This is done in the third section, where results for the 2T2A system will be presented for the strong-coupling and the bad-cavity regime and will be compared to the 2T1A and the 2T0A system. In the fourth section a method will be presented that allows us to describe the cascaded system in terms of the single-toroid system which has already been studied in some detail [ADW$^+$06a, DPA$^+$08a].

6.1 The theoretical model

The cascaded system we are interested in comprises two microtoroidal resonators with a single atom coupled to each of the toroids. The system is driven by an external light source which is experimentally realized with a laser. The coherent light of the laser is sent through a fibre (connecting the two toroids) and couples into the microcavities through the evanescent field. A schematic of the system is shown in Figure 6.1. We are interested in the output photon fluxes.

The theoretical model is, in principle, very similar to the model for spontaneous emission described in Section 5.1, but with an external, coherent driving term added to the system Hamiltonian.

6.1.1 Hamiltonian and master equation

To describe the driven system we have to take the external driving into account. How this is done was outlined in Section 4.2.2. If we allow for driving from both

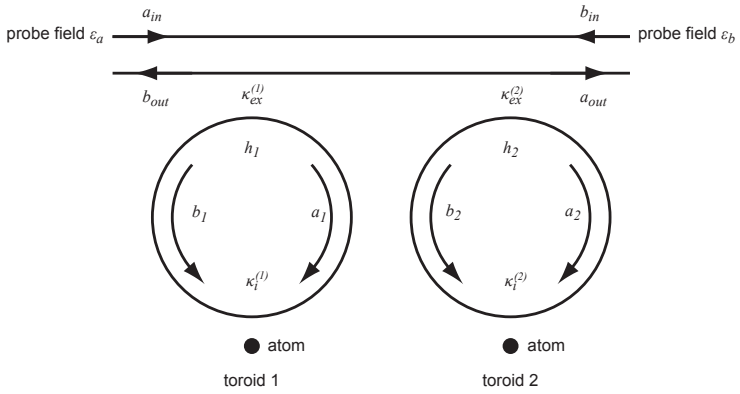

FIGURE 6.1: Schematic of a driven cascaded microtoroid system.

directions, the system Hamiltonian reads[1]

$$H = H_1 + H_2 + H_{12}\,, \tag{6.1}$$

with

$$\begin{aligned} H_1 &= \omega_{\mathrm{C}_1}(a_1^\dagger a_1 + b_1^\dagger b_1) + (h_1 a_1^\dagger b_1 + h_1^* b_1^\dagger a_1) + (\mathcal{E}_a^* e^{i\omega_\mathrm{p} t} a_1 + \mathcal{E}_a e^{-i\omega_\mathrm{p} t} a_1^\dagger) \\ &\quad + \sqrt{\kappa_{ex}^{(1)}/\kappa_{ex}^{(2)}}(\mathcal{E}_b^* e^{-i\phi_b} e^{i\omega_\mathrm{p} t} b_1 + \mathcal{E}_b e^{i\phi_b} e^{-i\omega_\mathrm{p} t} b_1^\dagger) \\ &\quad + \omega_{\mathrm{A}_1}\sigma_1^+\sigma_1^- + (g_1^* a_1^\dagger \sigma_1^- + g_1 \sigma_1^+ a_1) + (g_1 b_1^\dagger \sigma_1^- + g_1^* \sigma_1^+ b_1)\,, \end{aligned} \tag{6.2}$$

$$\begin{aligned} H_2 &= \omega_{\mathrm{C}_2}(a_2^\dagger a_2 + b_2^\dagger b_2) + (h_2 a_2^\dagger b_2 + h_2^* b_2^\dagger a_2) + (\mathcal{E}_b^* e^{i\omega_\mathrm{p} t} b_2 + \mathcal{E}_b e^{-i\omega_\mathrm{p} t} b_2^\dagger) \\ &\quad + \sqrt{\kappa_{\mathrm{ex}}^{(2)}/\kappa_{\mathrm{ex}}^{(1)}}(\mathcal{E}_a^* e^{-i\phi_a} e^{i\omega_\mathrm{p} t} a_2 + \mathcal{E}_a e^{i\phi_a} e^{-i\omega_\mathrm{p} t} a_2^\dagger) \\ &\quad + \omega_{\mathrm{A}_2}\sigma_2^+\sigma_2^- + (g_2^* a_2^\dagger \sigma_2^- + g_2 \sigma_2^+ a_2) + (g_2 b_2^\dagger \sigma_2^- + g_2^* \sigma_2^+ b_2)\,, \end{aligned} \tag{6.3}$$

$$\begin{aligned} H_{12} &= i\sqrt{\kappa_{\mathrm{ex}}^{(1)}\kappa_{\mathrm{ex}}^{(2)}}(e^{-i\phi_a} a_1^\dagger a_2 - e^{i\phi_a} a_2^\dagger a_1) \\ &\quad + i\sqrt{\kappa_{\mathrm{ex}}^{(1)}\kappa_{\mathrm{ex}}^{(2)}}(e^{-i\phi_b} b_2^\dagger b_1 - e^{i\phi_b} b_1^\dagger b_2)\,, \end{aligned} \tag{6.4}$$

where ω_p is the probe frequency and $\mathcal{E}_a$ ($\mathcal{E}_b$) a complex field amplitude for the driving in the direction of a_in (b_in). The other parameters are the same as in the modelling of spontaneous emission presented in Section 5.1.1.

To simplify the calculations in the following sections, we move to a frame rotating at the probe frequency ω_p.[2] The Hamiltonian in the rotating frame is

$$H' = H_1' + H_2' + H_{12}'\,, \tag{6.5}$$

[1] We set $\hbar = 1$ throughout this chapter.

[2] For more information about transforming to a rotating frame see Appendix B.

with

$$\begin{aligned}
H_1' &= \Delta\omega_{\mathrm{C}_1}(a_1^\dagger a_1 + b_1^\dagger b_1) + (h_1 a_1^\dagger b_1 + h_1^* b_1^\dagger a_1) + (\mathcal{E}_a^* a_1 + \mathcal{E}_a a_1^\dagger) \\
&\quad + \sqrt{\kappa_{ex}^{(1)}/\kappa_{ex}^{(2)}}(\mathcal{E}_b^* e^{-i\phi_b} b_1 + \mathcal{E}_b e^{i\phi_b} b_1^\dagger) \\
&\quad + \Delta\omega_{\mathrm{A}_1}\sigma_1^+\sigma_1^- + (g_1^* a_1^\dagger \sigma_1^- + g_1\sigma_1^+ a_1) + (g_1 b_1^\dagger \sigma_1^- + g_1^*\sigma_1^+ b_1)\,, \qquad (6.6) \\
H_2' &= \Delta\omega_{\mathrm{C}_2}(a_2^\dagger a_2 + b_2^\dagger b_2) + (h_2 a_2^\dagger b_2 + h_2^* b_2^\dagger a_2) + (\mathcal{E}_b^* b_2 + \mathcal{E}_b b_2^\dagger) \\
&\quad + \sqrt{\kappa_{\mathrm{ex}}^{(2)}/\kappa_{\mathrm{ex}}^{(1)}}(\mathcal{E}_a^* e^{-i\phi_a} a_2 + \mathcal{E}_a e^{i\phi_a} a_2^\dagger) \\
&\quad + \Delta\omega_{\mathrm{A}_2}\sigma_2^+\sigma_2^- + (g_2^* a_2^\dagger \sigma_2^- + g_2\sigma_2^+ a_2) + (g_2 b_2^\dagger \sigma_2^- + g_2^*\sigma_2^+ b_2)\,, \qquad (6.7) \\
H_{12}' &= i\sqrt{\kappa_{\mathrm{ex}}^{(1)}\kappa_{\mathrm{ex}}^{(2)}}(e^{-i\phi_a} a_1^\dagger a_2 - e^{i\phi_a} a_2^\dagger a_1) \\
&\quad + i\sqrt{\kappa_{\mathrm{ex}}^{(1)}\kappa_{\mathrm{ex}}^{(2)}}(e^{-i\phi_b} b_2^\dagger b_1 - e^{i\phi_b} b_1^\dagger b_2)\,, \qquad (6.8)
\end{aligned}$$

where $\Delta\omega_{\mathrm{C}_1} = \omega_{\mathrm{C}_1} - \omega_{\mathrm{p}}$ and $\Delta\omega_{\mathrm{C}_2} = \omega_{\mathrm{C}_2} - \omega_{\mathrm{p}}$ are detunings between the frequency of cavity 1 and cavity 2, respectively and the probe frequency, and $\Delta\omega_{\mathrm{A}_1} = \omega_{\mathrm{A}_1} - \omega_{\mathrm{p}}$ and $\Delta\omega_{\mathrm{A}_2} = \omega_{\mathrm{A}_2} - \omega_{\mathrm{p}}$ are detunings between the transition frequency of atom 1 and atom 2, respectively and the probe frequency.

The master equation for the system (in the rotating frame) reads,

$$\begin{aligned}
\dot{\rho} = -i\,[H', \rho] &+ (J_a \rho J_a^\dagger - \frac{1}{2}J_a^\dagger J_a \rho - \frac{1}{2}\rho J_a^\dagger J_a) + (J_b \rho J_b^\dagger - \frac{1}{2}J_b^\dagger J_b \rho - \frac{1}{2}\rho J_b^\dagger J_b) \\
&+ \kappa_{\mathrm{i}}^{(1)}(2a_1\rho a_1^\dagger - a_1^\dagger a_1 \rho - \rho a_1^\dagger a_1) + \kappa_{\mathrm{i}}^{(1)}(2b_1\rho b_1^\dagger - b_1^\dagger b_1\rho - \rho b_1^\dagger b_1) \\
&+ \kappa_{\mathrm{i}}^{(2)}(2a_2\rho a_2^\dagger - a_2^\dagger a_2\rho - \rho a_2^\dagger a_2) + \kappa_{\mathrm{i}}^{(2)}(2b_2\rho b_2^\dagger - b_2^\dagger b_2\rho - \rho b_2^\dagger b_2) \\
&+ \frac{\gamma_1}{2}(2\sigma_1^-\rho\sigma_1^+ - \sigma_1^+\sigma_1^-\rho - \rho\sigma_1^+\sigma_1^-) \\
&+ \frac{\gamma_2}{2}(2\sigma_2^-\rho\sigma_2^+ - \sigma_2^+\sigma_2^-\rho - \rho\sigma_2^+\sigma_2^-)\,, \qquad (6.9)
\end{aligned}$$

with the jump operators

$$J_a = \sqrt{2\kappa_{\mathrm{ex}}^{(1)}}a_1 + e^{-i\phi_a}\sqrt{2\kappa_{\mathrm{ex}}^{(2)}}a_2\,, \qquad (6.10)$$

$$J_b = \sqrt{2\kappa_{\mathrm{ex}}^{(2)}}b_2 + e^{-i\phi_b}\sqrt{2\kappa_{\mathrm{ex}}^{(1)}}b_1\,. \qquad (6.11)$$

6.1.2 Input and output fields

In Section 4.1, where the theory of inputs and outputs in optical cavities was presented, the output field operators were found to be

$$a_{\mathrm{out}}(t) = -a_{\mathrm{in}}(t) + J_a(t)\,, \qquad (6.12)$$

$$b_{\mathrm{out}}(t) = -b_{\mathrm{in}}(t) + J_b(t)\,. \qquad (6.13)$$

The inputs to modes a and b are coherent probe fields and can be written in terms of the driving fields that appear in the Hamiltonian

$$\langle a_{\rm in}\rangle = -\frac{i\mathcal{E}_a}{\sqrt{2\kappa_{\rm ex}^{(1)}}} \qquad \text{and} \qquad \langle b_{\rm in}\rangle = -\frac{i\mathcal{E}_b}{\sqrt{2\kappa_{\rm ex}^{(2)}}}\,. \tag{6.14}$$

In the case of sufficiently weak driving we need only consider the mean field. Hence the cavity output fields are

$$\langle a_{\rm out}(t)\rangle = \frac{i\mathcal{E}_a}{\sqrt{2\kappa_{\rm ex}^{(1)}}} + \langle J_a(t)\rangle\,, \tag{6.15}$$

$$\langle b_{\rm out}(t)\rangle = \frac{i\mathcal{E}_b}{\sqrt{2\kappa_{\rm ex}^{(1)}}} + \langle J_b(t)\rangle\,. \tag{6.16}$$

6.2 Analytical investigations – 2-toroids-no-atom system

For the simpler system consisting of two "plain" microtoroidal resonators, i.e. no atoms coupled to the microtoroids, we are able to carry out an analytical investigation. The 2T0A system is described by the Hamiltonian (6.5) and the master equation (6.9) when the atomic terms (the terms including the parameters g and γ) in these equations are set to zero.

When no atoms are coupled to the toroids, the system is entirely linear and we need only consider the mean field amplitudes.[3] Time derivatives of these mean amplitudes can be calculated from the master equation using the relation $\langle\dot{a}\rangle = \mathrm{Tr}[a\dot{\rho}]$. We find the following equations of motion:

$$\langle\dot{a}_1\rangle = -(\kappa_i^{(1)} + \kappa_{ex}^{(1)} + i\Delta\omega_{\mathrm{C}_1})\langle a_1\rangle - ih_1\langle b_1\rangle - i\mathcal{E}_a\,, \tag{6.17}$$

$$\begin{aligned}\langle\dot{a}_2\rangle = &-(\kappa_i^{(2)} + \kappa_{ex}^{(2)} + i\Delta\omega_{\mathrm{C}_2})\langle a_2\rangle - ih_2\langle b_2\rangle \\ &- 2e^{i\phi_a}\sqrt{\kappa_{ex}^{(1)}\kappa_{ex}^{(2)}}\langle a_1\rangle - i\sqrt{\kappa_{ex}^{(2)}/\kappa_{ex}^{(1)}}\mathcal{E}_a e^{i\Phi_a}\,,\end{aligned} \tag{6.18}$$

$$\begin{aligned}\langle\dot{b}_1\rangle = &-(\kappa_i^{(1)} + \kappa_{ex}^{(1)} + i\Delta\omega_{\mathrm{C}_1})\langle b_1\rangle - ih_1^*\langle a_1\rangle \\ &- 2e^{i\phi_b}\sqrt{\kappa_{ex}^{(1)}\kappa_{ex}^{(2)}}\langle b_2\rangle - i\sqrt{\kappa_{ex}^{(1)}/\kappa_{ex}^{(2)}}\mathcal{E}_b e^{i\Phi_b}\,,\end{aligned} \tag{6.19}$$

$$\langle\dot{b}_2\rangle = -(\kappa_i^{(2)} + \kappa_{ex}^{(2)} + i\Delta\omega_{\mathrm{C}_2})\langle b_2\rangle - ih_2^*\langle a_2\rangle - i\mathcal{E}_b\,. \tag{6.20}$$

[3] In the case that atoms are coupled to the toroids, the system is, in general, not linear but can be linearised for sufficiently weak driving.

Solving these equations in steady state yields

$$\langle a_1\rangle_{ss} = -\frac{i\mathcal{E}_a}{Z_1} - \frac{ih_1}{Z_1}\langle b_1\rangle_{ss}\,, \tag{6.21}$$

$$\langle a_2\rangle_{ss} = -\frac{i\mathcal{E}_a Y_a}{Z_2} + \frac{i\mathcal{E}_a X_a}{Z_1 Z_2} + \frac{ih_1 X_a}{Z_1 Z_2}\langle b_1\rangle_{ss} - \frac{ih_2}{Z_2}\langle b_2\rangle_{ss}\,, \tag{6.22}$$

$$\langle b_1\rangle_{ss} = -\frac{\mathcal{E}_a h_1^* + i\mathcal{E}_b Y_b Z_1}{h_1 h_1^* + Z_1^2} - \frac{X_b Z_1}{h_1 h_1^* + Z_1^2}\langle b_2\rangle_{ss}\,, \tag{6.23}$$

$$\begin{aligned}\langle b_2\rangle_{ss} = [&-i\mathcal{E}_b Z_1 Z_2(h_1 h_1^* + Z_1^2) + \mathcal{E}_a h_2^* X_a(h_1 h_1^* + Z_1^2) - \mathcal{E}_a h_1 h_1^* h_2^* X_a \\ &- \mathcal{E}_a h_2^* Y_a Z_1(h_1 h_1^* + Z_1^2) - i\mathcal{E}_b h_1 h_2^* Y_b Z_1 X_a] \\ &\cdot [Z_2^2 Z_1(h_1 h_1^* + Z_1^2) + h_2 h_2^* Z_1(h_1 h_1^* + Z_1^2) + h_1 h_2^* Z_1 X_a X_b]^{-1}\,,\end{aligned} \tag{6.24}$$

where the abbreviations

$$\kappa^{(1/2)} = \kappa_i^{(1/2)} + \kappa_{ex}^{(1/2)}\,, \tag{6.25}$$

$$Z_{1/2} = \kappa^{(1/2)} + i\Delta\omega_{\mathrm{C}_{1/2}}\,, \tag{6.26}$$

$$X_{a/b} = 2e^{i\phi_{a/b}}\sqrt{\kappa_{ex}^{(1)}\kappa_{ex}^{(2)}}\,, \tag{6.27}$$

$$Y_a = \sqrt{\kappa_{ex}^{(2)}/\kappa_{ex}^{(1)}}e^{i\phi_a}\,, \tag{6.28}$$

$$Y_b = \sqrt{\kappa_{ex}^{(1)}/\kappa_{ex}^{(2)}}e^{i\phi_b}\,, \tag{6.29}$$

have been used.

6.2.1 Photon fluxes

Having the mean field amplitudes, equations (6.21)-(6.24), the jump operators, equations (6.10) and (6.11), and the expressions for the output field amplitudes, equations (6.15) and (6.16), we can compute the steady state output photon fluxes, $|\langle a_{\mathrm{out}}\rangle_{\mathrm{ss}}|^2$ and $|\langle b_{\mathrm{out}}\rangle_{\mathrm{ss}}|^2$.

In the following, the output photon fluxes in the forward (a_{out}) and backward (b_{out}) direction are computed as a function of the probe frequency, ω_{p}. The system is driven from one side only ($\mathcal{E}_a \neq 0$ and $\mathcal{E}_b = 0$) and the output fluxes are normalized by the input flux, $|\langle a_{\mathrm{in}}\rangle|^2$. For simplicity we assume the toroids to be identical, i.e.,

$$\omega_{\mathrm{C}_1} = \omega_{\mathrm{C}_1} =: \omega_{\mathrm{C}}\,, \qquad h_1 = h_2 =: h\,, \tag{6.30}$$

$$\kappa_{\mathrm{ex}}^{(1)} = \kappa_{\mathrm{ex}}^{(2)} =: \kappa_{\mathrm{ex}}\,, \qquad \kappa_{\mathrm{i}}^{(1)} = \kappa_{\mathrm{i}}^{(2)} =: \kappa_{\mathrm{i}}\,. \tag{6.31}$$

Figure 6.2 shows the output photon flux with the parameters chosen to match the over-coupled regime, i.e. the external loss rate, κ_{ex}, satisfies the inequality

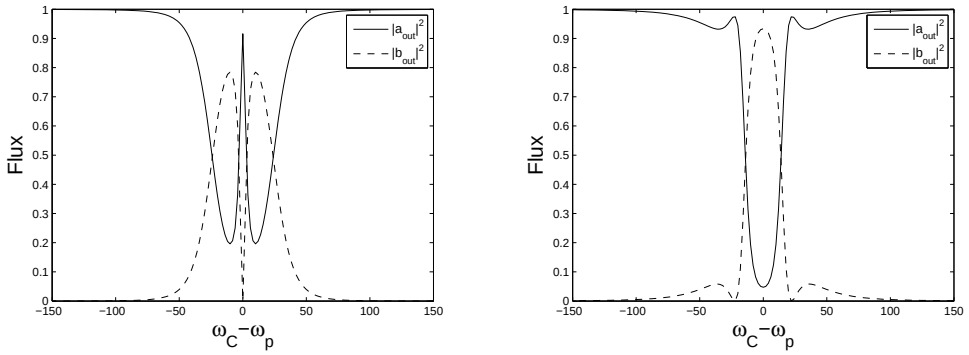

(a) $\phi_a = \pi$, $\phi_b = 0$ (b) $\phi_a = \phi_b = 0$

FIGURE 6.2: Normalized forward flux (solid line) and backward flux (dashed line), $|\langle a_{\rm out}\rangle|^2/|\langle a_{\rm in}\rangle|^2$ and $|\langle b_{\rm out}\rangle|^2/|\langle b_{\rm in}\rangle|^2$, as a function of probe detuning for different phase factors. The system is driven from one side, with a strength $\mathcal{E}_a = 0.2$. The other parameters are $h = 10$, $\kappa_{\rm ex} = 20$ and $\kappa_{\rm i} = 0.1$.

$\kappa_{\rm ex} > \sqrt{\kappa_{\rm i}^2 + h^2}$.[4] The output photon flux crucially depends on the phase factors, ϕ_a and ϕ_b, which vary with the separation between the two toroids. For the right choice of phase factors, $\phi_a = \pi$ and $\phi_b = 0$, the output photon flux exhibits an *electromagnetically-induced-transparency*-like (EIT-like) effect (Figure 6.2(a)). Whereas when the phase factors are chosen as $\phi_a = \phi_b = 0$ this effect does not occur (Figure 6.2(b)); instead the flux shows a "normal" absorption spectrum. When the probe frequency is close to the cavity frequency, light can couple into the cavity, where it is scattered to the b mode and reflected back, as indicated by an increase of flux in backward direction and a reduction of flux in forward direction.

EIT is characterized by a very narrow transparency peak in the center of a broader transmission dip. It occurs in atomic systems due to quantum interference effects between different excitation pathways to the upper energy level of an atom when it is coherently driven with an external laser [LI01]. In [MMSI04], it was theoretically shown that two coupled WGM resonators can "mimic the narrow linewidth obtained with EIT", and this was later on observed experimentally [XSP+06]. Also, in a slightly different alignment of the WGM resonators, the occurrence of EIT-like effects was predicted in [SCF+04] and experimentally shown in [NFSR05]. In all of these investigated WGM-resonator systems, it was crucial for the occurrence of EIT-like effects that the resonators are coupled in both directions, since the EIT-like effect (in the case of coupled WGM resonators) is a purely classical optical interference effect. In our case, this is satisfied by a finite interaction, h, of the two counter-propagating modes. When only driven from one side ($\langle a_{\rm in}\rangle$), a part of the light of the a mode is scattered into the b mode which provides for light being reflected back, and hence for

[4] The notation is from the single-toroid system, where for critical coupling, $\kappa_{\rm ex} = \sqrt{\kappa_{\rm i}^2 + h^2}$, the output photon flux in the forward direction is zero and all the light (which is not lost internally) is reflected back.

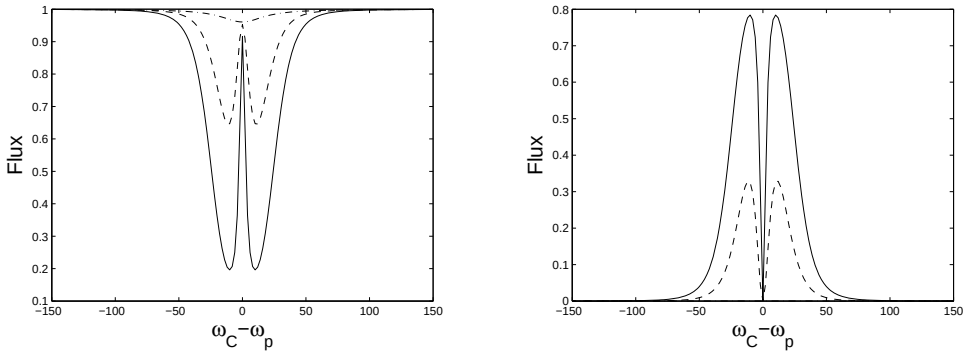

(a) (b)

FIGURE 6.3: Normalized forward flux (a) and backward flux (b), $|\langle a_{\rm out}\rangle|^2/|\langle a_{\rm in}\rangle|^2$ and $|\langle b_{\rm out}\rangle|^2/|\langle b_{\rm in}\rangle|^2$, as a function of probe detuning for $h = 10$ (solid line), $h = 5$ (dashed line) and $h = 0.1$ (dashed-dotted line). The system is driven from one side, with a strength $\mathcal{E}_a = 0.2$. The other parameters are $\kappa_{\rm ex} = 20$, $\kappa_{\rm i} = 0.1$, $\phi_a = \pi$ and $\phi_b = 0$. The backward flux for $h = 0.1$ is approximately zero and lies on top of the zero axis.

a coupling of the second toroid with the first. In the over-coupled regime considered here, the cavities decay primarily into the fibre ($\kappa_{\rm ex}$) and not into free space ($\kappa_{\rm i}$). Thus, there is a strong interference between incoming light and light which is coupled back into the fibre. In particular, light from the b mode that propagates "backwards" in the fibre can strongly interfere with the incoming light. In Figure 6.3 the photon flux is shown for different interactions strengths between the modes. For a small h almost no light is scattered into the b mode and reflected back (in the direction of $b_{\rm out}$), hence the coupling between the two toroids is mostly unidirectional (light from toroid 1 is coupled into toroid 2 but not vice versa) and the EIT-like effect does not occur.

The narrow transparency peak is determined by the internal loss rate, $\kappa_{\rm i}$, where, in particular the height of the peak decreases with increasing $\kappa_{\rm i}$. Figure 6.4 shows the output photon flux for different $\kappa_{\rm i}$.

In Figure 6.5 the output photon flux for a critical-coupled system is shown. For critical coupling the EIT-like effect does not occur. This can be explained by the fact that for the single-toroid system, the forward flux is zero for $\omega_{\rm p} \approx \omega_{\rm C}$, when the system is under the condition of critical coupling [Par06]. Hence, for driving from one side and independent cavities (linear system) the light is reflected back from the first cavity and does not couple into the second cavity. Therefore there are no interference effects between light from the first and the second cavity and the EIT-like feature does not occur.

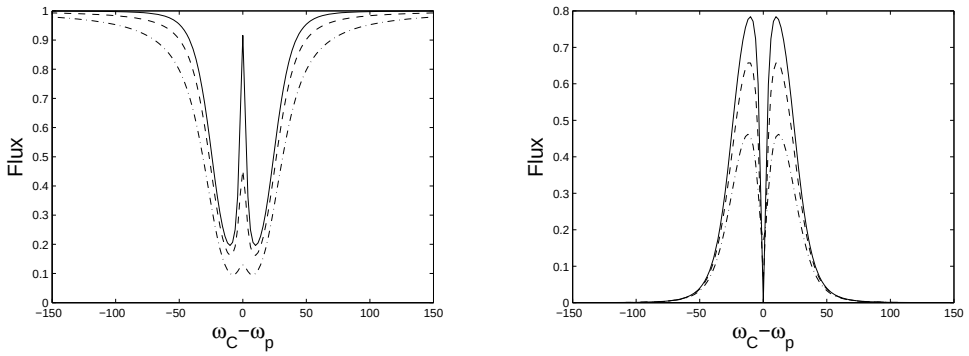

FIGURE 6.4: Normalized forward flux (a) and backward flux (b), $|\langle a_{\rm out}\rangle|^2/|\langle a_{\rm in}\rangle|^2$ and $|\langle b_{\rm out}\rangle|^2/|\langle b_{\rm in}\rangle|^2$, as a function of probe detuning for $\kappa_{\rm i} = 0.1$ (solid line), $\kappa_{\rm i} = 1$ (dashed line) and $\kappa_{\rm i} = 3$ (dash-dotted line). The system is driven from one side, with a strength $\mathcal{E}_a = 0.2$. The other parameters are $h = 10$, $\kappa_{\rm ex} = 20$, $\phi_a = \pi$ and $\phi_b = 0$.

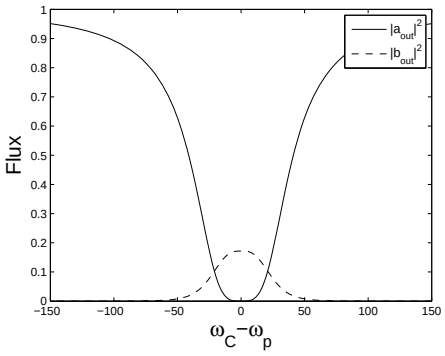

FIGURE 6.5: Normalized forward flux (solid line) and backward flux (dashed line), $|\langle a_{\rm out}\rangle|^2/|\langle a_{\rm in}\rangle|^2$ and $|\langle b_{\rm out}\rangle|^2/|\langle b_{\rm in}\rangle|^2$, as a function of probe detuning for a critical-coupled system. The system is driven from one side, with a strength $\mathcal{E}_a = 0.2$. The other parameters are $h = 10$, $\kappa_{\rm ex} = 14.1$ and $\kappa_{\rm i} = 10$, $\phi_a = \pi$ and $\phi_b = 0$.

6.3 Numerical investigations

To study the behaviour of the system we have to solve the master equation (6.9). For the general case (the 2T2A system), this is too complex to be done analytically and the results, in any case, become too cumbersome to be of use. Hence, we solve the master equation numerically.

6.3.1 Steady state method

We are, in particular, interested in the mean values of the photon output fields ($|\langle a_{\text{out}}\rangle|^2$ and $|\langle b_{\text{out}}\rangle|^2$) in steady state, which are calculated with the steady-state density operator, ρ_{ss}, as

$$\langle a_{\text{out}}\rangle_{\text{ss}} = \text{Tr}\left[a_{\text{out}}\rho_{\text{ss}}\right] \qquad \text{and} \qquad \langle b_{\text{out}}\rangle_{\text{ss}} = \text{Tr}\left[b_{\text{out}}\rho_{\text{ss}}\right] . \tag{6.32}$$

In order to perform these calculations we must find the steady-state density operator, ρ_{ss}. This is done by solving the master equation

$$\dot{\rho}_{\text{ss}} = \mathcal{L}\rho_{\text{ss}} = 0 , \tag{6.33}$$

with the Liouvillian $\mathcal{L}$ written in standard Lindblad form:

$$\mathcal{L} = -i\left[H, \cdot\right] + \sum_{j=1}^{n} C_j \cdot C_j^\dagger - \frac{1}{2}(C_j^\dagger C_j \cdot + \cdot C_j^\dagger C_j) , \tag{6.34}$$

where the C_j are the collapse operators due to damping. It is possible to write the $n \times n$ density matrix as a n^2 dimensional column-vector and the superoperator $\mathcal{L}$ as an $n^2 \times n^2$ matrix. The problem of solving the master equation in steady state is then reduced to finding the eigenvector belonging to the eigenvalue zero, which can be obtained by the inverse power method.

6.3.2 Fock space truncation

The strength of the driving field determines the approximate number of photons in the cavity and it is very unlikely that the photon number exceeds a maximum value N, given a certain set of parameters. Therefore, it is a good approximation to neglect all photon numbers larger than N. This is called the truncation of the Fock space of the cavity mode.

In our system, the total Hilbert space consists of the subspaces for the two atoms and the subspaces for the four cavity modes,

$$\mathcal{H}_{\text{total}} = \mathcal{H}_{\text{atom1}} \otimes \mathcal{H}_{\text{atom2}} \otimes \mathcal{H}_{a1} \otimes \mathcal{H}_{b1} \otimes \mathcal{H}_{a2} \otimes \mathcal{H}_{b2} . \tag{6.35}$$

For a two-level atom the dimension of the total Hilbert space is $d_{\mathcal{H}} = 4N^4$, where each cavity mode has the same truncation N. The dimension of the density matrix is the square of the dimension of the Hilbert space and the dimension of the Liouvillian

is $d_{\mathcal{H}}^4$, which is a very large number even for small truncations. Since in our weakly driven system the average photon number in each cavity mode was of the order 10^{-4}, it is sufficient to choose a truncation of $N = 1$. As a "rule of thumb", the truncation should be at least ten times larger than the average photon number.

6.3.3 Numerical results – strong-coupling limit

The numerical calculations were performed with the Quantum Optics Toolbox for MATLAB [Tan].

In the following, the numerical investigations are performed for the strong-coupling limit ($g >> \kappa, \gamma$), where the atom-cavity coupling exceeds the cavity damping and the atomic decay rate. The system is only driven from one side ($\mathcal{E}_a \neq 0$ and $\mathcal{E}_b = 0$) and we are interested in the output photon fluxes in the forward (a_{out}) and backward (b_{out}) direction as a function of the probe frequency ω_{p}. It is convenient to normalize the output fluxes by the input flux, $|\langle a_{\text{in}} \rangle|^2$. For simplicity we assume the toroids to be identical, i.e.,

$$\omega_{\text{C}_1} = \omega_{\text{C}_1} =: \omega_{\text{C}}\,, \qquad \omega_{\text{A}_1} = \omega_{\text{A}_1} =: \omega_{\text{A}}\,, \tag{6.36}$$

$$\kappa_{\text{ex}}^{(1)} = \kappa_{\text{ex}}^{(2)} =: \kappa_{\text{ex}}\,, \qquad \kappa_{\text{i}}^{(1)} = \kappa_{\text{i}}^{(2)} =: \kappa_{\text{i}}\,, \tag{6.37}$$

$$\gamma_1 = \gamma_2 =: \gamma\,, \qquad g_1 = g_2 =: g\,, \tag{6.38}$$

$$h_1 = h_2 =: h\,, \tag{6.39}$$

and the atoms and cavities to be resonant with each other ($\omega_{\text{C}} = \omega_{\text{A}}$).

In Figure 6.6 and Figure 6.7, the output photon fluxes (in the forward and backward direction) for the 2T2A, the 2T1A (where the remaining atom is coupled to toroid 1) and the 2T0A system are shown for the critical-coupled regime as a function of the probe detuning, $\Delta\omega_{\text{C}}$. The atom-cavity coupling, g, is in the first case taken to be real-valued (Figure 6.6) and in the other case to be imaginary (Figure 6.7), which corresponds to different positions of the atom around the toroid [ADW+06b]. The obtained output fluxes for the 2T2A and 2T1A system are similar to the output fluxes of the driven 1T1A system, which was investigated in [ADW+06b], and can be explained accordingly. For both systems, three dips occur in the forward flux, corresponding to an increased backward flux at these frequencies. This can be understood by considering the normal modes of the single toroid.[5] Similar to Section 5.5, the Hamiltonian of the single driven atom-toroid system can be written with the

[5] To be correct, in case of coupled cavities we need to find the normal modes of the total Hamiltonian and cannot just use the "local" normal modes of the separate cavities (which would be A and B). This involves finding the eigenvalues of the total Hamiltonian which seems near impossible to do analytically. However the "local" normal modes can explain the behaviour qualitatively.

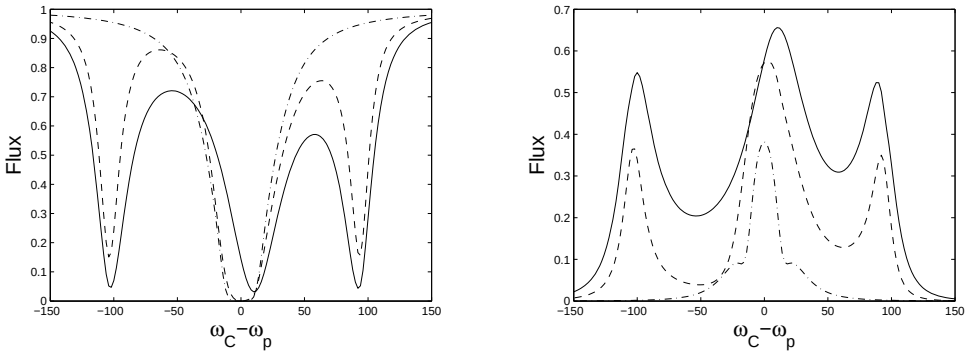

(a) forward flux (b) backward flux

FIGURE 6.6: Normalized forward flux (a) and backward flux (b), $|\langle a_{\rm out}\rangle|^2/|\langle a_{\rm in}\rangle|^2$ and $|\langle b_{\rm out}\rangle|^2/|\langle b_{\rm in}\rangle|^2$, as a function of probe detuning for a real-valued atom-cavity coupling $g = 70$. The fluxes are plotted for the 2T2A system (solid line), the 2T1A system (dashed line) and the 2T0A system (dashed-dotted line), all in the critical-coupled regime. The atom is resonant with the cavity ($\omega_{\rm A} = \omega_{\rm C}$) and is driven by $\mathcal{E}_a = 0.2$. The other parameters are $h = 10$, $\kappa_{\rm ex} = 11.2$, $\kappa_{\rm i} = 5$, $\gamma = 5$, $\phi_a = 0$ and $\phi_b = 0$.

normal modes, $A = (a + b)/\sqrt{2}$ and $B = (a - b)/\sqrt{2}$, as

$$\begin{aligned} H = {} & (\omega_{\rm C} + h)A^\dagger A + (\omega_{\rm C} - h)B^\dagger B + \omega_A \sigma^+\sigma^- \\ & + \frac{1}{\sqrt{2}}\left[\mathcal{E}_{\rm p}^*(A + B) + \mathcal{E}_{\rm p}(A^\dagger + B^\dagger)\right] \\ & + \sqrt{2}{\rm Re}\{g\}(A^\dagger\sigma^- + \sigma^+ A) - i\sqrt{2}{\rm Im}\{g\}(B^\dagger\sigma^- - \sigma^+ B)\,. \end{aligned} \tag{6.40}$$

We see that for a real coupling constant, the atom only couples to mode A, of frequency $\omega_{\rm C} + h$, and for a imaginary g only to mode B, of frequency $\omega_{\rm C} - h$. This can explain the reduction of the forward flux in the cascaded system at probe detunings $\Delta\omega_{\rm C} = -h \pm \sqrt{2}g$ (for a real-valued g) and $\Delta\omega_{\rm C} = h \pm \sqrt{2}|g|$ (for an imaginary g). The splitting of these two dips by the factor $2\sqrt{2}g$ is due to the vacuum Rabi splitting of the mode coupled to the atom. The reduction of the forward flux at approximately $\Delta\omega_{\rm C} = h$ and $\Delta\omega_{\rm C} = -h$, respectively, is the spectrum of the mode which is not coupled to the atom. It is noticeable that the "displacement" for the 2T1A is not as strong as for the 2T2A system, in particular for the dip in the middle. Also, it is noticeable that, generally, the peaks in the forward flux are much higher for the 2T1A system than for the 2T2A system. From an experimental point of view, this offers a way to distinguish between the two systems. The asymmetry in the output flux is due to the asymmetry in the system when it is driven only from one side.

The 2T0A system shows a "normal" absorption spectrum determined by the cavity loss rate κ and has already been discussed in Section 6.2. The results obtained by numerically solving the corresponding master equation agree with the results

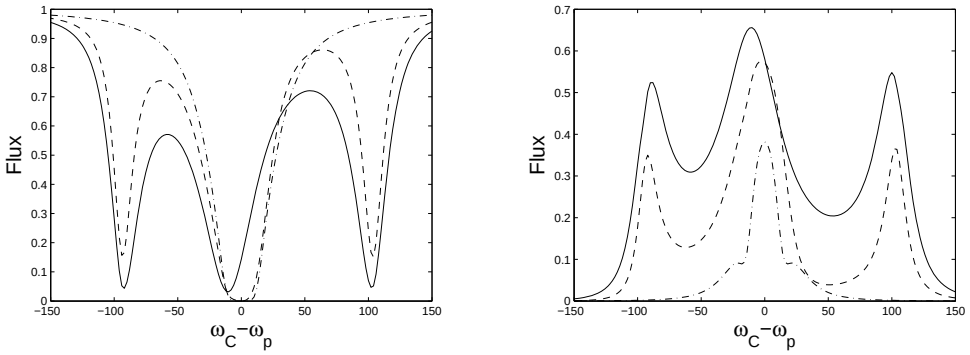

(a) forward flux (b) backward flux

FIGURE 6.7: Normalized forward flux (a) and backward flux (b), $|\langle a_{\text{out}}\rangle|^2/|\langle a_{\text{in}}\rangle|^2$ and $|\langle b_{\text{out}}\rangle|^2/|\langle b_{\text{in}}\rangle|^2$, as a function of probe detuning for a imaginary-valued atom-cavity coupling $g = 70i$. The fluxes are plotted for the 2T2A system (solid line), the 2T1A system (dashed line) and the 2T0A system (dashed-dotted line), all in the critical-coupled regime. The atom is resonant with the cavity ($\omega_{\text{A}} = \omega_{\text{C}}$) and is driven by $\mathcal{E}_a = 0.2$. The other parameters are $h = 10$, $\kappa_{\text{ex}} = 11.2$, $\kappa_{\text{i}} = 5$, $\gamma = 5$, $\phi_a = 0$ and $\phi_b = 0$.

obtained from the analytical investigation in the previous section.

For an over-coupled 2T2A system additional features can occur in the sidepeaks of the backward flux. These are shown in Figure 6.8 and are due to interference effects between the two coupled atom-toroid systems which do not occur in the single atom-toroid system nor in the 2T1A or the 2T0A system.

6.3.4 Numerical results – bad-cavity limit

In this section we investigate the three systems (2T2A, 2T1A and 2T0A) in the bad-cavity, strongly over-coupled regime, where the cavity loss rate exceeds all other parameters ($\kappa \gg \gamma, g$).

The output photon fluxes in the forward and backward directions are computed as a function of probe frequency by numerically solving the corresponding master equation in steady state. As in the previous section, we assume the toroids to be identical and the atoms and cavities to be resonant with each other. The system is only driven from one side ($\mathcal{E}_a \neq 0$ and $\mathcal{E}_b = 0$) and the output photon fluxes are normalized by the input flux $|\langle a_{\text{in}}\rangle|^2$.

The output fluxes for a sample set of parameters are shown in Figure 6.9. For the 2T0A system, the forward flux is approximately unity, corresponding to a backward flux of zero. For a single-toroid system in the strongly over-coupled regime, it was shown that "in the absence of an atom, virtually no light is coupled into the backward field" [PDAK09]. Hence, the incoming light is, at toroid 1 and at toroid 2, respectively, coupled into the forward field (apart from internal losses in the cavities), which leads to the obtained results. For the chosen parameters, where the

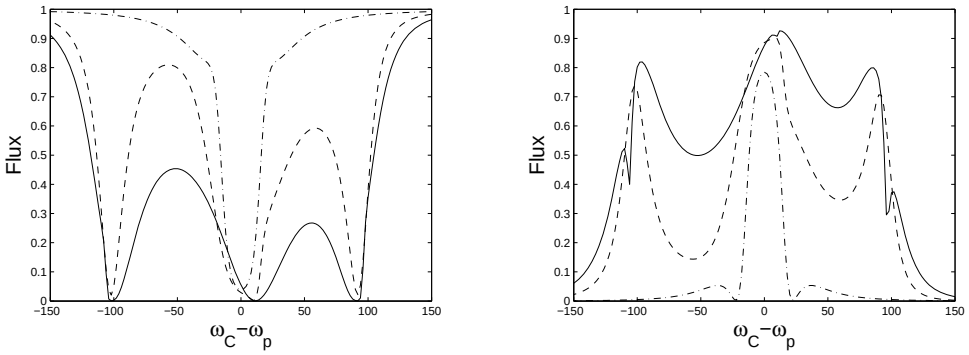

(a) forward flux (b) backward flux

FIGURE 6.8: Normalized forward flux (a) and backward flux (b), $|\langle a_{\rm out}\rangle|^2/|\langle a_{\rm in}\rangle|^2$ and $|\langle b_{\rm out}\rangle|^2/|\langle b_{\rm in}\rangle|^2$, as a function of probe detuning for a real-valued atom-cavity coupling $g = 70$. The fluxes are plotted for the 2T2A system (solid line), the 2T1A system (dashed line) and the 2T0A system (dashed-dotted line), all in the over-coupled regime. The atom is resonant with the cavity ($\omega_{\rm A} = \omega_{\rm C}$) and is driven by $\mathcal{E}_a = 0.2$. The other parameters are $h = 10$, $\kappa_{\rm ex} = 20$, $\kappa_{\rm i} = 1$, $\gamma = 5$, $\phi_a = 0$ and $\phi_b = 0$.

internal loss is much smaller than the coupling to the fibre, the forward flux shows a very broad, but very shallow absorption dip around resonance, which is not visible for the scale in the plot. In contrast, the forward flux of the 2T2A and the 2T1A system shows a clear absorption spectrum. For small detunings most of the light is reflected back, indicated by an increased photon flux in the backward direction. The linewidth scales with $\frac{g^2}{\kappa}$ and is, for the 2T2A system, approximately twice as large as for the 2T1A system. In particular, the full widths at half maximum can be determined to be $8\frac{g^2}{\kappa}$ and $4\frac{g^2}{\kappa}$, respectively, which correspond to the linewidths of the emission spectra obtained for the spontaneous emission systems.

6.4 Reflection and transmission coefficient

In this section we will describe the driven 2T2A system in terms of the properties of the single driven microtoroid described in [ADW+06a, ADW+06b, DPA+08a, DPA+08b]. This can be done for sufficiently weak driving fields where the response is essentially linear.

A cascaded system can be depicted as shown in Figure 6.10, where we restrict ourselves to driving from only one side.[6] A part of the input field, $\langle a_{\rm in}\rangle$, is reflected back at the first cavity and the other part is transmitted, where it in turn is reflected or transmitted at the second cavity. This transmission and reflection at a single cavity can be described in terms of a transmission coefficient T and reflection coefficient R. The total transmission coefficient F and total reflection coefficient B of a cascaded

[6] It is a simple task to apply the results obtained in this section to driving from the other side.

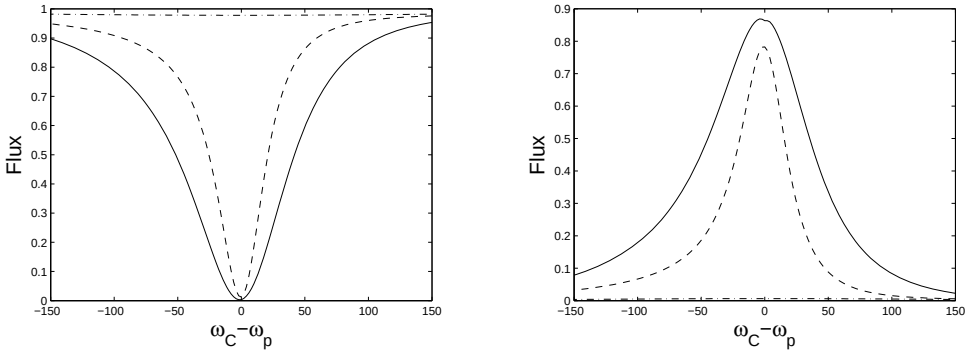

(a) forward flux (b) backward flux

FIGURE 6.9: Normalized forward flux (a) and backward flux (b), $|\langle a_{\rm out}\rangle|^2/|\langle a_{\rm in}\rangle|^2$ and $|\langle b_{\rm out}\rangle|^2/|\langle b_{\rm in}\rangle|^2$, as a function of probe detuning for the 2T2A system (solid line), the 2T1A system (dashed line) and the 2T0A system (dashed-dotted line). The systems are in the bad-cavity, strongly over-coupled regime with the parameters $h = 10$, $\kappa_{\rm ex} = 500$, $\kappa_{\rm i} = 1$, $g = 70$, $\gamma = 5$, $\phi_a = 0$, $\phi_b = 0$ and are driven with a strength $\mathcal{E}_a = 0.2$. The atom is resonant with the cavity ($\omega_{\rm A} = \omega_{\rm C}$).

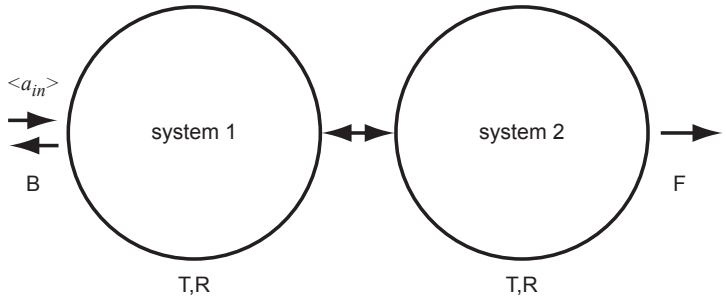

FIGURE 6.10: Schematic of a driven cascaded toroid system. $\langle a_{\rm in}\rangle$ is the input field amplitude, B the total backward reflection coefficient and F the total forward transmission coefficient. T and R denote the single-toroid transmission and reflection coefficients, respectively.

system consisting of two identical toroids is then,

$$\begin{aligned} F &= T^2 + T^2R^2 + T^2R^4 + \cdots = T^2(1 + R^2 + R^4 + \cdots) \\ &= \frac{T^2}{1 - R^2}\,, \end{aligned} \tag{6.41}$$

and

$$\begin{aligned} B &= R + RT^2 + R^3T^2 + R^5T^2 + \cdots = R(1 + T^2 + T^2R^2 + T^2R^4 + \cdots) \\ &= R\left(1 + \frac{T^2}{1 - R^2}\right)\,, \end{aligned} \tag{6.42}$$

where the geometrical series has been summed. With these coefficients the mean output amplitudes can be written in terms of the input amplitudes

$$\langle a_{\mathrm{out}}\rangle = F\langle a_{\mathrm{in}}\rangle \qquad \text{and} \qquad \langle b_{\mathrm{out}}\rangle = B\langle a_{\mathrm{in}}\rangle\,, \tag{6.43}$$

and the output fluxes yield

$$|\langle a_{\mathrm{out}}\rangle|^2 = |F\langle a_{\mathrm{in}}\rangle|^2 = |F|^2|\langle a_{\mathrm{in}}\rangle|^2\,, \tag{6.44}$$

$$|\langle b_{\mathrm{out}}\rangle|^2 = |B\langle a_{\mathrm{in}}\rangle|^2 = |B|^2|\langle a_{\mathrm{in}}\rangle|^2\,. \tag{6.45}$$

6.4.1 Expressions for the reflection and transmission coefficients

In order to be able to compute the output fluxes we need to know the transmission and reflection coefficients, F and B, of the cascaded system. This in turn means that we need to obtain expressions for the transmission and reflection at a single toroid.

Let us write the output field amplitudes of a single toroid in terms of the input, $\langle a_{\mathrm{in}}\rangle$,

$$\langle a_{\mathrm{out}}\rangle = -\langle a_{\mathrm{in}}\rangle + \sqrt{2\kappa_{\mathrm{ex}}}\langle a\rangle_{\mathrm{ss}} = \left(-1 + 2i\frac{\kappa_{\mathrm{ex}}}{\mathcal{E}_{\mathrm{p}}}\langle a\rangle_{\mathrm{ss}}\right)\langle a_{\mathrm{in}}\rangle\,, \tag{6.46}$$

$$\langle b_{\mathrm{out}}\rangle = \sqrt{2\kappa_{\mathrm{ex}}}\langle b\rangle_{\mathrm{ss}} = \left(2i\frac{\kappa_{\mathrm{ex}}}{\mathcal{E}_{\mathrm{p}}}\langle b\rangle_{\mathrm{ss}}\right)\langle a_{\mathrm{in}}\rangle\,, \tag{6.47}$$

where the expression for $\langle a_{\mathrm{in}}\rangle$ from equation (6.14) was used. Hence, we obtain for the transmission and reflection coefficient of a single toroid

$$T = -1 + 2i\frac{\kappa_{\mathrm{ex}}}{\mathcal{E}_{\mathrm{p}}}\langle a\rangle_{\mathrm{ss}} \qquad \text{and} \qquad R = 2i\frac{\kappa_{\mathrm{ex}}}{\mathcal{E}_{\mathrm{p}}}\langle b\rangle_{\mathrm{ss}}\,. \tag{6.48}$$

The only task left is to determine expressions for the mean amplitudes of the cavity modes in steady state ($\langle a\rangle_{\mathrm{ss}}$ and $\langle b\rangle_{\mathrm{ss}}$). The equations of motion for the mean amplitudes can be obtained from the master equation of the single-toroid system, which then have to be solved for the steady state to yield the wanted expressions. This was done by Parkins [Par06] and we will just state the results.

In case of an atom coupled to the toroid the mean field amplitudes, $\langle a\rangle_{\rm ss}$ and $\langle b\rangle_{\rm ss}$, are

$$\langle a\rangle_{\rm ss} = i\mathcal{E}_{\rm p}\frac{\chi[(\kappa+i\Delta_{\rm C})\chi+|g|^2]}{(ih\chi+g^{*2})(ih\chi+g^2)-[(\kappa+i\Delta_{\rm C})\chi+|g|^2]^2}\,, \tag{6.49}$$

$$\langle b\rangle_{\rm ss} = -i\mathcal{E}_{\rm p}\frac{\chi(ih\chi+g^2)}{(ih\chi+g^{*2})(ih\chi+g^2)-[(\kappa+i\Delta_{\rm C})\chi+|g|^2]^2}\,, \tag{6.50}$$

with the abbreviation

$$\chi = \frac{\gamma}{2}+i\Delta_{\rm A}\,, \tag{6.51}$$

where $\Delta_{\rm A}$ denotes the detuning between the atom frequency and the probe frequency, and $\Delta_{\rm C}$ the detuning between the cavity frequency and the probe frequency:

$$\Delta_{\rm A} = \omega_{\rm A}-\omega_{\rm p} \qquad \text{and} \qquad \Delta_{\rm C} = \omega_{\rm C}-\omega_{\rm p}\,. \tag{6.52}$$

The output amplitude for the forward ($\langle a_{\rm out}\rangle$) and the backward ($\langle b_{\rm out}\rangle$) directions can then be written as

$$\langle a_{\rm out}\rangle = \left(-1-2\kappa_{\rm ex}\frac{(\chi[(\kappa+i\Delta_{\rm C})\chi+|g|^2]}{(ih\chi+g^{*2})(ih\chi+g^2)-[(\kappa+i\Delta_{\rm C})\chi+|g|^2]^2}\right)\langle a_{\rm in}\rangle\,, \tag{6.53}$$

$$\langle b_{\rm out}\rangle = \left(\frac{2\kappa_{\rm ex}}{\mathcal{E}_{\rm p}}\frac{\chi(h\chi-ig^2)}{(ih\chi+g^{*2})(ih\chi+g^2)-[(\kappa+i\Delta_{\rm C})\chi+|g|^2]^2}\right)\langle a_{\rm in}\rangle\,. \tag{6.54}$$

Thus, we find for the transmission coefficient $T(\Delta_{\rm C})$ and the reflection coefficient $R(\Delta_{\rm C})$ of a single toroid

$$T(\Delta_{\rm C}) = -1-2\kappa_{\rm ex}\frac{\chi[(\kappa+i\Delta_{\rm C})\chi+|g|^2]}{(ih\chi+g^{*2})(ih\chi+g^2)-[(\kappa+i\Delta_{\rm C})\chi+|g|^2]^2}\,, \tag{6.55}$$

$$R(\Delta_{\rm C}) = \frac{2\kappa_{\rm ex}}{\mathcal{E}_{\rm p}}\frac{\chi(h\chi-ig^2)}{(ih\chi+g^{*2})(ih\chi+g^2)-[(\kappa+i\Delta_{\rm C})\chi+|g|^2]^2}\,. \tag{6.56}$$

6.4.2 Applying the transmission and reflection coefficient

We compute the output fluxes for a cascaded system, using equations (6.44) and (6.45), and compare the results to the fluxes obtained from numerically solving the master equation (see Section 6.3).

In Figure 6.11 the output fluxes $|\langle a_{\rm out}\rangle|^2$ and $|\langle b_{\rm out}\rangle|^2$ of a sample system are plotted for different driving strengths. It can be clearly seen that for weak driving the results obtained from the different methods match very well, whereas for stronger driving the plots start to deviate. For stronger driving the response is no longer linear and cannot be accurately described by the transmission and reflection coefficient method.

However, for a sufficiently weak driving this method provides a nice, intuitive way of determining transmission/reflection properties of such cascaded systems, and could in principle be applied to systems with more toroids.

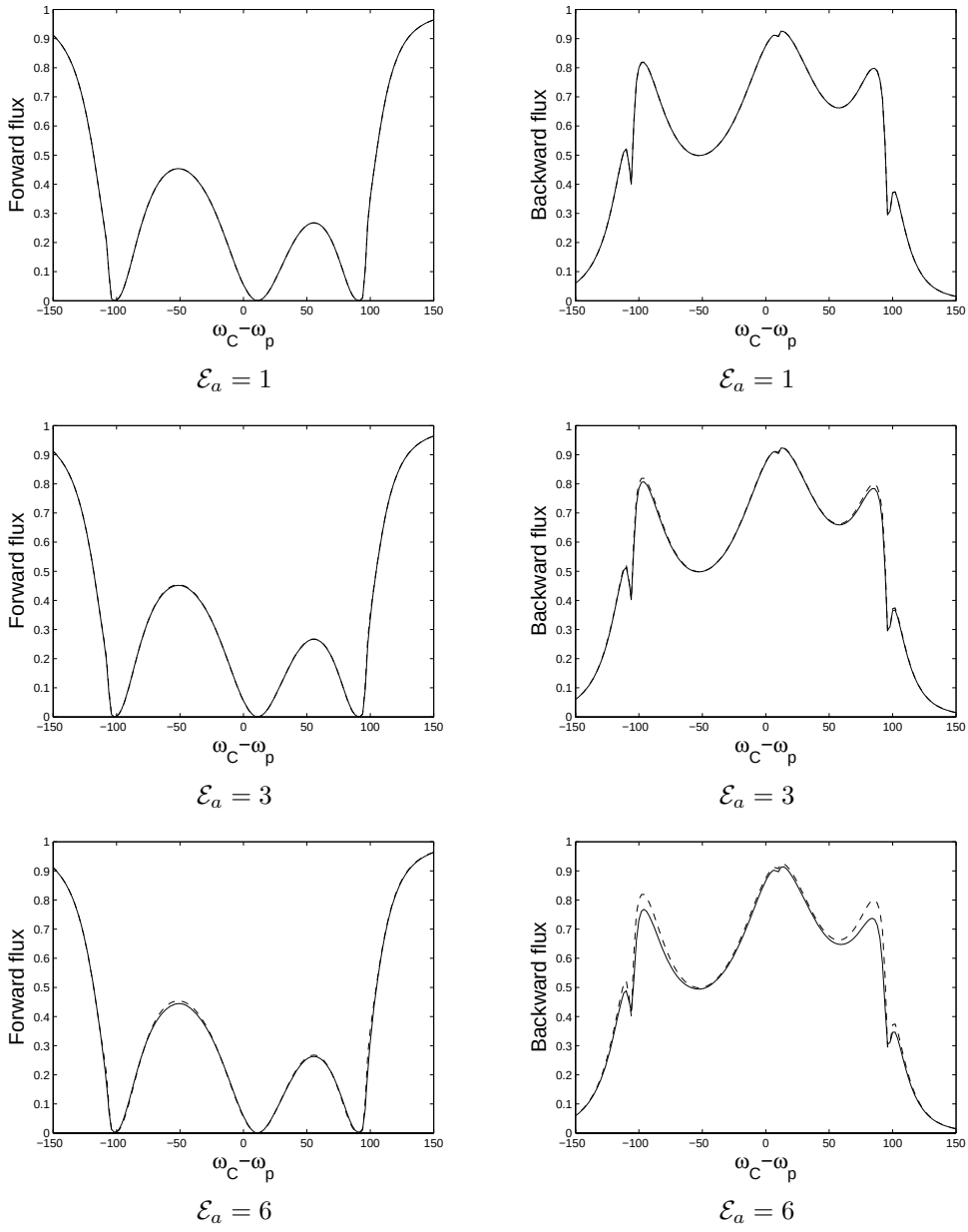

FIGURE 6.11: Normalized forward flux (left column) and backward flux (right column), $|\langle a_{\rm out}\rangle|^2/|\langle a_{\rm in}\rangle|^2$ and $|\langle b_{\rm out}\rangle|^2/|\langle b_{\rm in}\rangle|^2$, as a function of probe detuning, obtained by solving the master equation (solid line) and by the reflection/transmission method (dashed line). Fluxes are plotted for different driving strengths $\mathcal{E}_a = \{1, 3, 6\}$ for the atom on resonance with the cavity ($\omega_{\rm A} = \omega_{\rm C}$). The other parameters are $h = 10$, $\kappa_{\rm ex} = 20$, $\kappa_{\rm i} = 1$, $g = 70$, $\gamma = 5$, $\phi_a = 0$ and $\phi_b = 0$.

Chapter 7

Conclusion

7.1 Summary

In this thesis we investigated a cascaded cavity QED system consisting of two microtoroidal resonators connected via an optical fibre. The toroids act as cavities with two counter-propagating WGMs. In addition a single atom is coupled to each of the toroids by the evanescent field of its cavity modes. The main emphasis of this investigation was on the spontaneous emission of the cascaded system. Additional research was conducted on the coherently driven system, based upon previous work done for the driven single-toroid system [ADW$^+$06a, DPA$^+$08a].

We started in Chapter 5 with an analytical investigation of the spontaneous emission system. By employing a "Separation of the Liouvillian" we were able to transform the complicated two-time integrals over second-order correlation functions, from which the emission spectrum is usually calculated, to simpler one-time integrals. These one-time integrals are over the probability amplitudes of the state vector of the one-energy quantum subspace, for which we derived a set of equations of motion.

For the bad-cavity system, this set of equations of motion was solved by adiabatically eliminating the cavity modes, and analytical expressions for the emission spectra were found. These analytical results were compared to the emission spectra obtained by numerically solving the equations of motion for the probability amplitudes. It was found that in the bad-cavity limit the analytical results agree with the numerical results.

The emission spectra of the 2T2A system were compared to the emission spectra of the 2T1A and the 1T1A system for the bad-cavity regime. It was found that the linewidth of the 2T2A system is, by a factor of two, larger than in the other two systems. This was later explained by the occurrence of superradiance.

For the bad-cavity regime a master equation with the cavity modes adiabatically eliminated was derived. This master equation is novel, in the sense that depending on the chosen detuning (and neglecting the spontaneous emission of the atoms), it either describes a collective atomic decay (the so-called superradiance), an individual decay of each atom, or a combination of both. This master equation could qualitatively

explain the shape of the emission spectra in the bad-cavity regime.

The strong-coupling regime was investigated numerically, where we found a vacuum Rabi splitting in the emission spectra plus several other features which in part could be explained by the different coupling strength of the atom to the normal modes of the system. But some of the occurred features still remained unexplained.

The driven cascaded system was studied in Chapter 6. Analytical calculations were only possible for the 2T0A system where we computed the output photon flux. The occurrence of an EIT-like effect was shown, which crucially depends on the phase factors (corresponding to the separation of the toroids). For the 2T2A and the 2T1A system, analytical calculations were too cumbersome and therefore these systems were only investigated numerically. We computed the output fluxes for the strong-coupling and bad-cavity regimes by solving the master equation in steady state. These numerical solutions were obtained in the weak-excitation limit, and thus we were able to truncate the cavity mode Hilbert space to make the numerical computations feasible. For the strong-coupling regime, the results for the photon fluxes of the two systems could, similarly to the spontaneous emission system, be interpreted in terms of vacuum Rabi splitting and a different coupling strength of the atoms to the different normal modes of the system. For the bad-cavity regime, we found a "normal" absorption (transmission) spectrum for the forward (backward) flux where the linewidth of the 2T2A system is approximately twice as large as of the 2T1A system. This corresponds with the results obtained for the spectrum of the spontaneous emission system in the bad-cavity regime.

A method to describe the cascaded system in terms of the properties of the single-toroid system by means of reflection and transmission coefficients was developed. Its validity (agreement with the numerical results) was shown for relatively small driving fields, in which case the response of the toroids is essentially linear.

The mathematical treatment given in this thesis can, in principle, be applied to other, similar systems as well; e.g., semiconductor quantum dots or quantum wells inside a photonic crystal, micropillar or microdisk resonator. In this case, the semiconductor quantum dot or quantum well plays the role of the two-level atom which can emit and absorb photons, and the photonic crystal or the microresonator is a cavity where only certain optical modes are allowed. Cavity QED effects in solid-state materials have indeed been observed, e.g., strong coupling for single quantum dots in microresonator cavities of the type mentioned above has been obtained [RSL$^+$04, YSH$^+$04, PSM$^+$05].[1] Recently, experiments on solid state systems [SMPP08, SP07a] similar to the experiments on atomic systems [ADW$^+$06a, DPA$^+$08a] have been conducted. In these experiments, a single high quality GaAs microdisk coupled with an InAs quantum dot was driven by a coherent probe field using a fibre taper waveguide. This system is mathematically described in the same way as a single atom-toroid system [SP07b]. Therefore, the results obtained in this thesis are also relevant to solid state systems, e.g., a coupled two-microdisk

[1] A review of the progress in obtaining true quantum-optical strong-coupling effects in semiconductors can be found in [KGK$^+$06].

system.

7.2 Future directions

We derived the adiabatic master equation for the spontaneous emission system in the bad-cavity limit. From this equation, the emission spectrum of the system could be computed and could then be compared to the results obtained from the full model. These calculations were started, but could, unfortunately, not be concluded due to time restraints.[2]

In case of strong coupling, some features occurred in the emission spectra which are still unexplained.[3] The same holds for the strong-coupling regime in the driven system. Further investigation is required to figure out the nature of these features.

In general, the system is quite complex, having many tunable parameters. We restricted ourself, in this thesis, to a few, simple examples to investigate the essential behaviour. In particular, throughout the investigation of the bad-cavity regime we set the coupling between the modes to zero and we assumed, throughout the thesis, the cavities to be identical with no cavity-atom detuning present. In principle all these simplifications can be lifted, but it is questionable as to what extent the system will remain manageable to systematic investigations.

Another aspect to be investigated is the entanglement between the atoms when the system is driven. However, in order for a noticeable entanglement between the atoms to occur the system would need to be strongly driven. More photons would be present in the cavity modes, which means that the dimension of the truncated cavity-modes Hilbert space would need to be increased. Solving the master equation numerically in steady state by the method used in this thesis would become much more elaborate, if not impossible. To overcome these computational problems, a Quantum Trajectory method, e.g., a quantum Monte-Carlo simulation, could be used.[4] The evolution of the state vector and the effects of entanglement can be observed directly with this method. Alternatively, in the case of the bad-cavity regime, the external driving could be added to the master equation where the cavity modes have been adiabatically eliminated - equation (5.139). Numerical and even analytical investigations for strong driving could be done using this equation, which has a much lower dimensionality of the equations to be solved compared to the full master equation.

Finally, the atom-toroid system is a promising candidate for a future quantum network consisting of quantum nodes (atom-toroid subsystems) connected by a quantum channel (optical fibre). The coupled two-toroid system, investigated in this thesis, is only the first step in this direction. More toroids could be added to build up a complex network whose properties could then be studied.

[2] Initial calculations are presented in Appendix C.

[3] Namely, the dispersive like feature which seems to be connected to the coupling constant h. See Section 5.5.

[4] For an introduction to Quantum Trajectory theory see [Car08, Chap. 17-18].

Appendix A

Bad-Cavity Limit – Supplementary Calculations

In this chapter the calculation of Section 5.4, where we adiabatically eliminate the cavity modes to obtain a master equation for the atom alone, are presented in more detail.

After expanding out equation (5.121) we arrive at

$$
\begin{aligned}
\dot{\tilde{\rho}}_{\mathrm{A}} = -\Big(& |g_1|^2 \int_0^t dt' \mathrm{Tr}_{\mathrm{C}} \left[a_1 e^{\mathcal{L}_{\mathrm{C}}(t-t')} a_1^\dagger \tilde{\rho}_{\mathrm{C}}^{\mathrm{ss}}(t') \right] e^{-i\omega_{\mathrm{C}}(t-t')} \\
& \cdot \Big(\sigma_1^+(t)\sigma_1^-(t')\tilde{\rho}_{\mathrm{A}}(t') - \sigma_1^-(t')\tilde{\rho}_{\mathrm{A}}(t')\sigma_1^+(t) \Big) \\
& + |g_1|^2 \int_0^t dt' \mathrm{Tr}_{\mathrm{C}} \left[a_1^\dagger e^{\mathcal{L}_{\mathrm{C}}(t-t')} \tilde{\rho}_{\mathrm{C}}^{\mathrm{ss}}(t') a_1 \right] e^{i\omega_{\mathrm{C}}(t-t')} \\
& \cdot \Big(\tilde{\rho}_{\mathrm{A}}(t')\sigma_1^+(t')\sigma_1^-(t) - \sigma_1^-(t)\tilde{\rho}_{\mathrm{A}}(t')\sigma_1^+(t') \Big) \\
& + |g_2|^2 \int_0^t dt' \mathrm{Tr}_{\mathrm{C}} \left[a_2 e^{\mathcal{L}_{\mathrm{C}}(t-t')} a_2^\dagger \tilde{\rho}_{\mathrm{C}}^{\mathrm{ss}}(t') \right] e^{-i\omega_{\mathrm{C}}(t-t')} \\
& \cdot \Big(\sigma_2^+(t)\sigma_2^-(t')\tilde{\rho}_{\mathrm{A}}(t') - \sigma_2^-(t')\tilde{\rho}_{\mathrm{A}}(t')\sigma_2^+(t) \Big) \\
& + |g_2|^2 \int_0^t dt' \mathrm{Tr}_{\mathrm{C}} \left[a_2^\dagger e^{\mathcal{L}_{\mathrm{C}}(t-t')} \tilde{\rho}_{\mathrm{C}}^{\mathrm{ss}}(t') a_2 \right] e^{i\omega_{\mathrm{C}}(t-t')} \\
& \cdot \Big(\tilde{\rho}_{\mathrm{A}}(t')\sigma_2^+(t')\sigma_2^-(t) - \sigma_2^-(t)\tilde{\rho}_{\mathrm{A}}(t')\sigma_2^+(t') \Big) \\
& + g_1^* g_2 \int_0^t dt' \mathrm{Tr}_{\mathrm{C}} \left[a_2 e^{\mathcal{L}_{\mathrm{C}}(t-t')} a_1^\dagger \tilde{\rho}_{\mathrm{C}}^{\mathrm{ss}}(t') \right] e^{-i\omega_{\mathrm{C}}(t-t')} \\
& \cdot \Big(\sigma_2^+(t)\sigma_1^-(t')\tilde{\rho}_{\mathrm{A}}(t') - \sigma_1^-(t')\tilde{\rho}_{\mathrm{A}}(t')\sigma_2^+(t) \Big) \\
& + g_1 g_2^* \int_0^t dt' \mathrm{Tr}_{\mathrm{C}} \left[a_2^\dagger e^{\mathcal{L}_{\mathrm{C}}(t-t')} \tilde{\rho}_{\mathrm{C}}^{\mathrm{ss}}(t') a_1 \right] e^{i\omega_{\mathrm{C}}(t-t')} \\
& \cdot \Big(\tilde{\rho}_{\mathrm{A}}(t')\sigma_1^+(t')\sigma_2^-(t) - \sigma_2^-(t)\tilde{\rho}_{\mathrm{A}}(t')\sigma_1^+(t') \Big) \\
& + \dots
\end{aligned}
$$

$$
\begin{aligned}
&+ |g_1|^2 \int_0^t dt' \mathrm{Tr}_\mathrm{C} \left[b_1 e^{\mathcal{L}_\mathrm{C}(t-t')} b_1^\dagger \tilde{\rho}_\mathrm{C}^\mathrm{ss}(t') \right] e^{-i\omega_\mathrm{C}(t-t')} \\
&\qquad \cdot \left(\sigma_1^+(t)\sigma_1^-(t')\tilde{\rho}_\mathrm{A}(t') - \sigma_1^-(t')\tilde{\rho}_\mathrm{A}(t')\sigma_1^+(t) \right) \\
&+ |g_1|^2 \int_0^t dt' \mathrm{Tr}_\mathrm{C} \left[b_1^\dagger e^{\mathcal{L}_\mathrm{C}(t-t')} \tilde{\rho}_\mathrm{C}^\mathrm{ss}(t') b_1 \right] e^{i\omega_\mathrm{C}(t-t')} \\
&\qquad \cdot \left(\tilde{\rho}_\mathrm{A}(t')\sigma_1^+(t')\sigma_1^-(t) - \sigma_1^-(t)\tilde{\rho}_\mathrm{A}(t')\sigma_1^+(t') \right) \\
&+ |g_2|^2 \int_0^t dt' \mathrm{Tr}_\mathrm{C} \left[b_2 e^{\mathcal{L}_\mathrm{C}(t-t')} b_2^\dagger \tilde{\rho}_\mathrm{C}^\mathrm{ss}(t') \right] e^{-i\omega_\mathrm{C}(t-t')} \\
&\qquad \cdot \left(\sigma_2^+(t)\sigma_2^-(t')\tilde{\rho}_\mathrm{A}(t') - \sigma_2^-(t')\tilde{\rho}_\mathrm{A}(t')\sigma_2^+(t) \right) \\
&+ |g_2|^2 \int_0^t dt' \mathrm{Tr}_\mathrm{C} \left[b_2^\dagger e^{\mathcal{L}_\mathrm{C}(t-t')} \tilde{\rho}_\mathrm{C}^\mathrm{ss}(t') b_2 \right] e^{i\omega_\mathrm{C}(t-t')} \\
&\qquad \cdot \left(\tilde{\rho}_\mathrm{A}(t')\sigma_2^+(t')\sigma_2^-(t) - \sigma_2^-(t)\tilde{\rho}_\mathrm{A}(t')\sigma_2^+(t') \right) \\
&+ g_1^* g_2 \int_0^t dt' \mathrm{Tr}_\mathrm{C} \left[b_1 e^{\mathcal{L}_\mathrm{C}(t-t')} b_2^\dagger \tilde{\rho}_\mathrm{C}^\mathrm{ss}(t') \right] e^{-i\omega_\mathrm{C}(t-t')} \\
&\qquad \cdot \left(\sigma_1^+(t)\sigma_2^-(t')\tilde{\rho}_\mathrm{A}(t') - \sigma_2^-(t')\tilde{\rho}_\mathrm{A}(t')\sigma_1^+(t) \right) \\
&+ g_1 g_2^* \int_0^t dt' \mathrm{Tr}_\mathrm{C} \left[b_1^\dagger e^{\mathcal{L}_\mathrm{C}(t-t')} \tilde{\rho}_\mathrm{C}^\mathrm{ss}(t') b_2 \right] e^{i\omega_\mathrm{C}(t-t')} \\
&\qquad \cdot \left(\tilde{\rho}_\mathrm{A}(t')\sigma_2^+(t')\sigma_1^-(t) - \sigma_1^-(t)\tilde{\rho}_\mathrm{A}(t')\sigma_2^+(t') \right) \\
&+ \ldots \Big) + \tilde{\mathcal{L}}_\mathrm{A}\tilde{\rho}_\mathrm{A} \,. \qquad \text{(A.1)}
\end{aligned}
$$

where the "..." stands for all other possible combinations of operators $a_1^\dagger\sigma_1^-$, $a_1\sigma_1^+$, etc. of the Hamiltonian (5.123). There are 254 terms in total.

The traces can be evaluated with the relation

$$\langle \hat{O}_1(t)\hat{O}_2(t+\tau)\rangle = \mathrm{Tr}\left[\hat{O}_2 e^{\mathcal{L}\tau}\rho(t)\hat{O}_1\right] , \qquad \text{(A.2)}$$

$$\langle \hat{O}_1(t+\tau)\hat{O}_2(t)\rangle = \mathrm{Tr}\left[\hat{O}_1 e^{\mathcal{L}\tau}\hat{O}_2\rho(t)\right] , \qquad \text{(A.3)}$$

of the quantum regression formula from Section 3.2. Thus, we have to calculate second-order correlation functions in order to be able to compute the integrals. These correlation functions can be calculated with some other relations of the quantum regression formula (stated in Section 3.2), namely

$$\frac{d}{dt}\langle \hat{A}_\mu\rangle = \sum_\lambda M_{\mu,\lambda}\langle A_\lambda\rangle \,, \qquad \text{(A.4)}$$

$$\frac{d}{d\tau}\langle \hat{O}(t)\hat{A}_\mu(t+\tau)\rangle = \sum_\lambda M_{\mu,\lambda}\langle \hat{O}(t)\hat{A}_\lambda(t+\tau)\rangle \,, \qquad \text{(A.5)}$$

$$\frac{d}{d\tau}\langle \hat{A}_\mu(t+\tau)\hat{O}(t)\rangle = \sum_\lambda M_{\mu,\lambda}\langle \hat{A}_\lambda(t+\tau)\hat{O}(t)\rangle \,. \qquad \text{(A.6)}$$

Using these equations, we first need to compute equations of motion for a complete set of operators $\langle \hat{A}_\mu \rangle$ in order to obtain the constants $M_{\mu,\lambda}$ with relation (A.4). Then, with relations (A.5) and (A.6), we are able to derive the equations of motion for the second-order correlation functions which we eventually have to solve.

Since the traces in equation (A.1) are taken over the cavity modes, the mean values of our set of operators, $\langle \hat{A}_\mu \rangle$, are also taken over the cavity modes and can therefore be computed by

$$\frac{d}{dt}\langle \hat{A}_\mu \rangle = \mathrm{Tr}[\hat{A}_\mu \dot{\rho}_\mathrm{C}] \,, \tag{A.7}$$

with the reduced cavity density operator

$$\rho_\mathrm{C} = \mathrm{Tr}_\mathrm{C}\left[\rho\right] \,, \tag{A.8}$$

where ρ is given by equation (5.109). We transform to a rotating frame[1] (denoted by the tilde) which rotates at the atomic frequency, ω_A, and can then approximately set

$$\dot{\tilde{\rho}}_\mathrm{C} \approx \tilde{\mathcal{L}}_\mathrm{C} \tilde{\rho}_\mathrm{C} \,, \tag{A.9}$$

since the cavity damping rate, κ, exceeds all other parameters in the rotating frame.

We find the following equations of motion for our complete set of operators

$$\langle \dot{\tilde{a}}_1 \rangle = -\kappa_1 \langle \tilde{a}_1 \rangle \,, \tag{A.10}$$
$$\langle \dot{\tilde{a}}_1^\dagger \rangle = -\kappa_1 \langle \tilde{a}_1^\dagger \rangle \,, \tag{A.11}$$
$$\langle \dot{\tilde{a}}_2 \rangle = -2\sqrt{\kappa_1 \kappa_2} \langle \tilde{a}_1 \rangle - \kappa_2 \langle \tilde{a}_2 \rangle \,, \tag{A.12}$$
$$\langle \dot{\tilde{a}}_2^\dagger \rangle = -2\sqrt{\kappa_1 \kappa_2} \langle \tilde{a}_1^\dagger \rangle - \kappa_2 \langle \tilde{a}_2^\dagger \rangle \,, \tag{A.13}$$
$$\langle \dot{\tilde{b}}_1 \rangle = -\kappa_1 \langle \tilde{b}_1 \rangle - 2\sqrt{\kappa_1 \kappa_2} \langle \tilde{b}_2 \rangle \,, \tag{A.14}$$
$$\langle \dot{\tilde{b}}_1^\dagger \rangle = -\kappa_1 \langle \tilde{b}_1^\dagger \rangle - 2\sqrt{\kappa_1 \kappa_2} \langle \tilde{b}_2^\dagger \rangle \,, \tag{A.15}$$
$$\langle \dot{\tilde{b}}_2 \rangle = -\kappa_2 \langle \tilde{b}_2 \rangle \,, \tag{A.16}$$
$$\langle \dot{\tilde{b}}_2^\dagger \rangle = -\kappa_2 \langle \tilde{b}_2^\dagger \rangle \,. \tag{A.17}$$

The unidirectional coupling of the cavities can be seen very clearly from these equations. The time evolution of operator $\tilde{a}_1$ of the first cavity and $\tilde{b}_2$ of the second cavity, respectively is identical to what we would expect when considering only one cavity. Thus the cavity which is second in the propagation of the light does not have any influence on the first one. Also, it can be seen that the equations for the a and b modes are anti-symmetric which results from the opposite direction of propagation.

The two-time correlation function can be computed from equations (A.10)-(A.17) by applying the quantum regression formula. The only possible non-zero correlation

[1] For more information about transforming to a rotating frame see Appendix B.

functions are:

$$\frac{d}{d\tau}\langle\tilde{a}_1(t)\tilde{a}_1^\dagger(t+\tau)\rangle = -\kappa\langle\tilde{a}_1(t)\tilde{a}_1^\dagger(t+\tau)\rangle\,, \tag{A.18}$$

$$\frac{d}{d\tau}\langle\tilde{a}_1(t)\tilde{a}_2^\dagger(t+\tau)\rangle = -\kappa\langle\tilde{a}_1(t)\tilde{a}_2^\dagger(t+\tau)\rangle - 2\kappa\langle\tilde{a}_1(t)\tilde{a}_1^\dagger(t+\tau)\rangle\,, \tag{A.19}$$

$$\frac{d}{d\tau}\langle\tilde{a}_2(t)\tilde{a}_1^\dagger(t+\tau)\rangle = -\kappa\langle\tilde{a}_2(t)\tilde{a}_1^\dagger(t+\tau)\rangle\,, \tag{A.20}$$

$$\frac{d}{d\tau}\langle\tilde{a}_2(t)\tilde{a}_2^\dagger(t+\tau)\rangle = -\kappa\langle\tilde{a}_2(t)\tilde{a}_2^\dagger(t+\tau)\rangle - 2\kappa\langle\tilde{a}_2(t)\tilde{a}_1^\dagger(t+\tau)\rangle\,, \tag{A.21}$$

$$\frac{d}{d\tau}\langle\tilde{a}_1(t+\tau)\tilde{a}_1^\dagger(t)\rangle = -\kappa\langle\tilde{a}_1(t+\tau)\tilde{a}_1^\dagger(t)\rangle\,, \tag{A.22}$$

$$\frac{d}{d\tau}\langle\tilde{a}_1(t+\tau)\tilde{a}_2^\dagger(t)\rangle = -\kappa\langle\tilde{a}_1(t+\tau)\tilde{a}_2^\dagger(t)\rangle\,, \tag{A.23}$$

$$\frac{d}{d\tau}\langle\tilde{a}_2(t+\tau)\tilde{a}_1^\dagger(t)\rangle = -\kappa\langle\tilde{a}_2(t+\tau)\tilde{a}_1^\dagger(t)\rangle - 2\kappa\langle\tilde{a}_1(t+\tau)\tilde{a}_1^\dagger(t)\rangle\,, \tag{A.24}$$

$$\frac{d}{d\tau}\langle\tilde{a}_2(t+\tau)\tilde{a}_2^\dagger(t)\rangle = -\kappa\langle\tilde{a}_2(t+\tau)\tilde{a}_2^\dagger(t)\rangle - 2\kappa\langle\tilde{a}_1(t+\tau)\tilde{a}_2^\dagger(t)\rangle\,, \tag{A.25}$$

and the corresponding equations for the b modes

$$\frac{d}{d\tau}\langle\tilde{b}_1(t)\tilde{b}_1^\dagger(t+\tau)\rangle = -\kappa\langle\tilde{b}_1(t)\tilde{b}_1^\dagger(t+\tau)\rangle - 2\kappa\langle\tilde{b}_1(t)\tilde{b}_2^\dagger(t+\tau)\rangle\,, \tag{A.26}$$

$$\frac{d}{d\tau}\langle\tilde{b}_1(t)\tilde{b}_2^\dagger(t+\tau)\rangle = -\kappa\langle\tilde{b}_1(t)\tilde{b}_2^\dagger(t+\tau)\rangle\,, \tag{A.27}$$

$$\frac{d}{d\tau}\langle\tilde{b}_2(t)\tilde{b}_1^\dagger(t+\tau)\rangle = -\kappa\langle\tilde{b}_2(t)\tilde{b}_1^\dagger(t+\tau)\rangle - 2\kappa\langle\tilde{b}_2(t)\tilde{b}_2^\dagger(t+\tau)\rangle\,, \tag{A.28}$$

$$\frac{d}{d\tau}\langle\tilde{b}_2(t)\tilde{b}_2^\dagger(t+\tau)\rangle = -\kappa\langle\tilde{b}_2(t)\tilde{b}_2^\dagger(t+\tau)\rangle\,, \tag{A.29}$$

$$\frac{d}{d\tau}\langle\tilde{b}_1(t+\tau)\tilde{b}_1^\dagger(t)\rangle = -\kappa\langle\tilde{b}_1(t+\tau)\tilde{b}_1^\dagger(t)\rangle - 2\kappa\langle\tilde{b}_2(t+\tau)\tilde{b}_1^\dagger(t)\rangle\,, \tag{A.30}$$

$$\frac{d}{d\tau}\langle\tilde{b}_1(t+\tau)\tilde{b}_2^\dagger(t)\rangle = -\kappa\langle\tilde{b}_1(t+\tau)\tilde{b}_2^\dagger(t)\rangle - 2\kappa\langle\tilde{b}_2(t+\tau)\tilde{b}_2^\dagger(t)\rangle\,, \tag{A.31}$$

$$\frac{d}{d\tau}\langle\tilde{b}_2(t+\tau)\tilde{b}_1^\dagger(t)\rangle = -\kappa\langle\tilde{b}_2(t+\tau)\tilde{b}_1^\dagger(t)\rangle\,, \tag{A.32}$$

$$\frac{d}{d\tau}\langle\tilde{b}_2(t+\tau)\tilde{b}_2^\dagger(t)\rangle = -\kappa\langle\tilde{b}_2(t+\tau)\tilde{b}_2^\dagger(t)\rangle\,. \tag{A.33}$$

Keeping in mind that in the bad-cavity limit the steady state cavity modes are in the vacuum state (since a photon in the cavity is immediately lost to its environment) we see that the only non-zero mean values of two arbitrary cavity operators in steady state are

$$\langle\tilde{a}_1\tilde{a}_1^\dagger\rangle_{\rm ss} = \langle\tilde{a}_2\tilde{a}_2^\dagger\rangle_{\rm ss} = \langle\tilde{b}_1\tilde{b}_1^\dagger\rangle_{\rm ss} = \langle\tilde{b}_2\tilde{b}_2^\dagger\rangle_{\rm ss} = 1\,. \tag{A.34}$$

Using this as initial value when solving the differential equations (A.18)-(A.33) and setting $t \to \infty$ (long-time limit) we find for the non-zero correlation functions in

steady state

$$\langle \tilde{a}_1(t)\tilde{a}_1^\dagger(t+\tau)\rangle_{\rm ss} = \langle \tilde{a}_1(t+\tau)\tilde{a}_1^\dagger(t)\rangle_{\rm ss} = e^{-\kappa\tau}\,, \tag{A.35}$$

$$\langle \tilde{a}_2(t)\tilde{a}_2^\dagger(t+\tau)\rangle_{\rm ss} = \langle \tilde{a}_2(t+\tau)\tilde{a}_2^\dagger(t)\rangle_{\rm ss} = e^{-\kappa\tau}\,, \tag{A.36}$$

$$\langle \tilde{a}_1(t)\tilde{a}_2^\dagger(t+\tau)\rangle_{\rm ss} = \langle \tilde{a}_2(t+\tau)\tilde{a}_1^\dagger(t)\rangle_{\rm ss} = -2\kappa\tau e^{-\kappa\tau}\,, \tag{A.37}$$

$$\langle \tilde{b}_1(t)\tilde{b}_1^\dagger(t+\tau)\rangle_{\rm ss} = \langle \tilde{b}_1(t+\tau)\tilde{b}_1^\dagger(t)\rangle_{\rm ss} = e^{-\kappa\tau}\,, \tag{A.38}$$

$$\langle \tilde{b}_2(t)\tilde{b}_2^\dagger(t+\tau)\rangle_{\rm ss} = \langle \tilde{b}_2(t+\tau)\tilde{b}_2^\dagger(t)\rangle_{\rm ss} = e^{-\kappa\tau}\,, \tag{A.39}$$

$$\langle \tilde{b}_2(t)\tilde{b}_1^\dagger(t+\tau)\rangle_{\rm ss} = \langle \tilde{b}_1(t+\tau)\tilde{b}_2^\dagger(t)\rangle_{\rm ss} = -2\kappa\tau e^{-\kappa\tau}\,, \tag{A.40}$$

where, for the sake of simple analytic expressions, the damping constant, $\kappa := \kappa_1 = \kappa_2$, was assumed to be the same for the two cavities. Moving back to the non-rotating frame yields

$$\langle a_1(t)a_1^\dagger(t+\tau)\rangle_{\rm ss} = e^{(-\kappa+i\omega_{\rm A})\tau}\,, \tag{A.41}$$

$$\langle a_1(t+\tau)a_1^\dagger(t)\rangle_{\rm ss} = e^{(-\kappa-i\omega_{\rm A})\tau}\,, \tag{A.42}$$

$$\langle a_2(t)a_2^\dagger(t+\tau)\rangle_{\rm ss} = e^{(-\kappa+i\omega_{\rm A})\tau}\,, \tag{A.43}$$

$$\langle a_2(t+\tau)a_2^\dagger(t)\rangle_{\rm ss} = e^{(-\kappa-i\omega_{\rm A})\tau}\,, \tag{A.44}$$

$$\langle a_1(t)a_2^\dagger(t+\tau)\rangle_{\rm ss} = -2\kappa\tau e^{(-\kappa+i\omega_{\rm A})\tau}\,, \tag{A.45}$$

$$\langle a_2(t+\tau)a_1^\dagger(t)\rangle_{\rm ss} = -2\kappa\tau e^{(-\kappa-i\omega_{\rm A})\tau}\,, \tag{A.46}$$

and equivalently for the b modes

$$\langle b_1(t)b_1^\dagger(t+\tau)\rangle_{\rm ss} = e^{(-\kappa+i\omega_{\rm A})\tau}\,, \tag{A.47}$$

$$\langle b_1(t+\tau)b_1^\dagger(t)\rangle_{\rm ss} = e^{(-\kappa-i\omega_{\rm A})\tau}\,, \tag{A.48}$$

$$\langle b_2(t)b_2^\dagger(t+\tau)\rangle_{\rm ss} = e^{(-\kappa+i\omega_{\rm A})\tau}\,, \tag{A.49}$$

$$\langle b_2(t+\tau)b_2^\dagger(t)\rangle_{\rm ss} = e^{(-\kappa-i\omega_{\rm A})\tau}\,, \tag{A.50}$$

$$\langle b_2(t)b_1^\dagger(t+\tau)\rangle_{\rm ss} = -2\kappa\tau e^{(-\kappa+i\omega_{\rm A})\tau}\,, \tag{A.51}$$

$$\langle b_1(t+\tau)b_2^\dagger(t)\rangle_{\rm ss} = -2\kappa\tau e^{(-\kappa-i\omega_{\rm A})\tau}\,. \tag{A.52}$$

These expressions coincide with equations (5.130)-(5.132) if t is replaced by t' and τ by $t-t'$.

Appendix B

The Rotating Frame

In quantum optics it is widely used to move to a rotating frame, rotating with the characteristic, high optical frequency of the system. This is done to separate the rapid motion of the optical system from the slow motion that we are usually interested in. We will demonstrate the mathematical formalism of transforming a system to a rotating frame by an example.

Our sample system consists of an atom (described by the lowering and raising operator $\sigma^{\pm}$) coupled to a one-mode cavity (with the mode denoted by a) and driven by an external coherent light source with the strength $\mathcal{E}$. The Hamiltonian of the system is[1]

$$H = \omega_{\mathrm{A}}\sigma^{+}\sigma^{-} + \omega_{\mathrm{C}}a^{\dagger}a + (\mathcal{E}^{*}e^{i\omega_{\mathrm{p}}t}a + \mathcal{E}e^{-i\omega_{\mathrm{p}}t}a^{\dagger}) + (g^{*}a^{\dagger}\sigma^{-} + g\sigma^{+}a)\,, \tag{B.1}$$

where g is the atom-cavity coupling constant, ω_{A} the atomic transition frequency, ω_{C} the cavity frequency and ω_{p} the frequency of the driving field. The master equation of the system can be written as

$$\dot{\rho} = -i\,[H, \rho] + \mathcal{L}\rho\,, \tag{B.2}$$

with the Liouvillian

$$\mathcal{L} = \kappa(2a\cdot a^{\dagger} - a^{\dagger}a\cdot - \cdot a^{\dagger}a) + \frac{\gamma}{2}(2\sigma^{-}\cdot\sigma^{+} - \sigma^{+}\sigma^{-}\cdot - \cdot\sigma^{+}\sigma^{-})\,, \tag{B.3}$$

where κ is the cavity damping rate and γ the atomic damping rate.

We want to get rid of the fast varying exponential in the driving term and, hence, have to move to a frame rotating with the probe frequency, ω_{p}. Mathematical, this is done by moving to an interaction picture, e.g., by a unitary transformation of our system of the form

$$\tilde{H} = U^{\dagger}HU\,, \tag{B.4}$$

[1] We set $\hbar = 1$ throughout this chapter.

with the operator

$$U = e^{-iH_{\mathrm{T}}t}\,, \tag{B.5}$$

where H_{T} is the transformation Hamiltonian

$$H_{\mathrm{T}} = \omega_{\mathrm{p}}(\sigma^{+}\sigma^{-} + a^{\dagger}a)\,. \tag{B.6}$$

The transformation of the master equation yields

$$\begin{aligned}\dot{\tilde{\rho}} &= \dot{U}^{\dagger}\rho U + U^{\dagger}\dot{\rho}U + U^{\dagger}\rho\dot{U} \\ &= -i\left[H', \tilde{\rho}\right] + \tilde{\mathcal{L}}\tilde{\rho}\,,\end{aligned} \tag{B.7}$$

with $H' = \tilde{H} - H_{\mathrm{T}}$.

In the next step, we have to evaluate the transformed Hamiltonian $\tilde{H}$ and the transformed Liouvillian $\tilde{\mathcal{L}}$. With the commutator relations for the annihilation and creation operators of the cavity mode

$$\left[a^{\dagger}a, a^{\dagger}\right] = a^{\dagger}aa^{\dagger} - a^{\dagger}a^{\dagger}a = \left[a, a^{\dagger}\right]a^{\dagger} = a^{\dagger}\,, \tag{B.8}$$

$$\left[a^{\dagger}a, a\right] = a^{\dagger}aa - aa^{\dagger}a = \left[a^{\dagger}, a\right]a = -a\,, \tag{B.9}$$

and the Baker-Hausdorff formula

$$\exp(\alpha A)B\exp(-\alpha A) = B + \alpha\left[A, B\right] + \frac{\alpha^2}{2}\left[A, [A, B]\right] + \cdots\,, \tag{B.10}$$

we can show that

$$\exp(\alpha a^{\dagger}a)a^{\dagger}\exp(-\alpha a^{\dagger}a) = a^{\dagger}\exp(\alpha)\,, \tag{B.11}$$

$$\exp(\alpha a^{\dagger}a)a\exp(-\alpha a^{\dagger}a) = a\exp(-\alpha)\,. \tag{B.12}$$

In a similar way we can show that

$$\exp(\alpha\sigma_{+}\sigma_{-})\sigma_{+}\exp(-\alpha\sigma_{+}\sigma_{-}) = \sigma_{+}\exp(\alpha)\,, \tag{B.13}$$

$$\exp(\alpha\sigma_{+}\sigma_{-})\sigma_{-}\exp(-\alpha\sigma_{+}\sigma_{-}) = \sigma_{-}\exp(-\alpha)\,. \tag{B.14}$$

The second calculation is slightly more complicated and therefore, we will state it here. From the Baker-Hausdorff formula, we find

$$\begin{aligned}\exp(\alpha\sigma_{+}\sigma_{-})\sigma_{+}\exp(-\alpha\sigma_{+}\sigma_{-}) = \sigma_{+} &+ \alpha\left[\sigma_{+}\sigma_{-}, \sigma_{+}\right] \\ &+ \frac{\alpha^2}{2!}\left[\sigma_{+}\sigma_{-}, [\sigma_{+}\sigma_{-}, \sigma_{+}]\right] + \cdots\end{aligned} \tag{B.15}$$

with the commutator

$$\left[\sigma_{+}\sigma_{-}, \sigma_{+}\right] = \sigma_{+}\underbrace{\left[\sigma_{-}, \sigma_{+}\right]}_{=-\sigma_z} + \underbrace{\left[\sigma_{+}, \sigma_{+}\right]}_{=0}\sigma_{-} = -\sigma_{+}\sigma_z\,, \tag{B.16}$$

and

$$\begin{aligned}
[\sigma_+\sigma_-,[\sigma_+\sigma_-,\sigma_+]] &= -\left[\sigma_+\sigma_-,\sigma_+\sigma_z\right] \\
&= -\left\{\sigma_+\left[\sigma_-,\sigma_+\sigma_z\right]+\left[\sigma_+,\sigma_+\sigma_z\right]\sigma_-\right\} \\
&= -\{\sigma_+\sigma_+\underbrace{\left[\sigma_-,\sigma_z\right]}_{=\sigma_-}+\sigma_+\underbrace{\left[\sigma_-,\sigma_+\right]}_{-\sigma_z}\sigma_z \\
&\quad +\sigma_+\underbrace{\left[\sigma_+,\sigma_z\right]}_{=-\sigma_+}\sigma_- +\underbrace{\left[\sigma_+,\sigma_+\right]}_{=0}\sigma_z\sigma_-\} \\
&= \sigma_+ \,. \qquad \text{(B.17)}
\end{aligned}$$

Evaluating further, gives

$$\begin{aligned}
\exp(\alpha\sigma_+\sigma_-)\sigma_+\exp(-\alpha\sigma_+\sigma_-) &= \sigma_+ +\alpha(-\sigma_+\sigma_z)+\frac{\alpha^2}{2!}\sigma_+ \\
&\quad +\frac{\alpha^3}{3!}(-\sigma_+\sigma_z)+\frac{\alpha^4}{4!}\sigma_+ +\cdots \\
&= \sigma_+\{\underbrace{(1+\frac{\alpha^2}{2!}+\frac{\alpha^4}{4!}+\cdots)}_{\cosh\alpha}I_2 \\
&\quad -\underbrace{(\alpha+\frac{\alpha^3}{3!}+\cdots)}_{\sinh\alpha}\sigma_z\} \\
&= \sigma_+(\cosh\alpha I_2-\sinh\alpha\sigma_z) \\
&= \sigma_+\begin{pmatrix}\cosh\alpha-\sinh\alpha & 0\\ 0 & \cosh\alpha+\sinh\alpha\end{pmatrix} \\
&= \sigma_+\begin{pmatrix}e^{-\alpha} & 0\\ 0 & e^{\alpha}\end{pmatrix}=\begin{pmatrix}0 & e^{\alpha}\\ 0 & 0\end{pmatrix} \\
&= \sigma_+ e^{\alpha}\,, \qquad \text{(B.18)}
\end{aligned}$$

where we used $\cosh\alpha\pm\sinh\alpha=e^{\pm\alpha}$ and $\sigma_+=\begin{pmatrix}0 & 1\\ 0 & 0\end{pmatrix}$ in the second last line.

Finally, using equations (B.11)-(B.14), we find for the transformed Hamiltonian, $H'=\tilde{H}-H_{\mathrm{T}}$,

$$H' = \Delta\omega_{\mathrm{A}}\sigma^+\sigma^- +\Delta\omega_{\mathrm{C}}a^\dagger a+(\mathcal{E}^*a+\mathcal{E}a^\dagger)+(g^*a^\dagger\sigma^- +g\sigma^+a)\,, \qquad \text{(B.19)}$$

with the frequency detunings $\Delta\omega_{\mathrm{A}}=\omega_{\mathrm{A}}-\omega_{\mathrm{p}}$ and $\Delta\omega_{\mathrm{C}}=\omega_{\mathrm{C}}-\omega_{\mathrm{p}}$, and for the transformed Liouvillian

$$\tilde{\mathcal{L}} = \kappa(2a\cdot a^\dagger - a^\dagger a\cdot - \cdot a^\dagger a)+\frac{\gamma}{2}(2\sigma^-\cdot\sigma^+-\sigma^+\sigma^-\cdot -\cdot\sigma^+\sigma^-)=\mathcal{L}\,. \qquad \text{(B.20)}$$

Suppressing the tilde on $\tilde{\rho}$ in equation (B.7), we find a master equation,

$$\dot{\rho} = -i\left[H',\rho\right]+\mathcal{L}\rho\,, \qquad \text{(B.21)}$$

which is formally similar to master equation (B.2) and where, in the Hamiltonian H', the fast varying exponential term has been eliminated.

Appendix C

Adiabatic Master Equation – Initial Calculations

The adiabatic master equation was derived in Section 5.4. In the case that the cavities have equal properties and the atom-cavity coupling constant, g, and the atomic decay rate, γ, are the same for both subsystems, it can be written as[1]

$$\begin{aligned}\dot{\rho} = -i\,[H,\rho] &+ \frac{\Gamma}{2}(2\sigma_1^-\rho\sigma_1^+ - \sigma_1^+\sigma_1^-\rho - \rho\sigma_1^+\sigma_1^-) \\ &+ \frac{\Gamma}{2}(2\sigma_2^-\rho\sigma_2^+ - \sigma_2^+\sigma_2^-\rho - \rho\sigma_2^+\sigma_2^-) \\ &+ \frac{\Pi}{2}(2\sigma_1^-\rho\sigma_2^+ - \sigma_2^+\sigma_1^-\rho - \rho\sigma_2^+\sigma_1^-) \\ &+ \frac{\Pi}{2}(2\sigma_2^-\rho\sigma_1^+ - \sigma_1^+\sigma_2^-\rho - \rho\sigma_1^+\sigma_2^-)\,, \end{aligned} \tag{C.1}$$

with

$$\begin{aligned} H = &\left(\omega_\mathrm{A} - 2g^2\frac{\Delta\omega}{\kappa^2+\Delta\omega^2}\right)\left(\sigma_1^+\sigma_1^- + \sigma_2^+\sigma_2^-\right) \\ &+ 4g^2\frac{\kappa^2\Delta\omega}{(\kappa^2-\Delta\omega^2)^2+4\kappa^2\Delta\omega^2}\left(\sigma_2^+\sigma_1^- + \sigma_1^+\sigma_2^-\right)\,, \end{aligned} \tag{C.2}$$

$$\Gamma = \gamma + 4g^2\frac{\kappa}{\kappa^2+\Delta\omega^2}\,, \tag{C.3}$$

$$\Pi = -4g^2\frac{\kappa(\kappa^2-\Delta\omega^2)}{(\kappa^2-\Delta\omega^2)^2+4\kappa^2\Delta\omega^2}\,. \tag{C.4}$$

In this equation the cavity modes have been adiabatically eliminated and we are only left with the atomic operators. This is a great reduction of the complexity of the system, especially in terms of the dimension of the Hilbert space, which is, in the case of a two-level atom, reduced from $d_\mathcal{H} = 4N^4$ (with N the truncation of the

[1] We set $\hbar = 1$ throughout this appendix.

cavity modes) to $d_{\mathcal{H}} = 4$. The emission spectra for the bad-cavity regime can be calculated from the adiabatic master equation.

The emission spectra are given by equations (5.28)-(5.31), where we need to compute two-time integrals over second-order correlation functions of the cavity modes and atoms. These integrals can be analysed in a similar way to Section 5.1.2 by a "Separation of the Liouvillian". The only difference is that we need to use the adiabatic master equation when separating the Liouvillian. Therefore, we need to write the cavity mode operators in terms of atomic operators (e.g. $a = a(\sigma_i)$), so that we are able to write the two-time cavity mode functions in terms of two-time atomic functions (e.g., $\langle a^\dagger(t)a(t')\rangle = \langle a^\dagger(t)a(t')\rangle(\langle\sigma_i^+\sigma_i^-\rangle)$), from which we eventually can apply the formalism of "Separation of the Liouvillian". The cavity mode operators in terms of atomic operators are obtained by deriving the quantum Langevin equations for the cavity modes, which are of the form

$$\dot{a} = -i\,[a, H] - \kappa a + \xi\,, \tag{C.5}$$

where ξ is a (input) noise term,[2] and formally integrating them.

The quantum Langevin equations for the a modes yield

$$\dot{a}_1 = (-i\omega_{\mathrm{C}} - \kappa)a_1 + \kappa a_2 - ig\sigma_1^- + \xi_1\,, \tag{C.6}$$
$$\dot{a}_2 = (-i\omega_{\mathrm{C}} - \kappa)a_2 - \kappa a_1 - ig\sigma_2^- + \xi_2\,. \tag{C.7}$$

In matrix form, this can be written as

$$\frac{d}{dt}\begin{pmatrix} a_1 \\ a_2 \end{pmatrix} = \underline{A}\begin{pmatrix} a_1 \\ a_2 \end{pmatrix} + \underline{B}\begin{pmatrix} \sigma_1^- \\ \sigma_2^- \end{pmatrix} + \begin{pmatrix} \xi_1 \\ \xi_2 \end{pmatrix}, \tag{C.8}$$

with

$$\underline{A} = \begin{pmatrix} -i\omega_{\mathrm{C}} - \kappa & \kappa \\ -\kappa & -i\omega_{\mathrm{C}} - \kappa \end{pmatrix}, \tag{C.9}$$

$$\underline{B} = \begin{pmatrix} -ig & 0 \\ 0 & -ig \end{pmatrix}. \tag{C.10}$$

Formally integrating equation (C.8) yields

$$\begin{pmatrix} a_1(t) \\ a_2(t) \end{pmatrix} = e^{\underline{A}t}\begin{pmatrix} a_1(0) \\ a_2(0) \end{pmatrix} + \int_0^t dt' e^{\underline{A}(t-t')}\underline{B}\begin{pmatrix} \sigma_1^-(t') \\ \sigma_2^-(t') \end{pmatrix} + \int_0^t dt' e^{\underline{A}(t-t')}\begin{pmatrix} \xi_1(t') \\ \xi_2(t') \end{pmatrix}. \tag{C.11}$$

We can replace the atomic operators by

$$\sigma_i^-(t') = e^{-i\omega_{\mathrm{A}}t'}\tilde{\sigma}_i^-(t')\,, \tag{C.12}$$

[2] The noise term is assumed to be the vacuum field with a mean value of zero.

where we have separated the fast varying term, $e^{-i\omega_{\rm A}t'}$, from the slow varying term, $\tilde{\sigma}_i^-(t')$. Substituting this into equation (C.11) and ignoring the noise term (since we are only interested in the mean values, and the mean of any term which involves the noise term is zero) we obtain

$$\begin{pmatrix} a_1(t) \\ a_2(t) \end{pmatrix} = e^{\underline{A}t} \begin{pmatrix} a_1(0) \\ a_2(0) \end{pmatrix} + \int_0^t dt' e^{i\omega_{\rm A}(t-t')} e^{\underline{A}(t-t')} \underline{B} \begin{pmatrix} \tilde{\sigma}_1^-(t') \\ \tilde{\sigma}_2^-(t') \end{pmatrix} e^{-i\omega_{\rm A}t} \,. \tag{C.13}$$

The exponential function, $e^{\underline{A}t}$, rapidly decays to zero (since in the bad-cavity regime κ is large), therefore we can neglect the first term on the RHS of equation (C.13). On the other hand, the atomic operator, $\tilde{\sigma}_i^-(t')$, varies very slowly and can be assumed to be constant over the integration in the second term of the RHS. Evaluating the integral yields for the cavity modes,

$$a_1(t) = X_1\sigma_1^-(t) + X_2\sigma_2^-(t)\,, \tag{C.14}$$
$$a_2(t) = -X_2\sigma_1^-(t) + X_1\sigma_2^-(t)\,, \tag{C.15}$$

with

$$X_1 = i\frac{g}{2}\left(\frac{1}{-i\Delta\omega - i\kappa - \kappa} + \frac{1}{-i\Delta\omega + i\kappa - \kappa}\right), \tag{C.16}$$
$$X_2 = \frac{g}{2}\left(\frac{1}{-i\Delta\omega - i\kappa - \kappa} - \frac{1}{-i\Delta\omega + i\kappa - \kappa}\right), \tag{C.17}$$

where $\Delta\omega = \omega_{\rm C} - \omega_{\rm A}$. In a similar way, the b modes can be obtained, which yield

$$\begin{aligned} b_1(t) &= X_1\sigma_1^-(t) - X_2\sigma_2^-(t)\,, \\ b_2(t) &= X_2\sigma_1^-(t) + X_1\sigma_2^-(t)\,. \end{aligned} \tag{C.18}$$

Hence we are now able to write the two-time correlation functions for the cavity modes and therefore also the integrals the emission spectra are computed with, given by,

$$T^{(j)}_{{\rm side},\sigma}(\omega) = \frac{\gamma_j}{2\pi}\int_0^\infty dt \int_0^\infty dt'\, e^{-i\omega(t-t')}\langle\sigma_j^+(t)\sigma_j^-(t')\rangle\,, \tag{C.19}$$

$$\begin{aligned} T_{{\rm axis},a_{\rm out}}(\omega) &= \frac{1}{2\pi}\int_0^\infty dt \int_0^\infty dt'\, e^{-i\omega(t-t')}\langle a^\dagger_{\rm out}(t)a_{\rm out}(t')\rangle \\ &= \frac{\kappa}{2\pi}\int_0^\infty dt \int_0^\infty dt'\, e^{-i\omega(t-t')}\big(\langle a_1^\dagger(t)a_1(t')\rangle + \langle a_1^\dagger(t)a_2(t')\rangle \\ &\quad + \langle a_2^\dagger(t)a_1(t')\rangle + \langle a_2^\dagger(t)a_2(t')\rangle\big)\,, \end{aligned} \tag{C.20}$$

$$\begin{aligned} T_{{\rm axis},b_{\rm out}}(\omega) &= \frac{\kappa}{2\pi}\int_0^\infty dt \int_0^\infty dt'\, e^{-i\omega(t-t')}\big(\langle b_1^\dagger(t)b_1(t')\rangle + \langle b_1^\dagger(t)b_2(t')\rangle \\ &\quad + \langle b_2^\dagger(t)b_1(t')\rangle + \langle b_2^\dagger(t)b_2(t')\rangle\big)\,, \end{aligned} \tag{C.21}$$

in terms of two-time correlation functions of the atomic operators. We used the relations

$$a_{\text{out}}(t) = -a_{\text{in}}(t) + J_a(t)\,, \tag{C.22}$$
$$b_{\text{out}}(t) = -b_{\text{in}}(t) + J_b(t)\,, \tag{C.23}$$

and that the input, a_{in} and b_{in}, is the vacuum noise whose mean is zero.

The second-order correlation functions for the atomic operators can be obtained in terms of the probability amplitudes of the pure state of the one-energy quantum subspace, shown as,

$$|\bar{\psi}(t)\rangle = \alpha(t)|eg\rangle + \beta(t)|ge\rangle\,, \tag{C.24}$$

by separating the Liouvillian, similar to what was done in Section 5.1.2. We find

$$\langle\sigma_1^+(t)\sigma_1^-(t')\rangle = \alpha^*(t)\alpha(t')\,, \tag{C.25}$$
$$\langle\sigma_1^+(t)\sigma_2^-(t')\rangle = \alpha^*(t)\beta(t')\,, \tag{C.26}$$
$$\langle\sigma_2^+(t)\sigma_1^-(t')\rangle = \beta^*(t)\alpha(t')\,, \tag{C.27}$$
$$\langle\sigma_2^+(t)\sigma_2^-(t')\rangle = \beta^*(t)\beta(t')\,, \tag{C.28}$$

and for the equations of motion for the probability amplitudes

$$\dot{\alpha}(t) = Y_1\alpha(t) + Y_2\beta(t)\,, \tag{C.29}$$
$$\dot{\beta}(t) = Y_2\alpha(t) + Y_1\beta(t)\,, \tag{C.30}$$

with

$$Y_1 = -i\left(\omega_{\text{A}} - 2g\frac{\Delta\omega}{\kappa^2 + \Delta\omega^2}\right) - \frac{\Gamma}{2}\,, \tag{C.31}$$
$$Y_2 = -i\left(4g^2\frac{\kappa^2\Delta\omega}{(\kappa^2 - \Delta\omega^2)^2 + 4\kappa^2\Delta\omega^2}\right) - \frac{\Pi}{2}\,, \tag{C.32}$$

where Γ and Π are given by equation (C.3) and (C.4), respectively. The solutions for the probability amplitudes are

$$\alpha(t) = e^{Y_1 t}\left[\cosh\left(Y_2 t\right)\alpha(0) + \sinh\left(Y_2 t\right)\beta(0)\right]\,, \tag{C.33}$$
$$\beta(t) = e^{Y_1 t}\left[\sinh\left(Y_2 t\right)\alpha(0) + \cosh\left(Y_2 t\right)\beta(0)\right]\,. \tag{C.34}$$

These are essentially all the results needed for computing the emission spectra which could then be compared with the emission spectra obtained from the full model.

Bibliography

[ADW+06a] Takao Aoki, Barak Dayan, E. Wilcut, W. P. Bowen, A. S. Parkins, T. J. Kippenberg, K. J. Vahala, and H. J. Kimble, *Observation of strong coupling between one atom and a monolithic microresonator*, Nature **443** (2006), 671.

[ADW+06b] ———, *Supplementary Information - Observation of strong coupling between one atom and a monolithic microresonator*, Nature **443** (2006), 671.

[Aga70] G. S. Agarwal, *Master-Equation Approach to Spontaneous Emission*, Phys. Rev. A **2** (1970), 2038.

[BBM+07] A. D. Boozer, A. Boca, R. Miller, T. E. Northup, and H. J. Kimble, *Reversible State Transfer between Light and a Single Trapped Atom*, Phys. Rev. Lett. **98** (2007), 193601.

[BMB+04] A. Boca, R. Miller, K. M. Birnbaum, A. D. Boozer, J. McKeever, and H. J. Kimble, *Observation of the Vacuum Rabi Spectrum for One Trapped Atom*, Phys. Rev. Lett. **93** (2004), 233603.

[BSH71] R. Bonifacio, P. Schwendimann, and Fritz Haake, *Quantum Statistical Theory of Superradiance. I*, Phys. Rev. A **4** (1971), 302.

[Car93] H. J. Carmichael, *Quantum trajectory theory for cascaded open systems*, Phys. Rev. Lett. **70** (1993), 2273.

[Car99] ———, *Statistical Methods in Quantum Optics 1*, Springer, 1999.

[Car08] ———, *Statistical Methods in Quantum Optics 2*, Springer, 2008.

[CBR+89] H. J. Carmichael, R. J. Brecha, M. G. Raizen, H. J. Kimble, and P. R. Rice, *Subnatural linewidth averaging for coupled atomic and cavity-mode oscillators*, Phys. Rev. A **40** (1989), 5516.

[CG84] M. J. Collett and C. W. Gardiner, *Squeezing of intracavity and traveling-wave light fields produced in parametric amplification*, Phys. Rev. A **30** (1984), 1386.

[CZKM97] J.I. Cirac, P. Zoller, H. J. Kimble, and H. Mabuchi, *Quantum State Transfer and Entanglement Distribution among Distant Nodes in a Quantum Network*, Phys. Rev. Lett. **78** (1997), 3221.

[Deu85] D. Deutsch, *Quantum theory, the Church-Turing principle and the universal quantum computer*, Proceedings of the Royal Society of London A **400** (1985), 97.

[Dic54] R. H. Dicke, *Coherence in Spontaneous Radiation Processes*, Phys. Rev. **93** (1954), 99.

[DPA+08a] Barak Dayan, A. S. Parkins, Takao Aoki, E. P. Ostby, K. J. Vahala, and H. J. Kimble, *A Photon Turnstile Dynamically Regulated by One Atom*, Science **319** (2008), 1062.

[DPA+08b] ———, *Supporting Online Information: Information - A Photon Turnstile Dynamically Regulated by One Atom*, Science **319** (2008), 1062.

[Fey82] R. P. Feynman, *Simulating Physics with Computers*, International Journal of Theoretical Physics **21** (1982), 467.

[Fox06] Mark Fox, *Quantum Optics - An introduction*, Oxford University Press, 2006.

[Gar93] C. W. Gardiner, *Driving a quantum system with the output field from another driven quantum system*, Phys. Rev. Lett. **70** (1993), 2269.

[GZ04] C. W. Gardiner and P. Zoller, *Quantum Noise*, Springer, 2004.

[Jac07] John David Jackson, *Classical Electrodynamics Third Edition*, Wiley, 2007.

[JC63] E. T. Jaynes and F. W. Cummings, *Comparison of quantum and semiclassical radiation theories with application to the beam maser*, Proceedings of the IEEE **51** (1963), 89.

[KGK+06] G. Khitrova, H. M. Gibbs, M. Kira, S. W. Koch, and A. Scherer, *Vacuum Rabi splitting in semiconductors*, Nature Physics **2** (2006), 81.

[KS87] H. J. Kolobov and I.V. Sokolov, Opt. Spektrosk. **62** (1987), 112.

[Leh70a] R. H. Lehmberg, *Radiation from an N-Atom System. I. General Formalism*, Phys. Rev. A **2** (1970), 883.

[Leh70b] ———, *Radiation from an N-Atom System. II. Spontaneous Emission from a Pair of Atoms*, Phys. Rev. A **2** (1970), 889.

[LI01] M. D. Lukin and A. Imamoglu, *Controlling photons using electromagnetically induced transparency*, Nature **413** (2001), 273.

[Lou73] Rodney Loudon, *The Quantum Theory of Light*, Oxford University Press, 1973.

[MMSI04] L. Maleki, A. B. Matsko, A. A. Savchenkov, and V. S. Ilchenko, *Tunable delay line with interacting whispering-gallery-mode resonators*, Optics Letters **29** (2004), 626.

[Mon02] C. Monroe, *Quantum information processing with atoms and photons*, Nature **416** (2002), 238.

[MSI07] Pierre Meystre and Murray Sargent III, *Elements of Quantum Optics*, Springer, 2007.

[NFSR05] Ahmer Naweed, G. Farca, S. I. Shopova, and A. T. Rosenberger, *Induced transparency and absorption in coupled whispering-gallery microresonators*, Phys. Rev. A **71** (2005), 043804.

[Par06] A. S. Parkins, *Notes on: Microtoroid cavity QED*, unpublished, 2006.

[PDAK09] A. S. Parkins, B. Dayan, T. Aoki, and H. J. Kimble, *Microtoroid Cavity QED in the Bad-Cavity, Critically-Coupled and Over-Coupled Regimes*, unpublished, 2009.

[PSM+05] E. Peter, P. Senellart, D. Martrou, A. Lemaître, J. Hours, J. M. Gérard, and J. Bloch, *Exciton-Photon Strong-Coupling Regime for a Single Quantum Dot Embedded in a Microcavity*, Phys. Rev. Lett. **95** (2005), 067401.

[Pur46] E. M. Purcell, *Spontaneous emission probabilities at radio frequencies*, Phys. Rev. **69** (1946), 681.

[Ree93] M. A. Reed, *Quantum Dots*, Scientific American **1** (1993), 118.

[RSL+04] J. P. Reithmaier, G. Sęk, A. Löffler, C. Hofmann, S. Kuhn, S. Reitzenstein, L. V. Keldysh, V. D. Kulakovskii, T. L. Reinecke, and A. Forchel, *Strong coupling in a single quantum dot-semiconductor microcavity system*, Nature **432** (2004), 197.

[Sak94] J.J. Sakurai, *Modern Quantum Mechanics*, Addison-Wesley, 1994.

[SCF+04] David D. Smith, Hongrok Chang, Kirk A. Fuller, A. T. Rosenberger, and Robert W. Boyd, *Coupled-resonator-induced transparency*, Phys. Rev. A **69** (2004), 063804.

[SG08] R. J. Schoelkopf and S. M. Girvin, *Wiring up quantum systems*, Nature **451** (2008), 664.

[SMNE83] J. J. Sanchez-Mondragon, N. B. Narozhny, and J. H. Eberly, *Theory of Spontaneous-Emission Line Shape in an Ideal Cavity*, Phys. Rev. Lett. **51** (1983), 550.

[SMPP08] Kartik Srinivasan, Christopher P. Michael, Raviv Perahia, and Oskar Painter, *Investigations of a coherently driven semiconductor optical cavity QED system*, Phys. Rev. A **78** (2008), 033839.

[SP07a] Kartik Srinivasan and Oskar Painter, *Linear and nonlinear optical spectroscopy of a strongly coupled microdisk-quantum dot system*, Nature **450** (2007), 862.

[SP07b] ———, *Mode coupling and cavity-quantum-dot interactions in a fiber-coupled microdisk cavity*, Phys. Rev. A **75** (2007), 023814.

[SZ97] Marlan O. Scully and M. Suhail Zubairy, *Quantum Optics*, Cambridge University Press, 1997.

[Tan] S. M. Tan, *A quantum optics toolbox for Matlab 5.*

[TRK92] R. J. Thompson, G. Rempe, and H. J. Kimble, *Observation of normal-mode splitting for an atom in an optical cavity*, Phys. Rev. Lett. **68** (1992), 1132.

[Vah03] K. J. Vahala, *Optical microcavities*, Nature **424** (2003), 839.

[WM94] D. F. Walls and G. J. Milburn, *Quantum Optics*, Springer, 1994.

[XSP+06] Qianfan Xu, Sunil Sandhu, Michelle L. Povinelli, Jagat Shakya, Shanhui Fan, and Michal Lipson, *Experimental Realization of an On-Chip All-Optical Analogue to Electromagnetically Induced Transparency*, Phys. Rev. Letters **96** (2006), 123901.

[Yab87] Eli Yablonovitch, *Inhibited Spontaneous Emission in Solid-State Physics and Electronics*, Phys. Rev. Lett. **58** (1987), 2059.

[YSH+04] T. Yoshie, A. Scherer, J. Hendrickson, G. Khitrova, H. M. Gibbs, G. Rupper, C. Ell, O. B. Shchekin, and D. G. Deppe, *Vacuum Rabi splitting with a single quantum dot in a photonic crystal nanocavity*, Nature **432** (2004), 200.

[YVK99] J. Ye, D. W. Vernooy, and H. J. Kimble, *Trapping of Single Atoms in Cavity QED*, Phys. Rev. Lett. **83** (1999), 4987.

Glossary

1T1A	1-toroid-1-atom, 54
2T0A	2-toroids-no-atom, 54
2T1A	2-toroids-1-atom, 54
2T2A	2-toroids-2-atoms, 54
EIT	electromagnetically induced transparency, 79
WGM	whispering gallery mode, 12